TOOLS FOR IDENTIFYING FUNCTIONS OF TYPE III SECRETION SYSTEM EFFECTORS FROM *SHIGELLA FLEXNERI*

by

Saima Sidik

Submitted in partial fulfillment of the requirements
for the degree of Master of Science

at

Dalhousie University
Halifax, Nova Scotia
April 2012

DALHOUSIE UNIVERSITY

Department of Microbiology and Immunology

The undersigned hereby certify that they have read and recommend to the Faculty of Graduate Studies for acceptance a thesis entitled "TOOLS FOR IDENTIFYING FUNCTIONS OF TYPE III SECRETION SYSTEM EFFECTORS FROM *SHIGELLA FLEXNERI*" by Saima Sidik in partial fulfillment of the requirements for the degree of Master of Science

Dated: April 17, 2012

Supervisor: _____

Co-Supervisor: _____

Readers: _____

_____

Departmental Representative: _____

DALHOUSIE UNIVERSITY

DATE: April 17, 2012

AUTHOR: Saima Sidik

TITLE: TOOLS FOR IDENTIFYING FUNCTIONS OF TYPE III SECRETION SYSTEM EFFECTORS FROM *SHIGELLA FLEXNERI*

DEPARTMENT OR SCHOOL: Department of Microbiology and Immunology

DEGREE: MSc CONVOCATION: October YEAR: 2012

_____

Signature of Author

TABLE OF CONTENTS

LIST OF TABLES

LIST OF FIGURES

ABSTRACT

Shigellae are pathogenic bacteria that cause the disease shigellosis. Two methods for studying secreted effectors encoded by this pathogen's virulence plasmid are described.

First, protein microarrays were used to identify substrates of an E3 ubiquitin ligase called IpaH7.8. Second, a deletion collection containing mutants for every gene on the virulence plasmid was used in two screens: one to identify mutants that elicit atypical levels of Interleukin-8 (IL-8) from U937 cells, and one to identify mutants that bind the dye Congo red abnormally.

Although protein microarrays were an ineffective tool, the deletion collection proved valuable. Most mutants were less effective at sequestering Congo red than wild-type *S. flexneri,* although this ability was enhanced in several mutants. Four mutants, *ΔospB, Δorf186, ΔmxiH* and *ΔmxiK,* elicited higher levels of IL-8 from U937 cells than wild type *S. flexneri*. These results validate the use of the deletion collection as a tool for studying bacterial pathogenesis.

LIST OF ABBREVIATIONS USED

AfaE	Afimbrial Adhesin E
ANKRD13D	Ankyrin Repeat Domain 13 Family, Member D
ATP	Adenosine Triphosphate
C/EBP	CCAAT Enhancer Binding Proteins
Caco-2	Adenocarcinoma of the Colon - 2
CCL	CC Ligand
CD	Cluster of Differentiation
cDNA	Complementary Deoxyribonucleic Acid
CLB3	Cell Lysis Buffer 3
cm	Centimeter
CMV	Cytomegalovirus
CO_2	Carbon Dioxide
CR Units	Congo Red Units
CXCL	CXC Ligand
DH5a	Doug Hanahan Strain 5α
DMEM	Dulbecco's Modified Eagle Medium
DTT	Dithiothreitol
E. coli	*Escherichia coli*
EDTA	Ethylenediaminetetraacetic acid
EGF	Epidermal Growth Factor
ELISA	Enzyme Linked Immunosorbent Assay
ENA-78	Epithelial-Derived Neutrophil-Activating Peptide 78
FBS	Fetal Bovine Serum
FITC	Fluorescein isothiocyanate
GCSF	Granulocyte Colony Stimulating Factor
GFP	Green Fluorescent Protein
GlcNAc	N-acetylglucosamine
hBD3	Human Beta-Defensin 3
HCl	Hydrogen Chloride
HECT	Homologous to the E6-AP Carboxyl Terminus
HeLa	Henrietta Lacks
HIV-1	Human Immunodeficiency Virus - 1
IFN-γ	Interferon-γ
IkBa	Inhibitor of NF-κB type α
IKK	I Kappa B Kinase
IL	Interleukin
IpaH	Invasion Plasmid Antigen H
IPTG	Isopropyl β-D-1-thiogalactopyranoside
JAK	Janus Kinase
K48	Lysine 48
K63	Lysine 63
KCNAB1	Potassium voltage-gated channel, shaker-related subfamily, beta member 1

LB	Luria Bertani Broth
LC3	Light Chain 3
LPS	Lipopolysaccharide
M-CSF	Macrophage Colony Stimulating Factor
MAPK	Mitogen Activated Protein Kinase
MCP-2	Monocyte Chemoattractant Protein 2
MDCK	Madin Darby Canine Kidney
mg	Milligram
MIP	Macrophage Inflammatory Protein
mL	Millilitre
MLTKα	Mixed-Linkage Kinase-Like Mitogen-Activated Protein Triple Kinase
mM	Millimetre
MOI	Multiplicity of Infection
MOMP	Major Outer Membrane Protein
MxiE	Membrane Excretion Protein E
Nedd4	Neural Precursor Cell Expressed Developmentally Down Regulated Protein 4
NF-kB	Nuclear Factor Kappa Light Chain Enhancer of Activated B Cells
NK	Natural Killer
NP-40	Nonidet P-40
OD600	Optical Density at 600nm
Orf	Open Reading Frame
Osp	Outer *Shigella* Protein
p-ERK1/2	Phospho-Extracellular Signal Regulated Kinase 1/2
p-p38	Phospho-p38
PBS	Phosphate Buffered Saline
PBST	Phosphate Buffered Saline with Tween-20
PCR	Polymerase Chain Reaction
PEI	Polyethylenimine
pg	Picogram
PKN1	Protein Kinase N1
PMA	Phorbol 12-Myristate 13-Acetate
PMSF	Phenylmethanesulfonylfluoride
PRR	Pattern Recognition Receptor
PVDF	Polyvinylidene Difluoride
RANTES	Regulated Upon Activation, Normal T-Cell Expressed, and Secreted
RB	Retinoblastoma Protein
RFP	Red Fluorescent Protein
RING	Really Interesting New Gene
RIPA	Radioimmunoprecipitation Assay
RPM	Revolutions Per Minute
RPMI	Roswell Park Memorial Institute
S. aureus	*Staphylococcus aureus*
S. cerevisiae	*Saccharomyces cerevisiae*

S. flexneri	*Shigella flexneri*
SDS-PAGE	Sodium Dodecyl Sulfate Polyacrylamide Gel Electrophoresis
Sp1	Specificity Protein 1
Spa	Surface Presentation Antigen
SspH1	Salmonella Secreted Protein H1
STAT	Signal Transducer and Activator of Transcription
T3SS	Type III Secretion System
TAK1	Transforming Growth Factor β-Activated Kinase 1
Tal	Tumor Susceptibility Gene 101 Associated Ligase
TECK	Thymus Expressed Chemokine
TLR	Toll-Like Receptor
TNFα	Tumor Necrosis Factor α
TRAF6	TNF Receptor Associate Factor 6
TSB	Trypticase Soy Broth
Tsg101	Tumor Susceptibility Gene 101
Ubc4	Ubiquitin Conjugating Protein 4
UBCH5B	Ubiquitin Conjugating Enzyme from Humans 5b
UFD1L	ubiquitin fusion degradation 1 like
RIOK3	Right Open Reading Frame Kinase 3
µg	Microgram
UI	Uninfected
µL	Microlitre
vir	Virulence Protein
WHO	World Health Organization

ACKNOWLEDGEMENTS

Thank you to all the members of the Rohde lab, past and present. In particular, thank you to Julie Ryu, who performed the protoarray screens, to Ameer Jarrar, who did some of the western blots in Figure 9, and to Amit Mishra, who contributed to Figure 1 and to the Congo red screen. Also thank you to Julie, Ameer and Dr. Jeremy Benjamin for creating the *S. flexneri* deletion collection, which has been a big part of my project. Thank you to Jesse Rusak for the invaluable help with all things computer-related.

Thank you to Drew Leidal, Dr. Denys Khaperskyy, Dr. Sharon Oldford, Yisong Wei and Kristin Hunt for their help throughout my project. These people were instrumental in the fluorescent microscopy, the stable cell line creation and the cytokine work. Thank you to Hana James and Dr. Andy Stadnyk for supplying the HT-29 and Caco-2 cells, to Dr. Rafael Garduño for supplying the U937 cells, to Dr. Peter Wentzell for his help ranking the results of the protoarray screens, and to Naoko Onodera for creating the phylogenetic tree shown in Figure 2. Also thanks to Dr. Craig McCormick for supplying the HeLa cells and LC3-GFP HeLa cells, and for his enthusiasm in my project.

Thank you to Dr. Jean Marshall, my co-supervisor, for always being generous with her time, knowledge and reagents, and to the other members of my supervisory committee, Dr. Brent Johnston and Dr. John Archibald, for their insight and support.

Most of all, thank you to my supervisor, Dr. John Rohde, who's a pretty awesome guy to work for.

Chapter 1: Introduction

1.1: *Shigellae* as Pathogens

1.1.1: Epidemiology of Shigellosis

Shigellae are gram-negative bacteria that cause the gastrointestinal disease shigellosis, which is characterized by fever, abdominal cramps and bloody diarrhea. These pathogens spread via the fecal-oral route, and are most prevalent in places where sanitation conditions are poor, such as developing countries or daycare centres and nursing homes in developed countries (Center for Disease Control, 2009). There are four species within the genus *Shigella*: *S. flexneri, S. sonnei, S. dysenteriae* and *S. boydii* (Sansonetti, 2001). *S. dysenteriae* is associated with large outbreaks of shigellosis, such as those that sometimes occur in refugee camps (Kernéis *et al*, 2009), and infections with this pathogen are often deadly due to its ability to produce Shiga toxin: an inhibitor of protein synthesis (Strockbine *et al*, 1988). *S. flexneri, S. sonnei* and *S. boydii*, are not as dangerous to adults as *S. dysenteriae*, although infections with these strains can still be deadly to children. These three species are endemic to Africa and parts of Asia (Sansonetti, 2001). *S. flexneri* is the most commonly studied laboratory strain, and will be the focus of this thesis.

In 1999, the World Health Organization (WHO) estimated that approximately one hundred million people contract shigellosis every year, and approximately one million die. Mortality is most common in young children, with 61% of deaths being in children under the age of five (Kotloff *et al*, 1999). A more recent study performed in south-east

Asia in 2006 found that the incidence of shigellosis was 2.1 cases per 1,000 people: a higher level than would have been predicted using the WHO's estimate of disease prevalence. Therefore, the frequency of shigellosis seems to be rising, at least in this part of the world. These researchers also recorded high levels of antibiotic resistance with, for example, as many as 84% of *S. flexneri* strains being resistant to ampicillin (von Seidlein *et al*, 2006). Antibiotic resistance has been reported in many other studies of shigellosis (e.g. El-Gendy *et al*, 2012, Özmert *et al*, 2005), and the cause is usually attributed to the ubiquitous availability, and poor regulation, of antibiotics in the developing world (Sack *et al*, 2001, Sansonetti, 2006). *S. boydii* encoding the gene *ndm1*, which confers resistance to a class of antibiotics called "β-lactams," (Cantón and Lumb, 2011), has also recently been identified in water samples from India. This is particularly worrisome, as *ndm1* confers resistance to a wide range of antibiotics (Walsh *et al*, 2011). The wide-spread distribution of shigellosis, the high death rate among children, and the rise of antibiotic resistance among this disease's etiological agents illustrate the severe effect that *Shigellae* have on inhabitants of the developing world, and the need to study these pathogens.

1.1.2: Route of *Shigellae* Infection

Shigellae spread via the fecal-oral route. After ingestion, these pathogens travel to the colon, where they cross the epithelial barrier through specialized immune cells known as "M cells" (Wassef *et al*, 1989). After this transition, *Shigellae* invade epithelial cells through the basolateral surface, as well as macrophages and dendritic cells found beneath the epithelial layer (Mounier *et al*, 1992, Phalipon and Sansonetti, 2007). This leads to a highly proinflammatory cytokine environment characterized by high levels of the cytokine Interleukin-8 (IL-8, Philpott *et al*, 2000), which leads to recruitment of

neutrophils (Beatty and Sansonetti, 1997). Neutrophils are capable of killing *S. flexneri*, and are thought to be a major factor in the clearance of this pathogen (Read, 1975, Phalipon and Sansonetti, 2007). Much of the IL-8 elicited in response to *S. flexneri* infection is produced by epithelial cells as a result of an interaction between peptidoglycan from *S. flexneri* and the intracellular receptor Nod1. Activation of Nod1 leads to stimulation of the JNK and NF-κB pathways, which leads to production of proinflammatory cytokines (Girardin *et al*, 2001, Girardin and Philpott, 2004).

1.1.3: *S. flexneri's* Virulence Plasmid and the Type III Secretion System

S. flexneri encodes the majority of its virulence factors on a large (approximately 200 kb) plasmid that is often referred to as the "virulence plasmid" (Buchrieser et al, 2000). The virulence plasmid encodes proteins necessary to construct a structure called a Type III Secretion System (T3SS) that is comprised of a hollow staff, or "needle complex" anchored to the bacterial inner and outer membranes. This structure is highly conserved in *S. flexneri* and other gram-negative bacteria such as *Salmonella enterica* and *Escherichia coli* (Marlovits and Stebbins, 2010). The T3SS is comprised of over twenty proteins, which include MxiD, MxiG, MxiJ, MxiH, MxiI and MxiM (Blocker *et al*, 2001, Schuth and Maurelli, 2001, Phalipon and Sansonetti, 2007). The T3SS components assemble to form needles that penetrate host cells and facilitate the transport of other proteins involved in virulence. The substrates of the T3SS, generally referred to as "effectors," are delivered, or injected, from the bacteria to the cytoplasm. At the base of this needle are the proteins Spa33 and Spa47. Spa33 is a component of the "C-ring" (Morita-Ishihara *et al*, 2006). This structure has been proposed to act as a sorting platform that dictates the order in which effectors are secreted (Lara-Tejero *et al*, 2011).

Spa47 is an ATPase involved in regulating secretion of effectors through the needle complex (Johnson and Blocker, 2008). Three secreted effectors, IpaB, IpaC and IpaD, promote rearrangement of the host cell's actin cytoskeleton, leading to internalization of bacteria through a process known as "macropinocytosis" (High et al, 1992, Ménard et al, 1993, Adam et al, 1995). Upon entry of the bacterium, a second group of effectors work to subvert the host cell's innate immune system and promote the survival of *S. flexneri* (Parsot, 2009). Figure 1 provides a visual explanation of *S. flexneri's* T3SS.

Genes encoding components of the T3SS, as well as several effectors, are encoded by a region of the virulence plasmid known as the "entry region," and are under the control of the transcription factors VirF and VirB. Expression of the entry region is regulated by temperature, with transcription being activated at 37°C (Phalipon and Sansonetti, 2007). Effectors that are regulated by VirF and VirB represent a "first wave" of effectors that is dedicated to promoting entry of the bacterium (Parsot, 2009).

First-wave effectors are produced prior to activation of the T3SS, and are stored in the bacterial cytoplasm in a secretion-competent state in association with chaperones (Ménard *et al*, 1994, Ogawa *et al*, 2003, Niebuhr *et al*, 2000 Page *et al*, 2002, Hachani *et al*, 2008, Parsot *et al*, 2005). IpaB and IpaC, two effectors involved in promoting invasion of epithelial cells, maintain a spatial separation in the bacterial cytoplasm by associating independently with the chaperone IpgC (Ménard *et al*, 1994). Upon activation of the T3SS, IpaB and IpaC are transported into the host cell, and IpgC goes on to interact with the bacterial transcription factor MxiE to stimulate production of a second set of effectors. Similarly, the effector IpgD is bound by a chaperone called IpgE while in the bacterial cytoplasm. After the T3SS is assembled, IpgD is released and translocated into the host cell cytoplasm, where it goes on to promote actin rearrangement and

invasion (Niebuhr *et al*, 2000). IpgA, a third chaperone, is necessary for translocation of the effector IcsB through the T3SS (Ogawa *et al*, 2003). IcsB has been implicated in allowing *S. flexneri* to avoid being destroyed by autophagosomes (Ogawa *et al*, 2005). The most versatile of *S. flexneri's* chaperones, Spa15, has been shown to regulate IpaA, IpgB1, IpgB2, OspB, OspD1 and OspC3 (Page *et al*, 2002, Hachani *et al*, 2008, Parsot *et al*, 2005). IpaA, IpgB1 and IpgB2 are all involved in actin rearrangement and invasion (Parsot, 2009). OspB is involved in modulating the immune response to *S. flexneri* (Zurawski *et al*, 2009), and OspD1 works with MxiE to regulate transcription of bacterial genes (Parsot *et al*, 2005). The diversity of Spa15's interacting partners and their roles in *S. flexneri's* pathogenesis underscores the importance of chaperones in coordinating an infection.

One such first wave effector, IcsB, allows *S. flexneri* to avoid being degraded through autophagy: a process eukaryotic cells use to recycle proteins and organelles, as well as to protect themselves against pathogens. IcsB binds to the surface protein IcsA. IcsA promotes actin polymerization, thereby allowing *S. flexneri* to use the host's cytoskeletal machinery to move within cells. When IcsB is deleted, the mammalian protein Atg5 binds to IcsA and allows host cells to destroy *S. flexneri* through the process of autophagy. IcsB masks IcsA, thereby preventing Atg5 from recognizing it (Ogawa *et al,* 2005). This bacterial defense mechanism was identified in Madin Darby Canine Kidney (MDCK) cells, and whether or not other effectors are involved in subverting the autophagy machinery in other cell types, or *in vivo*, is unknown.

Activity of the T3SS stimulates transcription of a second wave of effectors that are under the control of the transcription factor MxiE. These "second wave" effectors include OspG, OspD3, OspE1, OspE2, and members of the IpaH family of effectors

(Parsot, 2009, Phalipon and Sansonetti, 2007). Many second wave effectors are involved in modulating the host immune response so as to optimize *S. flexneri's* environment and promote its proliferation and spread (Nataro *et al*, 1995, Kim *et al*, 2005, Kim *et al*, 2009). Some first wave effectors, such as OspB and OspF, work to subvert the host immune response, as well (Zurawski *et al*, 2009). These interactions will be discussed in more detail in Chapter 1.3.

The IpaHs are a family of twelve proteins, five of which are encoded by the virulence plasmid and seven of which are chromosomal (Onodera *et al*, submitted to Journal of Bacteriology). The IpaHs are E3 ubiquitin ligases (Rohde et al, 2007), and one member of this family, IpaH9.8, targets a component of the NF-κB pathway known as Nemo for destruction by the proteasome (Ashida et al, 2009). One focus of this thesis is to identify substrates of another member of this family: IpaH7.8. A more extensive overview of these proteins is given in Chapters 1.5 and 1.6.

1.1.4: Congo Red

S. flexneri is used frequently to study Type III Secretion Systems due to its ability to bind a synthetic dye known as Congo red. Congo red induces assembly of the T3SS and secretion of effectors at 37°C and in the absence of mammalian cells (Parsot *et al*, 1995). Virulent strains of *S. flexneri* also sequester this dye, making their colonies appear red on agar plates containing Congo red. Avirulent strains, such as the virulence plasmid-cured strain BS176, sequester Congo red inefficiently, giving them a pink appearance. This property is a useful research tool, as it associates a phenotype with activation of the T3SS, which is helpful in identifying factors that alter Type III Secretion.

The ultimate goal of the *Shigella* research community is to understand all the mechanisms through which the effectors orchestrate an infection. This thesis describes a few steps that I have taken down this road.

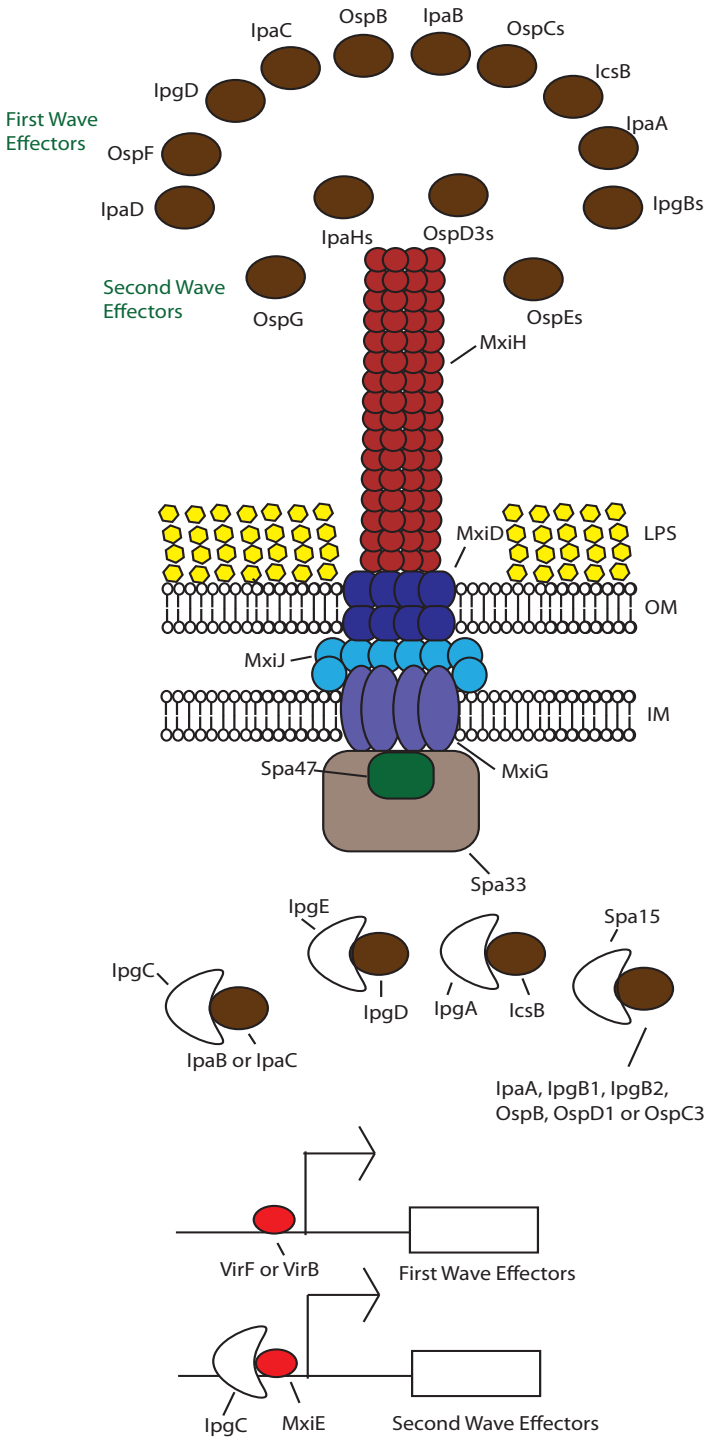

Figure 1: Effectors and needle components produced by *S. flexneri*. LPS = Lipopolysaccharide, OM = Outer Membrane, IM = Inner Membrane. This figure was created in part by Amit Mishra and Julie Ryu.

1.2*: S. flexneri's* Interaction With Macrophages

After crossing the epithelial barrier of the colon, *S. flexneri* is phagocytosed by the macrophages residing beneath. Once inside, *S. flexneri* breaks out of phagocytic vacuoles and enters the cytoplasm (Phalipon and Sansonetti, 2007). Macrophages are a major contributor to the immune response to bacterial infections, and part of this thesis describes research on the interaction between this cell type and effectors encoded by *S. flexneri*.

1.2.1: Pyroptosis of Macrophages

Macrophages infected by *S. flexneri* undergo a type of proinflammatory cell death that was initially characterized as a type of apoptosis (Zychlinsky *et al*, 1992, Zychlinsky *et al*, 1996). It has since been proposed that this type of death be referred to as "pyroptosis" because apoptosis is inherently anti-inflammatory (Fink and Cookson, 2005, Suzuki *et al*, 2007). Hallmarks of pyroptosis include activation of the protease Caspase-1, which is involved in cytokine processing, and the subsequent release of proinflammatory cytokines (Fink and Cookson, 2005). Upon infection with *S. flexneri*, Caspase-1 is bound and activated by the effector IpaB (Hilbi et al, 1998). This leads to the release of the cytokines Interleukin-1β (IL-1β, Zychlinsky *et al*, 1994) and Interleukin-18 (IL-18 Sansonetti, 2000). Sansonetti and coworkers (2000) used the mouse pulmonary model of shigellosis to show that mice lacking Caspase-1 had significantly higher bacterial burdens and succumbed to infection significantly more frequently than wild-type mice. The same study found that injection of recombinant IL-1β into Caspase-1 mutant mice lead to even higher bacterial loads and a higher death rate than Caspase-1 mutant mice, whereas injection of recombinant IL-18 returned bacterial load and death rate to

that of wild-type mice. This demonstrates that although the inflammation associated with release of IL-1β may promote colonization of infected tissue by *S. flexneri*, aspects of pyroptosis are necessary to clear *S. flexneri*. This dichotomy is typical of *S. flexneri* infections, in which a strong, early inflammatory response, while being necessary to clear the infection, also damages the surrounding tissue and allows *S. flexneri* to infiltrate a wide area (Phalipon and Sansonetti, 2007).

1.2.2: Immunogenic Surface Proteins

In addition to the IpaB-dependent cytokines released during the process of pyroptosis, pattern recognition receptors (PRRs) encoded by macrophages respond to *S. flexneri's* surface molecules, enhancing the contribution of this cell type to the immune response. For example, a surface protein that Pore and coworkers (2010) refer to as "Major Outer Membrane Protein" (MOMP) is recognized by the PRR Toll Like Receptor 2 (TLR2). This leads to production of the cytokines IL-1β, IL-6, Tumor Necrosis Factor α (TNFα), Interferon-γ (IFN-γ) and IL12-p70, as well as an increase in mRNA levels corresponding to CCL3 (MIP-1α), CCL4 (MIP-1β) and CCL5 (RANTES) (Pore *et al*, 2010). As Chapter 1.3 will illustrate, *S. flexneri* is well adapted to the immunological environment produced by macrophages and other immune cells, and often manipulates cellular factors to tailor this environment in ways that promote its survival and spread.

1.3: *S. flexneri* Manipulates the Host Immune Response to Shape the Cytokine Environment

The early stages of *S. flexneri* infections are dominated by the highly proinflammatory innate immune response associated with pyroptosis of macrophages and

release of IL-8 from epithelial cells (Suzuki *et al*, 2007, Philpott *et al*, 2000). The degree to which this environment is shaped by the host and the extent to which *S. flexneri* influences it are matters currently under investigation by many labs, and there are numerous examples of *S. flexneri's* effectors manipulating the host's immune response, presumably to create an optimal environment for its survival and spread. One of my research initiatives involved identifying new interactions between effectors and host immune factors, and so a few examples of previously characterized interactions are described below to put these results in context.

1.3.1: Cytokines Elicited by MxiE-Dependent Factors

Sperandio *et al* (2008) showed that one or more second-wave effector(s) regulates expression of antimicrobial peptides and cytokines produced by epithelial cells. These factors included hBD3, a cationic peptide capable of permeabilizing cell membranes and possessing a chemotactic property for neutrophils (Scudiero *et al*, 2010), as well as various chemokines that attract macrophages and lymphocytes to the site of infection, such as CCL3, CCL4, CCL20 (MIP-3α) and CCL25 (TECK). Lower expression of the genes encoding these proteins correlated with an increase in *S. flexneri's* ability to progress towards intestinal crypts, and lower numbers of dendritic cells being recruited to the area of infection (Sperandio *et al*, 2008).

1.3.2: Effectors that Interfere with Immunological Signaling Pathways

A number of effectors interfere with the NF-κB and MAP Kinase signaling pathways. These include a kinase called OspG that interacts with an E2 ubiquitinating enzyme called UbcH5b, which is involved in ubiquitinating the protein Inhibitor of NF-

κB type α (IkBα). In resting conditions, IkBα binds to the transcription factor NF-κB. Upon infection, its ubiquitination and subsequent destruction allow NF-κB to enter the nucleus and transcribe many genes encoding proteins involved in innate immunity (Kim *et al*, 2005). OspG has been associated with high levels of IκBα, and it is assumed that its interaction with UbcH5b is responsible for blocking IκBα degradation. A *ΔospG* mutant elicits more inflammation upon infection of a rabbit's ileal loop than a wild-type strain of *S. flexneri*, indicating the direct consequence of OspG's action on the host's immunological response (Kim *et al*, 2005). Enterohemorrhagic *E. coli* (EHEC) encodes a homologue of OspG known as NleH1. NleH1 inhibits phosphorylation of the NF-κB subunit RPS3, thereby preventing it from activating transcription of its target genes (Wan *et al*, 2011).

OspF inactivates the phosphorylated mitogen activated protein kinases p-p38 and p-ERK1/2 through the removal of phosphate groups, and a *ΔospF* mutant induces more inflammation and attracts more neutrophils to the site of infection than a wild-type strain in a rabbit ileal loop model of infection (Li *et al*, 2007, Arbibe *et al*, 2007). OspF and OspB interact with the transcription factor Retinoblastoma Protein (RB), and epithelial cells infected with a *ΔospB* mutant produce more IL-8 than those infected with wild-type *S. flexneri* (Zurawski *et al*, 2009).

1.3.3: Effectors that Modify Lipopolysaccharide

Effectors are also involved in modifying components of *S. flexneri* itself to manipulate the immune response. The proteins MsbB1 and MsbB2 are effectors that do not fit into the typical first wave/second wave hierarchy, as they are not under the control of any either VirF, VirB or MxiE (Le Gall *et al*, 2005). MsbB1 and MsbB2 are involved

in modifying the lipid A component of Lipopolysaccharide (LPS): a highly immunogenic glycoprotein found on the surfaces of gram-negative bacteria (White, 2007). A mutant lacking both *msbB1* and *msbB2* elicited less TNF and caused less tissue damage than wild-type *S. flexneri* when used to infect monocytes and rabbit ileal loops. Animals infected with *ΔmsbB* mutant strains also had lower bacterial loads than wild-type *S. flexneri* infected animals, implying that it is advantageous for *S. flexneri* to modify LPS so as to enhance inflammation and tissue destruction, probably to promote its spread throughout the surrounding tissue (d'Hauteville *et al*, 2002). Whether these two effectors are secreted through the T3SS or modify LPS intracellularly before its assembly remains uncharacterized.

1.3.4: An Effector that Interferes with T-Cell Migration

Konradt *et al* (2011) have recently obtained an example of an effector that interferes directly with the ability of immune cells to respond to *S. flexneri* infections. This group found that *S. flexneri* delivers the effector IpgD into CD4+ T cells, either after invading or by using its T3SS while the bacterium remains outside the T cell. IpgD, a phosphoinositide 4-phosphatase, interferes with proteins that cross-link components of the cell's cytoskeleton to the membrane. This prevents the cell from polarizing its cytoskeleton, rendering it unable to move directionally. *S. flexneri* is therefore able to limit the number of CD4+ T cells available to respond to infection.

1.3.5: A Broad View of Bacterial Effectors

The ability to interfere with host defense mechanisms is, of course, a common theme among pathogenic bacteria. Effectors that modify host factors post-translationally

are commonly employed as a strategy to shut down signaling pathways (Galán, 2009, Mattoo *et al*, 2007, Stavrinides *et al*, 2008). For example, the *Yersinia* effector YopJ acetylates serine and threonine residues on proteins in the Map Kinase pathway, thereby preventing these proteins from being phosphorylated and therefore activated (Galán, 2009). Another example of an effector that induces a post-translational modification is VopS from *Vibrio parahaemolyticus,* which attaches an adenosine 5'-monophosphate group to several cellular factors involved in actin rearrangement, thereby changing the actin dynamics in the infected cell and loosening cell-cell adhesions (Galán, 2009, Casselli *et al*, 2008).

Subversion of the Map Kinase pathway is also illustrated by the classical toxin Lethal Factor, or LF, from *Bacillus anthracis*. LF is a protease capable of cleaving most Map Kinase Kinase isoforms (Mattoo *et al*, 2007). Similarly, the effector CT441 from *Chlamydia sp*. cleaves the p65 subunit of NF-κB, thereby reducing production of many proinflammatory cytokines (Mattoo *et al*, 2007). Knowledge regarding interactions such as these is crucial for the development of new treatments for, and vaccines against, diseases such as shigellosis.

1.4: Deletion Collections and their Uses in Research

The feasibility of high-throughput studies has increased substantially in recent years with creations such as pinning robots for the manipulation of thousands of yeast or bacterial strains, and next-generation sequencing, which allows analysis of a whole genome within a few days. Deletion collections are a critical component of this new, high-throughput way of studying biology. These are collections of mutant strains of a particular organism, each lacking one gene. The Rohde lab has created an *S. flexneri*

deletion collection in which each gene on the virulence plasmid has been deleted. One focus of this thesis involves using the deletion collection to dissect the roles of previously uncharacterized or poorly characterized effectors.

1.4.1: The *Saccharomyces cerevisiae* Deletion Collection

The *Saccharomyces cerevisiae* deletion collection has been a widely used tool in molecular biology since its completion nearly ten years ago (Glaever *et al*, 2002). Glaever and coworkers (2002) first used this collection to study responses to stresses such as high salt concentration or using galactose as a carbon source. These experiments revealed the involvement of many previously unidentified genes in these processes, thus validating the use of the deletion collection as a research tool. Since then, the *S. cerevisiae* deletion collection has lead to new discoveries closely related to human health. For example, Steinmetz *et al* (2002) screened the deletion collection for genes involved in respiration, thereby identifying candidates for genes involved in human mitochondrial disorders. In fact, the extent of the yeast deletion collection's success is still being discovered as this tool is combined with emerging technologies such as next-generation sequencing and robotics. For example, Tong and coworkers (2001) applied pinning robots to the yeast deletion collection to develop a high-throughput method for creating double mutants to identify genes with redundant functions.

1.4.2: The *Escherichia coli* Deletion Collection

In 2006, an *E. coli* deletion collection called the Keio collection was completed (Baba *et al*, 2006). One of the early experiments performed using this tool involved screening the collection for mutants that were hypersensitive to antibiotics (Tamae *et al*,

2008). This screen identified potential targets for "codrugs," or drugs that could be used in combination with antibiotics to enhance their effects. The Keio collection has also allowed for genetic manipulation of *E. coli* in ways that were previously not feasible. For example, Typas *et al* (2008) used the collection to develop a technique for creating double-mutants in *E. coli*. This has allowed the group to identify genetic interactions by identifying double mutants with growth phenotypes that are more severe than those observed for either of the single mutants.

1.5: Ubiquitin and E3 Ubiquitin Ligases

1.5.1: Functions of Ubiquitination

The IpaHs are a family of twelve effectors, five of which are encoded by the virulence plasmid, and seven of which are chromosomal (Onodera *et al*, submitted to Journal of Bacteriology). These effectors have recently been characterized as bacterial ubiquitin ligases which have evolved to interact with mammalian ubiquitination machinery (Rohde *et al*, 2007). Ubiquitin is a 76 amino acid protein that can be conjugated to lysine residues on substrate proteins as a type of post-translational modification. Moreover, chains of ubiquitin linked through one of its seven lysine residues can form after an initial ubiquitin has been conjugated to its substrate (Hershko and Ciechanover, 1998). The most commonly known function of ubiquitination involves the addition of ubiquitin polymers linked through the lysine at amino acid position 48, or K48. Proteins modified by such an ubiquitin chain are targeted for destruction by a complex of proteases known as the "proteasome" (Xu *et al*, 2009). However, other functions for ubiquitination have also been documented. Chains of ubiquitin linked

through the lysine at position 63, or K63, stabilize proteins and create scaffolding between multiple proteins to facilitate signaling. An example of this can be found in the NF-κB signaling cascade. A protein called TRAF6 mediates formation of K63 linked ubiquitin chains attached to itself and a protein known as Nemo, an activator of IKK activity. A complex of proteins known as TAK1 interacts with both of these ubiquitin chains, resulting in the activation of Nemo, which eventually leads to NF-κB entering the nucleus (Sun *et al*, 2004). Linear chains of ubiquitin linked via the N-terminal methionine residue are also known to occur, and Nemo is also modified by these "Met1" chains. The exact function of Met1 chains conjugated to Nemo is not clear, but cells lacking the ability to form Met1 chains show defects in their ability to degrade IκBα, indicating that these chains are necessary to ensure proper functioning of the NF-κB pathway (Behrends and Harper, 2011).

Monoubiquitination plays an important biological role by regulating localization of proteins and protein complexes. A single ubiquitin molecule conjugated to a protein often signals that the protein should be endocytosed or exocytosed. For example, monoubiquitination of Epidermal Growth Factor Receptor (EGFR) results in it being endocytosed and degraded by the lysosome (Haglund *et al*, 2003).

1.5.2: The Ubiquitin Cascade

The conjugation of ubiquitin to a protein is a three-step process. The process begins with an enzyme simply known as "E1" binding the glycine residue at the C-terminal end of ubiquitin. The E1 then passes ubiquitin to one of the approximately 20 E2 enzymes produced by humans. The E2 then interacts with one of several hundred E3 enzymes. Humans produce two broad families of E3 enzymes: those containing HECT-

domains and those containing RING domains. In the case of HECT E3s, ubiquitin is transferred from the E2 to the E3, then to a substrate protein that interacts with the E3. RING-domain E3s, however, bring the E2 into close proximity with the substrate protein, and then ubiquitin is passed directly from the E2 to the substrate (Hershko and Ciechanover, 1998).

1.5.3: HECT-Domain E3 Ubiquitin Ligases

E2 enzymes interact with the N-terminal region of HECT domains. The C-terminal domain contains a cysteine residue to which ubiquitin is passed (Huibregtse *et al*, 1995). These two domains are connected by a flexible linker region. This region is thought to bend, thereby moving the E2 into close proximity with the cysteine that will receive ubiquitin. Ubiquitin is then passed from the E3 to a substrate (Huang *et al*, 1999). HECT-domain E3s interact with their substrates through one of several protein-protein interaction domains. The best characterized HECTs contain a WW protein interaction domain, characterized, as the name implies, by two conserved tryptophan residues. This domain interacts preferentially with proteins containing (L/P)PXY motifs. The strong preference of some HECT-domain E3s for this particular domain is useful in identifying substrates of these enzymes (Bernassola *et al*, 2008).

1.5.4: RING-domain E3 Ubiquitin Ligases

RING-domain E3s are named after their most prominent feature: a rigid polypeptide comprised of seven conserved cysteines cross-linked by two zinc ions and several less-conserved residues. The U-box family of E3 ubiquitin ligases are a sub-set of RING-type E3s possessing a similar structure in which the cysteines and zinc ions have

been replaced by charged and polar residues that maintain a finger-like structure through hydrogen bonding (Deshaies and Joazeiro, 2009). RING and U-box domains interacts with E2 enzymes and substrate proteins. Because the binding sites for E2s and substrate proteins are separated spatially, it is thought that binding to RING-domains triggers a conformational change in the E2~ubiquitin conjugate, which brings ubiquitin into close proximity with a lysine residue on the substrate protein, thereby mediating transfer of ubiquitin to this lysine. However, this process is not well understood (Petroski *et al*, 2005).

1.5.5: The IpaH Family of E3 Ubiquitin Ligases

The Invasion Plasmid Antigen H effectors (IpaHs) define a third class of E3 ubiquitin ligases. These E3s, which are each approximately 530 amino acids in length, contain a catalytic cysteine, and appear to function similarly to HECT-domain E3s, although their structure is distinct (Singer *et al*, 2008, Zhu *et al*, 2008). There are twelve IpaHs encoded by *S. flexneri*. Figure 2 shows a phylogenetic tree illustrating the relationships between these proteins, which are all highly conserved. A thirteenth protein not shown on this tree shares sequence similarity with the N-terminal region of the IpaHs, but has a large C-terminal deletion, and most likely does not encode a functional E3 ubiquitin ligase. As this tree illustrates, there are three pairs of IpaHs that are nearly identical. These include IpaH1 and IpaH6, IpaH2.5 and IpaH1.4, and IpaH4 and IpaH5. These pairs are likely to have resulted from very recent gene duplication events. (Onodera *et al*, submitted to Journal of Bacteriology). Homologues of the IpaHs exist in *Pseudomonas spp, Rhizobium spp, Salmonella spp* and *Yersinia spp* (Hicks and Galán, 2010). In *S. flexneri*, transcription of the *ipaHs* is under the control of the transcription

factor MxiE, and deletion of MxiE has been shown to dramatically attenuate levels of this family of proteins (Mavris *et al*, 2002).

The IpaHs consist of an N-terminal Leucine Rich Repeat domain (LRR domain) and a C-terminal E3 catalytic domain. The LRR domain consists of seven repeats of 21 amino acids, each containing five leucine residues in conserved positions, followed by two LRRs containing different patterns of leucine residues. Deleting the LRR domain has no effect on the ability of the IpaHs to polymerize ubiquitin *in vitro*, but a mutant of *ipaH9.8* that lacked the LRR domain was unable to ubiquitinate its substrate from yeast, Ste7 (Zhu *et al*, 2008). This implies that the LRR domain is involved in substrate recognition. The C-terminal domain consists of twelve α-helices. The salient feature of this domain is a catalytic cysteine residue that is thought to receive ubiquitin from E2 enzymes before passing it to substrates. This cysteine is located in a labile region that links helices eight and nine. Mutating this cysteine to either alanine or serine eliminates the ability of the IpaHs to bind ubiquitin (Zhu *et al*, 2008, Singer *et al*, 2008).

Levin and coworkers (2010) have shown that IpaH-family effectors differ from mammalian E3 ubiquitin ligases in their interactions with E2 enzymes. This group showed that SspH1, unlike mammalian E3 ubiquitin ligases, binds only to E2-ubiquitin conjugates, and not to uncharged E2 enzymes. A polyubiquitin chain then accumulates on the active site of the E2 enzyme, rather than on the E3. This is consistent with one of several models of ubiquitin chain formation proposed by Hochstrasser and coworkers (2006) in regards to HECT-domain E3s. In this model, ubiquitin is transferred from the E2 to the E3, then back to the E2 after it has picked up an additional ubiquitin molecule, with the process repeating until a chain containing multiple ubiquitin molecules has formed.

IpaH3 has been shown to catalyze K48-linked ubiquitin chains (Zhu *et al*, 2008), whereas IpaH9.8 catalyzes K29-linked chains (Ashida *et al*, 2010). Both of these chain types target substrates for destruction by the proteasome (Xu *et al*, 2009). A logical hypothesis regarding the function of the IpaHs is that they ubiquitinate mammalian proteins involved in host defense, thereby causing these proteins to be destroyed by the proteasome and promoting survival of *S. flexneri*. As Chapter 1.6 will show, early reports regarding substrates of IpaHs and their homologues support this hypothesis.

1.5.6: E3 Ubiquitin Ligases Secreted by *Legionella pneumophila, Salmonella enterica* and *Pseudomonas syringae*

Production of E3 ubiquitin ligases by bacteria has been documented previously. For example, Kubori and coworkers (2010) identified a *Legionella pneumophila* effector called LubX that contains a U-box domain and ubiquitinates another bacterial effector, SidH, thereby targeting SidH for destruction by the proteasome. This group addressed the biological significance of the LubX "metaeffector" using a *Drosophila melanogaster* model of *L. pneumophila* infection. A *ΔlubX* mutant showed hyperlethality to flies when compared to wild-type or *ΔsidH L. pneumophila*, and bacterial counts in flies infected with the *ΔlubX* strain were lower than those in flies infected with wild-type. It is possible that the hyperlethality associated with the *ΔlubX* mutant prevents *L. pneumophila* from reaching its maximal infectivity, thereby accounting for the low bacterial counts that were observed. LubX also ubiquitinates the mammalian protein Clk1, which is involved in splice-site selection. Whether or not this ubiquitination results in Clk1 being destroyed by the proteasome, and the role this could play in *L. pneumophila* pathogenesis, is unclear (Kubori *et al*, 2008).

The *L. pneumophila* effector AnkB is also an E3 ubiquitin ligase. AnkB conjugates K48-linked ubiquitin chains to proteins on the surface of the *Legionella* Containing Vacuole, or LCV, which is the intracellular compartment in which *L. pneumophila* lives and replicates. Proteolytic degradation of these ubiquitinated proteins yields a source of amino acids for *L. pneumophila*, and a mutant lacking *ankB* shows growth defects (Price *et al*, 2011).

Salmonella typhimurium encodes four E3 ubiquitin ligases. SspH1 (which is absent from some strains), SspH2 and SlrP are all IpaH-homologues (Hicks and Galán, 2010). SspH1 targets the mammalian protein, but whether or not this effect occurs *in vivo* is unknown **(**Rohde *et al*, 2007, Haraga and Miller, 2006). The consequences of this interaction are discussed in Chapter 1.6. SlrP interacts with the mammalian protein Thioredoxin: a redox protein that reduces a myriad of other proteins (Holmgren and Lu, 2010, Bernal-Bayard *et al*, 2009). A line of HeLa cells expressing *slrP* had a higher rate of death than HeLa cells not expressing *slrP* (Bernal-Bayard *et al*, 2009). SopA is a structural mimic of HECT-domain E3 enzymes. Although the substrates of SopA are unknown, a strain producing a mutant of *sopA* defective for E3 enzyme activity induced lower levels of neutrophil recruitment than wild-type *S. typhimurium* (Hicks and Galán, 2010). Although SopA bears structural resemblance to HECT-domain E3s, the E2 recognition site and the catalytic cysteine are closer together than in eukaryotic HECT E3s. This means that the conformational changes that are thought to occur when E2s bind to eukaryotic HECT domain E3s, which bring ubiquitin into close proximity to the catalytic cysteine, may be unnecessary in the case of SopA. This raises the possibility that SopA belongs to yet another new class of E3 ubiquitin ligases (Diao *et al*, 2008).

SopB, another of *S. typhimurium's* effectors, is not an E3 enzyme, but is monoubiquitinated at multiple sites by a yet-unidentified E3 ubiquitin ligase. SopB produced by a mutant lacking bacterially-encoded E3 ubiquitin ligases is still ubiquitinated, indicating that the protein responsible for this effect is probably encoded by the host (Patel *et al*, 2009). SopB localizes to the plasma membrane early after infection, where it induces actin rearrangements and promotes macropinocytosis (Patel and Galán, 2006, Zhou *et al*, 2001). Later during infection, SopB is monoubiquitinated and moves to the *Salmonella* containing vacuole (SCV), where it is necessary for intracellular replication of *S. typhimurium* (Hernandez *et al*, 2004, Mallo *et al*, 2008). A strain encoding a mutant of *sopB* in which all the lysine residues were mutated, rendering it unable to be ubiquitinated, induces a prolonged period of actin remodeling at the plasma membrane, and a defect in intracellular replication of *S. typhimurium* (Patel *et al*, 2009).

The ability to hijack the ubiquitin pathway is not limited to human pathogens. *Pseudomonas syringae,* is a bacterium that causes bacterial speck disease on tomato and *Arabidopsis* plants (Hicks and Galán, 2010). AvrPtoB is an effector secreted by *P. syringae* that contains a RING-finger domain and has E3 ubiquitin ligase activity (Janjusevic *et al*, 2006). AvrPtoB ubiquitinates Fen kinase (Rosebrock *et al*, 2007), Flagellin-sensing receptor kinase 2 (Göhre *et al*, 2008) and Chitin Elicitor Receptor Kinase 1 (Gimenez-Ibanez *et al*, 2009), which are all involved in plant immunity. The net effect is that AvrPtoB suppresses programmed cell death, thereby promoting survival of *P. syringae* (Janjusevic *et al*, 2006).

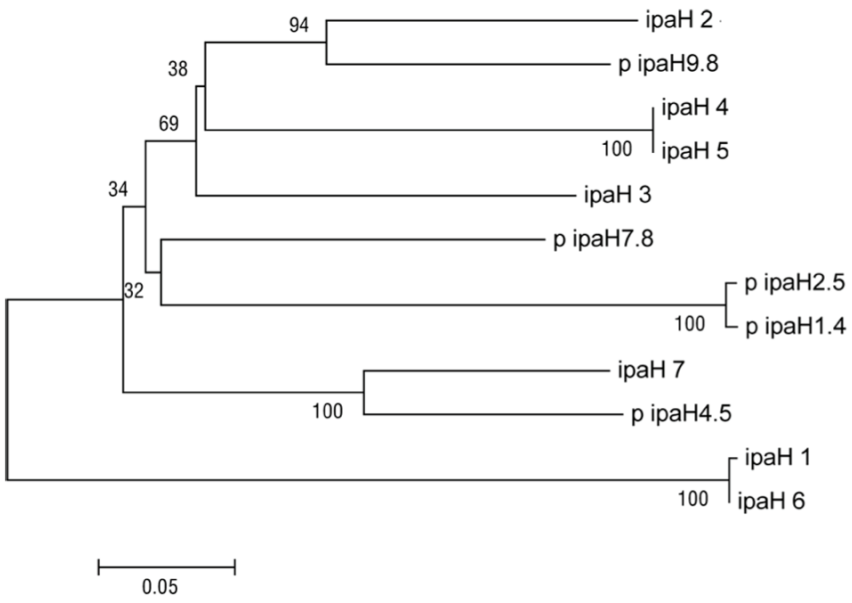

Figure 2: A phylogenetic tree showing the *ipaH* genes from *S. flexneri* serotype 5a (M90T-Sm). This tree was constructed based on the neighbour-joining method using a 515 amino acid data set. Genes found on the virulence plasmid are indicated by a "p" preceding the name of the gene. Bootstrap values are shown at each node, and a measure of genetic distance is given below the tree. This figure was created by Naoko Onodera.

1.6: Substrates and Functions of the IpaHs and Their Homologues

1.6.1: SspH1 Ubiquitinates PKN1 *In Vitro*

Substrates have been reported for IpaH9.8 and its homologue from *Salmonella enterica*, SspH1. SspH1 was shown to interact with the mammalian Protein Kinase N1 (PKN1) before the SspH proteins were known to be ubiquitin ligases (Haraga and Miller, 2006). After its characterization as an E3 enzyme, SspH1 was shown to ubiquitinate PKN1 *in vitro* (Rohde *et al*, 2007).

PKN1 interferes with NF-κB-mediated transcription: an effect also observed in association with SspH1. It seems likely that the interaction between PKN1 and SspH1 causes PKN1 to interfere with the NF-κB signaling pathway during an *S. enterica* infection (Haraga and Miller, 2006). However, questions remain, as proteolytic degradation of PKN1 is not consistent with the theory that SspH1 would somehow enhance this protein's ability to downregulate NF-κB signaling. *In-vivo* ubiquitination of PKN1 by SspH1 has yet to be demonstrated, so perhaps these proteins also interact in a ubiquitin-independent manner. Alternatively, ubiquitination of PKN1 by SspH1 may serve a function other than to target PKN1 for destruction by the proteasome. PKN1 has also been shown to phosphorylate MLTKα: a MAP triple kinase in the p38 MAPK pathway (Takahashi *et al*, 2003). This raises the possibility that SspH1 affects innate immunity through signaling pathways other than NF-κB.

1.6.2: IpaH9.8 Ubiquitinates Ste7 from Yeast and Nemo from Humans

IpaH9.8 was characterized as an E3 ubiquitin ligase following the observation that, when expressed in *Saccharomyces cerevisiae,* IpaH9.8 inhibits a MAP Kinase

pathway necessary to produce mating pheromones. Proteasome-dependent degradation of the MAP Kinase Kinase Ste7 is responsible for this block in production. Although IpaH9.8 ubiquitinates Ste7, its homologue in mammalian cells is not a substrate of IpaH9.8 (Rohde *et al*, 2007). IpaH9.8 was later shown to ubiquitinate and destroy the mammalian protein Nemo (Ashida *et al*, 2009). Nemo is part of the IKK complex, which is part of the pathway that leads to ubiquitination of IκBα, thereby allowing NF-κB to enter the nucleus and serve its function as a transcription factor. The relationship between substrates of SspH1 and IpaH9.8 and the NF-κB and MAP Kinase cascades is reminiscent of the functions of OspG and OspF, which also interfere with these two pathways.

1.6.3: Phenotypes Associated with IpaH7.8

Although a substrate for IpaH7.8 has not been identified, this effector has been reported to play a role in *S. flexneri's* escape from phagocytic vacuoles inside macrophages. Fernandez-Prada *et al* (2000) reported that a *ΔipaH7.8* strain of *S. flexneri* remained in vacuoles longer than wild-type *S. flexneri* after infection of human and murine macrophages. However, this group's results are largely based on a technique involving treating infected macrophages with chloroquin and gentamicin to kill bacteria inside vacuoles and outside cells, respectively, and their results demonstrate that this technique has a high degree of variability. This variability leads the reader to wonder if the group's results are overstated. In addition, Paetzold and coworkers (2007) were unable to replicate the results of Fernandez-Prada's group. However, Paetzold and coworkers noted that a *ΔipaH7.8* mutant was less toxic to macrophages than wild-type *S.*

flexneri, as assessed by release of Lactate Dehydrogenase over the course of three hours. The identification of substrates of IpaH7.8 is one focus of this thesis.

1.7: Protein Microarrays as a Tool for Identifying Substrates of E3 Ubiquitin Ligases

Protein microarrays, or "protoarrays" are glass slides covered in a layer of nitrocellulose with numerous proteins spotted on each slide. Protoarrays covering large portions of the yeast and human proteomes have recently become available from Invitrogen. Dr. Daniela Rotin and her lab at the University of Toronto have pioneered the use of these arrays for the identification of substrate of HECT-domain E3 ubiquitin ligases from the Nedd4 family, which contain a WW protein-protein interaction domain (Gupta *et al*, 2007, Persaud *et al*, 2009), and I have attempted to apply this technology to the identification of targets of IpaH7.8.

1.7.1: Identifying Substrates of Rsp5

The Rotin lab first used Invitrogen's protoarrays to identify novel substrates of the yeast E3 ubiquitin ligase Rsp5 (Gupta *et al*, 2007). This group applied a reconstituted ubiquitination pathway including purified E1, Ubc4 (an E2 enzyme), Rsp5, FITC-labeled Ubiquitin and ATP to protein arrays and interpreted conjugation of FITC-Ubiquitin to a protein on the array as evidence of ubiquitination. Rsp5 is a HECT domain E3, and is known to ubiquitinate proteins containing (L/P)PXY motifs. Gupta *et al* found that whereas only 7% of proteins in the yeast proteome contain (L/P)PXY motifs, 72% of the top 40 proteins from their screen contained these sequences. Moreover, twelve of these 40 proteins had already been implicated as substrates of Rsp5. This screen also identified

20 proteins that had not previously been characterized as substrates of Rsp5. The authors went on to validate one of these substrates *in vivo*.

1.7.2: Identifying Substrates of Nedd4-1 and Nedd4-2

Rsp5 is part of a family of HECT-domain E3 ubiquitin ligases called the Nedd4 family. The Rotin lab has also used protoarray screening to identify substrates of two human Nedd4 family E3s, Nedd4-1 and Nedd4-2, as well as Nedd4-1 from rats. Again, at least half of the top 50 hits for each screen contained an (L/P)PXY motif, and the researchers were able to validate several hits from each screen *in vivo* (Persaud *et al*, 2009). The success achieved by the Rotin group motivated our group to use protoarrays to try to identify substrates of IpaH7.8.

1.8: Research Described in this Thesis

This thesis describes two areas of research: characterization of protein microarrays, or "protoarrays" as a tool for identifying substrates of the IpaHs, and characterization of the *S. flexneri* deletion collection as a tool for studying bacterial pathogenesis. Attempts to confirm putative substrates of IpaH7.8 identified through protoarrays were not successful, and the substrates of IpaH7.8 remain unknown. From this, I conclude that protoarrays are a difficult tool to use for the identification of substrates of bacterial effectors. Because of the association of several putative substrates of IpaH7.8 with autophagy, I also tested the hypothesis that IpaH7.8 plays a role in *S. flexneri's* ability to avoid being destroyed through autophagy in HeLa cells. However, as Chapter 3.2 shows, this is not the case.

The *S. flexneri* deletion collection proved to be a valuable tool for studying effectors secreted by this pathogen. I used the deletion collection in two screens: one in which the ability of seventy eight mutants to elicit IL-8 from U937 cells was assessed, and another in which I looked for *S. flexneri* mutants that differ from wild-type in their ability to bind the dye Congo red. I identified *ΔmxiH, ΔmxiK, ΔospG* and *ΔospB* as mutants that elicit higher levels of IL-8 than wild-type *S. flexneri*. I also identified several mutants for effectors of unknown function that are more Congo red-positive than wild-type *S. flexneri*. Mutants for genes encoding two effectors, IpaH1.4 and OspD2, were more Congo red-negative than mutants for other genes in the same families, indicating that the functions of these effectors may be distinct from other closely-related effectors. Lastly, I identify several cytokines that may be affected by factors encoded by the virulence plasmid.

Chapter 2: Materials and Methods

2.1: Growth and Maintenance of Bacterial Strains, Use of Antibiotics and Construction of Mutants

Shigella flexneri serotype 5a (M90T) was used throughout this study (Allaoui *et al*, 1992). This strain is resistant to streptomycin and is sometimes referred to as "M90T-Sm." I have referred to it as simply M90T in an effort to be consistent with the majority of *S. flexneri* literature. The virulence plasmid encoded by M90T is named "pwr100." Figure 3 shows a representation of the DNA sequence of pwr100. S. *flexneri* was grown overnight at 37°C in 30 mg/mL trypticase soy broth (TSB) when liquid cultures were needed, or on 30 mg/mL TSB with 20 mg/mL agar and 0.01% Congo red when a solid matrix was required. The *Escherichia coli* (*E. coli*) strains DH5α and BL-21 (DE3) were maintained in or on Luria Bertani broth (10 mg/mL tryptone, 5 mg/mL yeast extract and 10 mg/mL sodium chloride) with or without 20 mg/mL agar. Frozen stocks were made by adding 15% glycerol to liquid cultures grown overnight at 37°C, and these stocks were stored at -80°C. When applicable, antibiotics were added to the medium at the following final concentrations:

Table 1 Antibiotic Concentrations

Antibiotic	Final concentration
Ampicillin	100 μg/mL
Gentamicin	5 μg/mL
Kanamycin	25 μg/mL on solid medium or 12.5 μg/mL in liquid medium
Spectinomycin	100 μg/mL
Tetracycline	5 μg/mL
Streptomycin	100 μg/mL
Chloramphenicol	25 μg/mL

Mutant strains included in the *S. flexneri* deletion collection were constructed using λ-red recombination as described in Baba *et al* (2006). Briefly, tetracycline knock-out cassettes were generated by performing PCR using a tetracycline resistance gene characterized by Karlinsey (2007) as template and primers containing 50 nucleotides of the sequence flanking the gene that was to be deleted. These PCR products were electroporated into wild-type *S. flexneri* (M90T) containing the plasmid pKD46 (GenBank Accession number AY048746, Datsenko and Wanner, 2000), which encodes the λ-red recombination machinery from λ phage. The resulting bacteria were grown for two hours in liquid medium at 37°C with shaking at 200 RPM, then plated on medium containing tetracycline to select for bacteria containing the desired deletion mutation. These deletions were confirmed by the ability to amplify a PCR product using a primer inside the tetracycline resistance cassette and a primer in the flanking DNA sequence. Tetracycline resistance cassettes were later removed via the introduction of a plasmid encoding flippase machinery capable of promoting recombination between FRT sites flanking the tetracycline resistance cassette (Cherepanov *et al*, 1995).

All deletions began at the second codon of the gene being deleted and ended before the sixth codon from the end of the gene. After removal of the tet cassette, these two ends of the genes were divided by an 81 nucleotide in-frame scar sequence containing the FRT site and several additional amino acids on each side. The final collection contains one hundred and three mutants out of the approximately 110 genes encoded by the virulence plasmid.

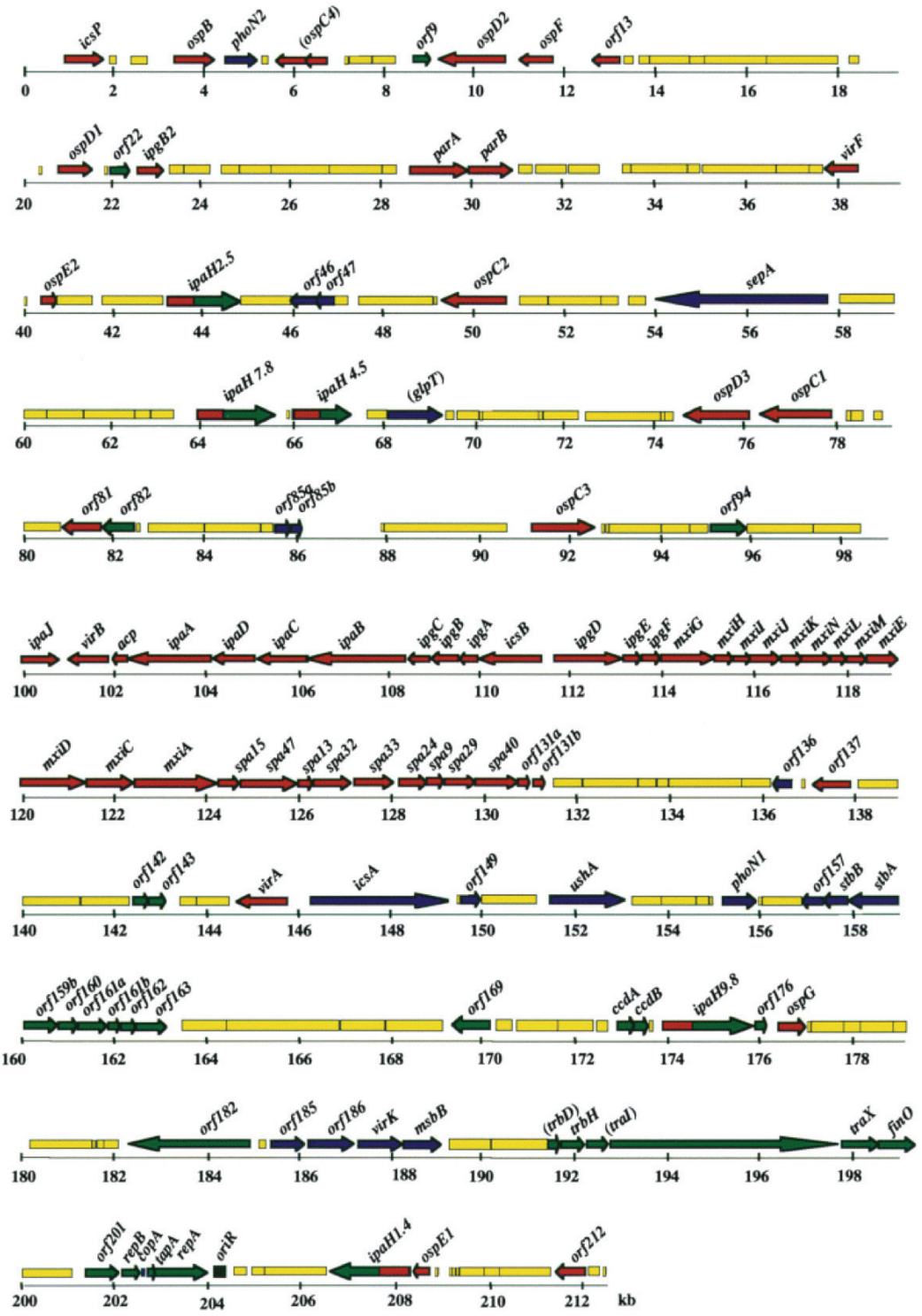

Figure 3: A representation of the DNA sequence of pwr100: the virulence plasmid of *S. flexneri* serotype 5a (M90T). This figure is adapted from Buchrieser *et al* (2000).

2.2: Identifying Putative Targets of IpaH7.8 Using Protoarrays

Protoarray human protein microarrays (Version five) purchased from Invitrogen (Burlington, ON) were used in binding and ubiquitination assays to determine putative substrates of IpaH7.8 and SspH1. These arrays contained approximately 9,483 proteins, each spotted in duplicate. The majority of these proteins were GST-tagged, and were isolated from insect cells. Binding and ubiquitination reactions were performed essentially as described in Persaud and coworkers (2009). Briefly, the arrays were rinsed with 10 mLs of phosphate buffered saline (PBS, Bioshop catalogue number PBS405.1, Burlington, ON), plus 1% Tween-20 (1% PBST) for approximately 1 minute, then incubated with blocking buffer (500 mM hepes pH 7.5, 250 mM sodium chloride, 0.08% triton X-100, 25% glycerol, 20 mM glutathion, 1.5% bovine serum albumin) for thirty minutes at room temperature. Arrays were then incubated with 1X charging buffer (25 mM Tris pH 7.5, 50 mM sodium chloride, 5 mM adenosine triphosphate, 10 mM magnesium chloride, 0.1 mM dithiothreitol) for five minutes at room temperature. Two protoarrays were incubated in the dark with 300 µL of binding reaction mix (50 µg/mL FITC-IpaH7.8 or FITC-SspH1, 1X charging buffer) for one hour. Two protoarrays were incubated with 300 µL ubiquitination reaction mix (19.3 µg/mL E1, 24.1 µg/mL UbcH5b, 28.9 µg/mL IpaH7.8 or SspH1, 28.9 µg/mL FITC-Ubiquitin, 1X charging buffer) for two hours. These incubations were done in the dark. All protoarrays were then washed three times for five minutes with 1% PBST.

Protoarrays were exposed to light of 494 nm, and the fluorescence resulting from conjugation of FITC-labeled ubiquitin (in the case of ubiquitination assays) or FITC-labeled IpaH7.8 or SspH1 (in the case of binding assays) to proteins on the protoarrays was imaged using ProScan Array HT software (Perkin Elmer, Waltham, MA) with a

microarray scanner from Perkin Elmer. An appropriate method of ranking the results from the protoarrays was developed based on sage advice from Dr. Peter Wentzell (Dalhousie University, Department of Chemistry). Briefly, images of the protoarrays were processed using GenePix Pro microarray analysis software (Molecular Devices, Sunnyvale, CA) to determine the median fluorescent intensities of the pixels corresponding to the areas occupied by the proteins on the protoarrays. To correct for the effect of a protein's position on an array, an estimate of the local background fluorescence was subtracted from the median fluorescent value for each protein. These background values were determined from the median fluorescence of a ring around each protein. These rings had diameters three times that of the protein spots, and excluded pixels that were part of neighbouring protein spots as well as pixels immediately outside protein spots.

Because each protein is present in duplicate on each array, the corrected median fluorescent values for each protein were averaged to obtain one value per protein per array. A histogram of these values resembled a normal distribution with a long tail on the end with the highest values. This tail contained between 175 and 300 proteins, depending on the array. The proteins corresponding to these values were considered worthy of consideration. The top 50 results were selected from each array, as 50 was deemed the highest number that might be feasible to analyze. This is consistent with the ranking strategy used by Persaud and coworkers (2009). The top 50 results from each binding assay were compared to each other, those from the two ubiquitination assays were compared, and all four lists were compared. By using two arrays for each screen and only considering proteins that were among the fifty most fluorescent proteins on both arrays, we ensured that the results from these assays were reproducible. Proteins that were

common between the lists were selected to create lists of binding hits, ubiquitination hits, and a high confidence data set, respectively. This method is similar to that used by the Rotin lab to rank the results of their protoarray screens (Persaud *et al*, 2009) except that the Rotin lab was able to normalize their results to account for the amount of protein present on each spot. Unfortunately, we did not have access to a complete set of data regarding protein amount per spot, so we were unable to perform this normalization. The Rotin group used version four of Invitrogen's human protoarrays, whereas we used version five. This discrepancy may account for the difference in availability of information regarding protein amount per spot.

2.3: *In Vitro* Ubiquitination Reactions

In vitro ubiquitination reactions contained the following reagents: E1 (0.5 μg, purchased from Boston Biochem in Cambridge, MA) UbcH5b (An E2 enzyme, 2 μg), IpaH7.8 or IpaH9.8 purified by members of the Rohde lab (approximately 2 μg), FLAG-tagged Ubiquitin purchased from Boston Biochem (1 μg), and various substrate proteins purified by the Rohde lab (see Chapter 2.6 for details). Reactions containing IpaH9.8 and its known substrate, Nemo (Ashida et al, 2010), were also performed. Effectors isolated from *S. flexneri* were sometimes used in place of IpaH7.8 or IpaH9.8. Approximately 1 mg of Ste11-4:Ste7:Kss1 complex was added to these reactions as a positive control when indicated. Five times Charging buffer (25 mM Tris-HCl pH7.5, 50 mM sodium chloride, 5 mM magnesium chloride, 4 mM adenosine triphosphate, 0.25 mM dithiothreitol) was added to a final concentration of 1X. Forty μL reactions were incubated at room temperature for one hour, then stopped with 15 μL of Lamelli buffer (50 mM Tris-HCl pH 6.8, 2% sodium dodecyl sulfate, 100 mM dithiothreitol, 10% glycerol). Reactions

were boiled for five minutes, and then frozen at -20°C or loaded directly on SDS-PAGE gels ranging from 8% to 10% acrylamide, depending on the size of the putative substrate being analyzed.

2.4: *S. flexneri* Effector Isolation

A 2 mL culture of wild-type *S. flexneri* was grown for sixteen hours at 37°C, then sub-cultured into 10 mLs at a ratio of 1:100 and grown at 37°C with shaking at 200 RPM for four hours. This culture was pelleted at 1,800 g for ten minutes at 37°C, then resuspended in 1 mL of PBS. Congo red was added to a final concentration of 150 μg/mL, and the mixture was incubated at 37°C for thirty minutes. The cells were then pelleted at 1,800 g for one minute at room temperature, and the supernatant, which contained the effector proteins, was transferred to a clean tube. Glycerol was added to the effectors to a final concentration of 10%. The effectors were frozen at -20°C for short-term storage (one month or less), or -80°C for long-term storage.

2.5: Cloning Top Hits from Protoarray Screens for Substrates of IpaH7.8

Clones of *rab34*, *cortactin*, *KCNAB1*, *p62*, *tal*, *ANKRD13D*, *UFD1L* and *RIOK3* cDNA were obtained from the sources listed in Table 2. Polymerase chain reaction (PCR) amplification was performed using primers indicated in Table 2 to obtain versions of these genes that lacked stop codons so as to allow the addition of C-terminal histidine tags. These primers also contained *attB* sites to facilitate cloning into Gateway vectors. A RIOK3-encoding plasmid purchased from ATCC already contained *attB* sites, and lacked a stop codon, and so PCR was not necessary in this instance. These PCR products were then cloned into the gateway vector pDONR201, using a BP reaction kit (a tool

allowing recombination between *attB* and *attP* sites found in Gateway entry and donor vectors, respectively) purchased from Invitrogen (catalogue number 11789-020, Burlington, ON). After sequencing, LR reactions (which, similarly to BP reactions, facilitate recombination between the *attL* and *attR* sites that are characteristic of gateway donor and destination vectors, respectively) were performed using an LR reaction kit also purchased from Invitrogen (catalogue number 11791-020) to move these constructs into the Gateway plasmid pET-DEST42, which conjugated a 6X histidine tag to the C-terminal end of each gene. These constructs were transformed into the *E. coli* strain BL-21 (DE3).

Table 2 Reagents used to clone putative substrates of IpaH7.8

Gene	Forward Primer	Reverse Primer	Source of Template Plasmid
Rab34	ggggacaagtttgtacaaa aaagcaggctcgatgaac attctggcacccgt	ggggaccactttgtacaa gaaagctgggtgtgggc aacatgtgggcttct	Invitrogen image clone no. MGC3902651
Cortactin	ggggacaagtttgtacaaa aaagcaggctcgatgtgg aaagcttcagcagg	ggggaccactttgtacaa gaaagctgggtgctgcc gcagctccacatagt	Invitrogen image clone no. MGC3637586
KCNAB1	ggggacaagtttgtacaaa aaagcaggctcgatgcaa gtctccatagcctg	ggggaccactttgtacaa gaaagctgggtgtgatct atagtccttcttgc	University of Toronto SIDNET ID 2061761
P62	ggggacaagtttgtacaaa aaagcaggctcgatggcg tcgctcaccgtgaag	ggggaccactttgtacaa gaaagctgggtgcaacg gcgggggatgctttg	Addgene cat. no. 28027
Tal	ggggacaagtttgtacaaa aaagcaggctcgatgccg ctcttcttccggaag	ggggaccactttgtacaa gaaagctgggtggctgc tgtggtagatgcggag	A gift from Dr. Karen Bedard
ANKRD13D	ggggacaagtttgtacaaa aaagcaggctcgatgtcct gtggtcggctggg	ggggaccactttgtacaa gaaagctgggtggtgct cagtgagtgacagctg	ATCC cat. no. 10436423
UFD1L	ggggacaagtttgtacaaa aaagcaggctcgatgttct ctttcaacatgttcgacc	ggggaccactttgtacaa gaaagctgggtggggct ttcttccctttttacg	ATCC image clone no. MGC13073
RIOK3			Addgene cat. no. 23537
Nemo	ggggacaagtttgtacaaa aaagcaggctcgatgaata ggcacctctggaagag	ggggaccactttgtacaa gaaagctgggtgctcaat gcactccatgacatg	University of Toronto SIDNET ID V106307-1 OCAAP38C4

2.6: Protein Purifications

BL-21 (DE3) *E. coli* was transformed with the plasmid pET-DEST42 containing cDNA corresponding to the protein being purified. Seven hundred and fifty mLs of

culture containing BL-21 (DE3) with the appropriate plasmid were grown to an OD_{600} of approximately 0.6 in the presence of 100 μg/mL ampicillin. Isopropyl β-D-1-thiogalactopyranoside (IPTG) was added to a final concentration of 0.2 mM to activate transcription of the gene encoding the protein to be purified, and the culture was then incubated at 18°C overnight with shaking at 200 RPM. The bacteria were then pelleted at 4,300 g for fifteen minutes at 4°C and resuspended in 25 mLs of buffer A (50 mM Tris-HCl pH 7.4, 200 mM sodium chloride, 5 mM imidazole and 5 mM beta-mercaptoethanol). 150 μL of phenylmethanesulfonylfluoride (PMSF) was added, and the cells were sonicated for four bursts of thirty seconds with one minute rests between bursts. Cell debris were pelleted at 48,000 g for thirty minutes at 4°C, and the supernatant, or crude extract, was transferred to a clean tube.

Two hundred and fifty μL of cobalt resin beads (Thermo Scientific catalogue number 89964, Asheville, NC) was prepared by washing three times in 1 mL of buffer A, and then resuspended in 500 μL of buffer A. The beads were then transferred to the tube containing the *E. coli* crude extract, which was incubated on a rocking platform at 4°C for one hour. The beads were pelleted at 4,300 g for one minute, and then resuspended in 1 mL of buffer A. The beads were washed twice with 1 mL of buffer A, then twice with one mL of buffer A1 (50mM Tris-HCl pH 7.4, 200 mM sodium chloride, 30 mM imidazole, 5 mM beta-mercaptoethanol). Proteins were eluted three times in 500 μL of buffer B (50 mM Tris-HCl pH 7.4, 200 mM sodium chloride, 500 mM imidazole, 5 mM beta-mercaptoethanol). The eluates were pooled and the isolated protein was concentrated using a 10 kD vivaspin dialysis column (GE Healthcare catalogue number 28-9322-25, Charlotte, NC). The concentrated protein was then resuspended in 500 μL of

PBS plus 10% glycerol and stored at -80°C until use. Western blots and silver stained gels used to confirm protein purifications are shown in Figure 4.

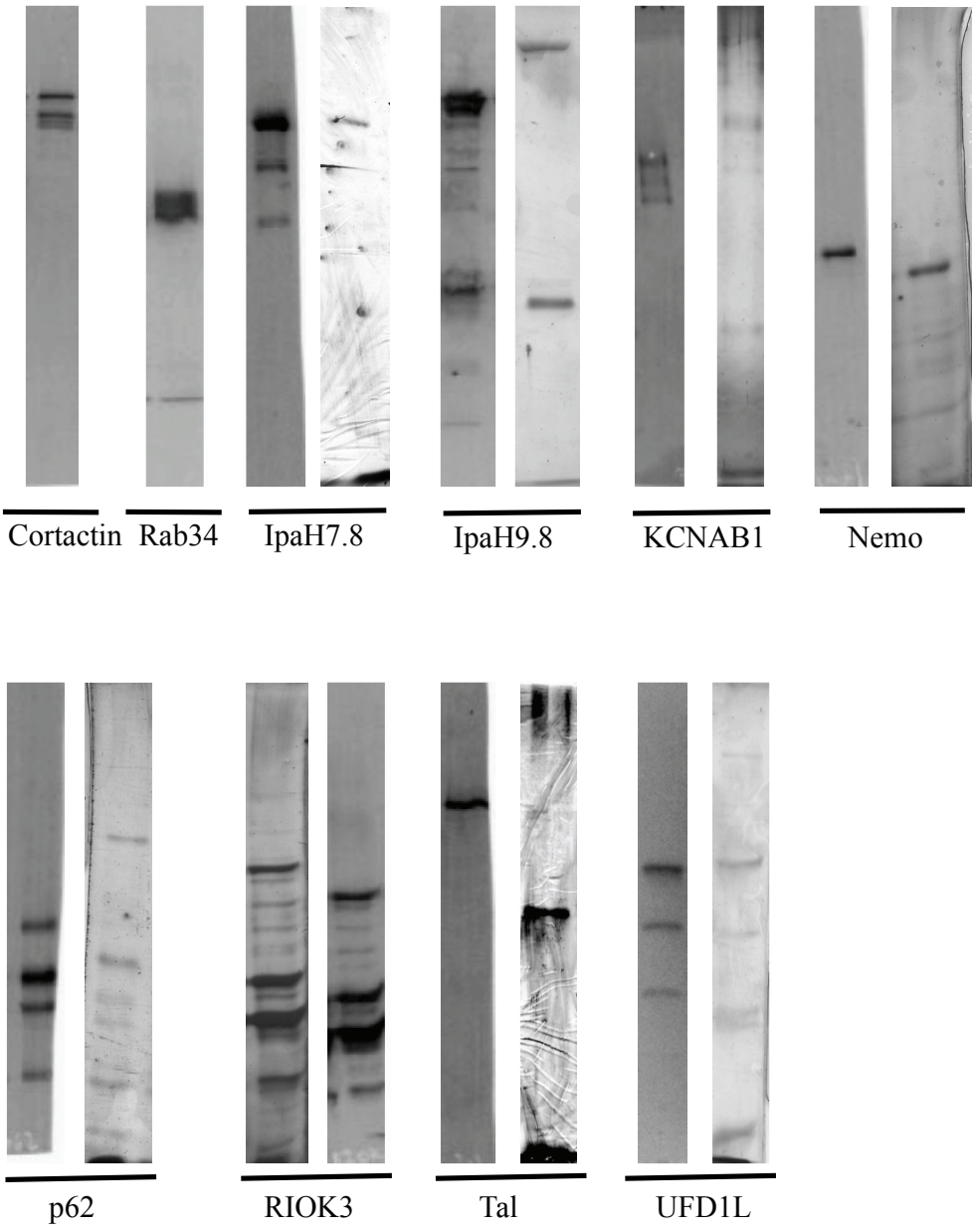

Figure 4: Western blots and silver stained gels are shown for each protein that was purified. In each case, an image of the western blot precedes that of the silver stain. Western blots were performed using antibodies against the purified proteins, except in the cases of RIOK3 and UFD1L when antibodies against the histidine tags fused to these proteins were used. Coomassie stains were performed in place of silver stains for Cortactin and Rab34 purifications, but these images are not shown as the concentrations of the proteins were not high enough for bands to be observed.

2.7: Tissue Culture Maintenance and Infections

HeLa cells were maintained in Dulbecco's Modified Eagle Medium (DMEM, Sigma catalogue number D6429, Oakville, ON) plus 10% Fetal Bovine Serum (FBS) at 37°C with 5% Carbon Dioxide (CO_2). Before infections, HeLa cells were plated in six-well dishes and grown to confluency. HeLa cells were washed three times with DMEM and then given fresh serum free medium approximately one hour before infecting. HeLa cells were infected with 100 µL of a culture of *S. flexneri* grown to an OD_{600} of 0.3, corresponding approximately to a multiplicity of infection of 10. The strains of *S. flexneri* used to infect contained the *E. coli* protein Afimbrial Adhesin E (AfaE) which enhances the ability of *S. flexneri* to adhere to tissue culture cells, thereby expediting infection. HeLa cells were allowed to cool to room temperature for fifteen minutes before infecting, and were left at room temperature for fifteen minutes after infecting to allow bacteria to settle and adhere to the HeLa cells. HeLa cells were then incubated at 37°C with 5% CO_2 until the desired time points. Cells were then washed with 500 µL of PBS and then resuspended in 500 µL of Lamelli Buffer (50 mM Tris-HCl pH 6.8, 2% sodium dodecyl sulfate, 100 mM dithiothreitol, 10% glycerol). HeLa cells were removed from 6-well dishes using cell scrapers, then boiled for five minutes and stored at -20°C until use.

HT-29 cells were maintained in DMEM plus 15% FBS and U937 cells were maintained in Roswell Park Memorial Institute medium (RPMI-1640, Sigma catalogue number R8758) plus 10% FBS and 2 mM glutamine. HT-29 cells were seeded in six-well dishes and grown to confluency before infection. U937 cells were activated by being exposed to 60 pg/mL phorbol 12-myristate 13-acetate (PMA) and incubated at 37°C with 5% CO_2 for ten minutes and then seeded at a density of $4x10^6$ cells/well in a six-well dish

sixteen to twenty hours before infection. Both cell types were given fresh serum-free medium approximately one hour before infection. The same infection protocol used for HeLa cells was then used to infect HT-29 and U937 cells.

2.8: Gentamicin Protection Assays

Cells were infected for one hour, then the medium was removed and replaced with medium containing 50 μg/mL gentamicin, which will kill external *S. flexneri* without penetrating mammalian cells at this concentration. Cells were incubated at 37°C for an additional thirty minutes, then the media was removed, the cells were washed with 500 μL of PBS, then the cells were lysed with 500 μL of lysis buffer (0.1% NP-40, 50 mM Tris-HCl pH 7.5, 5 mM Ethylenediaminetetraacetic acid (EDTA), 10% glycerol, 100 mM sodium chloride). Eight one-in-ten serial dilutions of the cell lysate were made using TSB as diluent. Fifty μL of each dilution was plated on a Congo red TSB agar plate and incubated overnight at 37°C. A dilution containing between thirty and one hundred colonies was selected and the colonies were counted.

2.9: Immunoprecipitations of Putative Substrates from Caco-2 and U937 Cells

Twelve 8.5 cm diameter cell culture plates were seeded with Caco-2 cells and grown to confluency or seeded with 8.25 x 10^7 U937 cells activated with phorbol myristate acetate (PMA, see Chapter 2.7 for details). Cells were given fresh serum-containing medium and allowed to cool to room temperature for fifteen minutes prior to infection. Wild-type and *ΔmxiE S. flexneri* was grown to an OD_{600} of approximately 0.3, and 500 μL of M90T was added to six of the twelve cell culture plates and 500 μL of *ΔmxiE S. flexneri* was added to the other six plates. The plates were incubated at 37°C

with 5% CO_2 for four hours. All cells and buffers were kept on ice for the remainder of the protocol. Cells were lysed with 2 mLs of CLB3 buffer (0.05 M Tris-HCl pH 7.4, 100 mM sodium chloride, 5 mM EDTA, 0.1% NP-40, 10% glycerol with one protease inhibitor tablet (catalogue number 05892791001, Roche, Laval, QC) added to 10 mLs of buffer). Cells were then scraped from the plates and transferred to clean tubes, where they were incubated in the CLB3 buffer for thirty minutes. Cell debris was pelleted at 23,500 g for twenty minutes at 4°C, and the supernatant (or crude extract) was transferred to clean tubes. Two point five µL of benzonase nuclease (Sigma catalogue number E1014-5KU) was added to each millilitre of crude extract to degrade nucleic acids, and the mixture was incubated on ice for five minutes. The samples were then centrifuged at 23,500 g for twenty minutes at 4°C and the supernatant was transferred to a clean tube. Fifty µL of 10% formalin-fixed *Staphylococcus aureus* (*S. aureus)* was added to each millilitre of cell lysate, and the mixture was incubated at 4°C for thirty minutes with constant agitation to absorb proteins that bind non-specifically to Protein A on the surface of *S. aureus*. The *S. aureus* was pelleted at 23,500 g for one minute at 4°C, and the supernatant was transferred to a clean tube. Five µL (approximately 5 µg) of antibody corresponding to the protein being immunoprecipitated was added to the supernatant, and this mixture was incubated on ice for one hour. Fifty µL of 10% *S. aureus* was added to each milliliter of sample to allow binding of the antibody to Protein A, and the mixture was incubated at 4°C for one hour with constant agitation. The samples were then spun at 23,500 g for one minute at 4°C, and the supernatant was removed. The pellet was washed with 500 µL of wash 1 (10 mM Tris-HCl pH 8.0, 1 M sodium chloride, 0.1% NP-40, one Roche tablet per 10 mLs) followed by 500 µL of wash 2 (10 mM Tris-HCl pH 8.0, 0.1 M sodium chloride, 0.1% NP-40, 0.1% sodium dodecyl sulfate, one Roche tablet per 10

mLs) and 500 µL of wash 3 (10 mM Tris pH 8.0, 0.1% NP-40, one Roche tablet per 10 mLs). The samples were then washed with 500 µL of RIPA buffer (10 mM Tris-HCl pH 8.0, 100 mM EDTA, 1% NP-40, 0.5% sodium deoxycholate, 1% sodium dodecyl sulfate, one Roche tablet per 10 mLs) and resuspended in 500 µL of Lamelli buffer. The samples were incubated at 37°C for ten minutes, and the *S. aureus* was then pelleted at 23,500 g for one minute. The supernatants, containing immunoprecipitated proteins, were transferred to clean tubes and stored at -80°C until use.

2.10: Cytokine Collection and Analysis

U937 cells were activated using PMA to allow the cells to differentiate and become macrophage-like cells (see Chapter 2.7 for details) and seeded in six-well dishes (10^6 cells per well) or 96-well dishes (6.25×10^4 cells per well) approximately four hours before infecting. One hour before infecting, the medium was removed and fresh RPMI-1640 containing 10% FBS, 2 mM glutamine, 100 µg/mL soybean trypsin inhibitor and 1 mM HEPES was added. *S. flexneri* strains were grown to an OD_{600} of approximately 0.3, then diluted 1 in 100 (if infecting in six-well plates) or 1 in 1600 (if infecting in 96-well plates) using TSB as diluent and 10 µL of *S. flexneri* culture was added to each well of U937 cells. This corresponds approximately to a multiplicity of infection of 0.01. Cells were incubated at 37°C with 5% CO_2 for sixteen hours. Medium was collected and centrifuged at 500 g for ten minutes, then transferred to clean tubes to remove residual U937 cells and *S. flexneri*. Chloramphenicol and gentamicin were then added to final concentrations of 50 µg/mL and 10 µg/mL, respectively. Samples were stored at -80°C until use.

RayBio human cytokine array number three and RayBio human chemokine array were purchased from RayBiotech, Inc (Norcross, GA). Luminex beads were purchased from Millipore (Billerica, MA). In both cases, assays were performed using the kits' recommendations. Briefly, Luminex is a process that involves applying a sample containing cytokines to beads conjugated to antibodies against these cytokines. These beads fluoresce, allowing them to be sorted in a way similar to fluorescent-activated cell sorting (FACS). The feasibility of sorting allows for multiplexed analysis, with beads conjugated to antibodies against multiple cytokines analyzed in the same well of a 96-well dish. RayBio cytokine arrays contain antibodies against numerous cytokines immobilized on nitrocellulose membranes. Samples containing cytokines can be applied to these membranes, and the cytokines will bind to their respective antibody spots. After treatment with a biotinylated secondary antibody, these arrays can be developed using labeled Streptavidin and developed using X-ray film. Densitometry was performed using Quantity One software from BioRad (Mississauga, ON) to quantify cytokine levels on RayBio arrays. Criteria for identifying significant results were that the spots representing the cytokines had to have densities at least 10% greater than the background density value, and there had to be at least a 1.5-fold difference in density between treatment groups. The IL-8 ELISA kit was purchased from R&D Systems. ELISAs were performed in plates purchased from Corning, Inc (catalogue number 3690, Corning, NY) using the kit's protocol, with the exceptions that the coating antibody was diluted in sodium bicarbonate coating buffer (100 mM sodium bicarbonate, 500 mM sodium chloride, pH 8.3) instead of PBS, and the plates were incubated with the samples at 4°C overnight instead of two hours at room temperature. ELISAs were developed using an

amplification kit from Invitrogen (catalogue number 19589-019) and read using a Benchmark Plus plate reader from BioRad.

2.11: Trypan Blue Staining

Trypan blue exclusion was used to determine the number of live and dead cells after infecting U937 cells for cytokine analysis. Trypan blue staining was also used before seeding cells in cell culture dishes to ensure that the majority of the cells were alive. Cells were resuspended in PBS, then 20 µL of resuspended cells were mixed with 20 µL of trypan blue (Thermo Scientific, catalogue number SV30084.01). Cells were then counted using a hemocytometer (catalogue number 0267110, Fisher Scientific, Ottawa, ON).

2.12: Generation and Transformation Calcium Competent DH5α and Electrocompetent *S. flexneri*

Five hundred mLs of DH5α or *S. flexneri* cells were grown to an OD_{600} of 0.6, then pelleted at 5000 g and 4°C for 15 minutes and resuspended in 50 mLs of cold 100 mM calcium chloride, in the case of DH5α, or cold water, in the case of *S. flexneri*. Cells were pelleted again under the same conditions and resuspended in 5mLs of their respective solutions plus 15% glycerol. 100 µL aliquots were frozen at -80°C until use.

When it was necessary to transform a plasmid into DH5α or *S. flexneri*, an aliquot was removed from the freezer and thawed on ice. The desired amount of plasmid was added to the cells. DH5α. cells were incubated on ice for twenty minutes, and *S. flexneri* was electroporated immediately. DH5α cells were then heat shocked at 42°C for forty five seconds and incubated on ice for an additional two minutes. *S. flexneri* cells were

electroporated at 2.5V. The cells were added to 1 mL of LB broth, in the case of DH5α, and TSB broth, in the case of *S. flexneri,* and incubated at 37°C with shaking at 200 RPM for one to two hours. The cells were plated on LB or TSB agar plates containing an appropriate antibiotic for plasmid selection.

2.13: Plasmid Preps

A culture of DH5α containing the desired plasmid was grown at 37°C with shaking at 200 RPM for approximately sixteen hours. One and a half mL of the culture was pelleted at 12,000 g for one minute, then resuspended in 100 µL of cell resuspension buffer (1% ethylene glycol, 1 mM sodium azide, 10 mM Tris-HCl pH 8.0). One hundred and fifty µL of lysis buffer (2% sodium dodecyl sulfate, 0.15 M sodium hydroxide, 0.025 M sodium iodate, 10 mM EDTA) was then added to the resuspended cells, and the mixture was incubated at room temperature for four minutes. The lysis was then stopped by the addition of 200 µL of Acid Iodide Precipitate (2.5 M cesium chloride, 0.25 M tartaric acid, 0.25 M sodium iodide) Cell debris were pelleted at 12,000 g for one minute, and the supernatant was transferred to a new tube containing 200 µL of PEG-ethanolamine (37% polyethylene glycol, 4 M monoethanolamine). This mixture was incubated at room temperature for 5 minutes, then the DNA was pelleted at 12,000 g for 5 minutes. The supernatant was discarded, and the pellet was washed three times with isopropanol. The pellet was then allowed to dry, and resuspended in 50 µL of water. Minipreps were stored at -20°C until use. (Huitema, 2012)

2.14: Cloning *ipaH7.8, ipaH7.8 C357A* and *orf186*

IpaH7.8 was cloned into the plasmid pGEM-T Easy, which was acquired as part of a pGEM cloning kit (Promega catalogue number A1360, Madison, WI). Cloning was performed following instructions from the manufacturer. Briefly, PCR using Taq DNA Polymerase (New England Biolabs, Pickering, ON, catalogue number M0267L) and the primers *ipaH7.8*-for and *ipaH7.8*-rev (Table 3) was performed. One colony of M90T *S. flexneri* was suspended in 100 µL of water, and 1 µL was used as template in each 25 µL PCR reaction. Taq DNA polymerase leaves an additional adenosine molecule at the 3' end of a synthesized strand of DNA, resulting in "A-overhangs." (Clark, 1988) These hybridize with "T-overhangs" at the 3' ends of linearized pGEM-T Easy. DNA ligase supplied with the kit was added to a reaction containing the PCR product and linear pGEM-T Easy, and the reaction was incubated at 4°C for approximately 16 hours. The ligated plasmid was then transformed into calcium-competent DH5α as described in Chapter 2.12.

A clone of *ipaH7.8* in which the nucleotides encoding a cysteine at amino acid position 357 were mutated to encode an alanine was generated using a Stratagene QuikChange Site Directed Mutagenesis kit (Stratagene catalogue number 200519, Santa Clara, CA) with ipaH7.8-pGEM-T Easy used as a template plasmid. Again, cloning was performed according to the manufacturer's instructions. Briefly, PCR was performed using the primers *ipaH7.8*-C357A-for and *ipaH7.8*-C357A-rev (table 3) and *ipaH7.8*-pGEM-T Easy as template**.** The PCR product was purified using a Qiagen gel extraction kit (Toronto, ON, catalogue number 28704) and then digested using the restriction enzyme Dpn1 to degrade methylated (i.e., template) plasmid. The reactions were then transformed into calcium competent DH5α.

Orf186 was cloned into the Xbal and SalI sites of pBluescript II SK+. PCR amplification was performed using the primers indicated in Table 3. Digestions were performed using the appropriate enzymes from New England Biolabs, and then ligated using T4 DNA ligase (New England Biolabs catalogue number M0202L). The ligation reaction was incubated at 4°C overnight, then transformed directly into *S. flexneri*.

All plasmids constructed as part of this study were sequenced by Genewiz, Inc (South Plainfield, NJ).

Table 3 *ipaH7.8* and *orf186* cloning primers

Construct	Forward Primer	Reverse Primer
ipaH7.8-pGEM-T Easy	tcatttaactcattactgtctcgatattc	ctttatccagtcatacaaggactt
ipaH7.8-C357A-pGEM-T Easy	gatgccactgagagcgctgaggaccgtg tcgcgc	gcgcgacacggtcctcagcgctctcagtggcatc
orf186-pBluescript II SK+	gaattctctagatatgaatatactattta cggaatcatcaccg	ctcgaggtcgacttacttgtgcttcgctaatgt gag

2.15: Stable Cell Lines

The Retro-X tet-off Advanced inducible expression system from Clontech (Mountain View, CA) was used in an attempt to create HeLa cells expressing *ipaH7.8*. ϕNX cells (Kinsella and Nolan, 1996) were transfected with the plasmid pRetroX-Tet-Off-Advanced using polyethylenimine (PEI) transfection reagent. Supernatant, containing Tet-Off-Advanced viral particles, was collected from these cells three days later. HeLa cells were transduced with the Tet-Off-Advanced virus by applying supernatant from the ϕNX cells to the HeLa cells in the presence of 5 μg/mL polybrene and centrifuging for two hours at 500 g. G418 was added at a concentration of 1 mg/mL twenty four hours later to select for transduced cells. Selection was maintained until

G418-sensitive HeLa cells were dead (approximately five days), and then the level of G418 was reduced to 100 μg/mL. These Tet-off HeLa cells were maintained in 100 ng/mL doxycycline to prevent binding of the tTA-advanced transactivator protein encoded by pRetroX-Tet-Off Advanced to tet operator sequences. These tet-off HeLa cells were then used to regulate expression of response vectors. The efficacy of the Tet activator protein was tested by transducing tet-off HeLa cells with a virus encoding the pRetroX-Tight-Pur-Luc response vector, which encodes luciferase under the control of the tet operator sequence, and measuring the amount of luciferase produced when doxycycline was removed from the cells. pRetroX-Tight-Pur-Luc virus was made as described above for pRetroX-Tet-Off-Advanced. A Dual Luciferase Reporter Assay system from Promega (Catalogue number E1910, Madison, WI) was used to assess production of Luciferase.

ipaH7.8 and a mutant in which the cysteine at position 357 was mutated to alanine were cloned into pRetroX-Tight-Pur, with and without FLAG tags, using primers described in Table 4. The strains M90T and DH5α transformed with the *ipaH7.8-C357*-pGEM-T Easy plasmid (Chapter 2.14) were used as template for the colony PCR required for this cloning. Viruses encoding these constructs were made as described for the Tet-Off-Advanced virus. Tet-Off HeLa cells were transduced with these viruses as described above for transduction with the Tet-Off-Advanced virus. Selection was performed starting twenty four hours after transduction using 1 μg/mL puromycin. After a well of puromycin-sensitive HeLa cells was dead (approximately two days later), the level of puromycin was reduced to 0.25 μg/mL. Doxycycline was removed, and IpaH7.8 levels were assessed two days later by western blot (See Chapter 2.17 for details).

Tet-off HeLa cells were also transiently transfected with *ipaH7.8* cloned into the Not1 and Apa1 sites of pcDNA3. Tet-off HeLa cells were seeded in a six-well dish and grown to approximately 70% confluency. The cells were then transfected with 2 μg of DNA per well using Fugene transfection reagent (Promega catalogue number E2311). Twenty four hours later, cells were lysed and levels of IpaH7.8 were assessed by western blot.

Table 4 Primers used to create an *ipaH7.8*-expressing HeLa cell line

Construct	Forward Primer	Reverse Primer
ipaH7.8-pRetroX-Tight-Pur and ipaH7.8-C357A-pRetroX-Tight-Pur	GGATCCGCGGCCGC ATGTTCTCTGTAAAT AATACACACTCATCA G	ACGCGTGAATTCTTA TGAATGGTGCAGTCG TGAGC
ipaH7.8-FLAG-pRetroX-Tight-Pur and ipaH7.8-C357A-FLAG-pRetroX-Tight-Pur	GGATCCGCGGCCGC ATGTTCTCTGTAAAT AATACACACTCATCA G	ACGCGTGAATTCTTA CTACTTATCATCATC ATCCTTGTAATCTGA ATGGTGCAGTCGTGA GC

2.16: Fluorescent Microscopy

HeLa cells were seeded on 2.2 cm diameter cover slips in 12-well plates for 24 hours prior to infection. Cells were given fresh medium three hours before infection with *S. flexneri*. *S. flexneri* strains containing the plasmid pmCherry (Clontech catalogue number 632522) and expressing the *E. coli* adhesin AfaE were grown to an OD_{600} of approximately 0.3, and 200 μL of culture was added to HeLa cells that had been allowed to cool to room temperature for fifteen minutes. The HeLa cells were incubated at room temperature for an additional fifteen minutes, then transferred to 37°C, where they were incubated until the desired time points.

Cover slips onto which HeLa cells had been seeded were washed twice in cold PBS after infection, then incubated in 4% paraformaldehyde/PBS for ten minutes on ice. Cover slips were washed three times in PBS and mounted on slides using Prolong Gold antifade mounting media (Invitrogen catalogue number P36930). Slides were analyzed using a Zeiss Axiovert microscope.

2.17: Polyacrylamide Gel Electrophoresis, Silver Staining and Western Blotting

Polyacrylamide gels were poured using the protocol found in Sambrook and Russell (2001) and gel casters purchased from Hoefer (Holliston, MA). Gels were run at 150V and transferred at either 0.5 A overnight or 1.5 A for two hours to polyvinylidene fluoride (PVDF) using a wet transfer apparatus purchased from Hoefer. Silver Stains were performed using a BioRad silver staining kit (catalogue number 161-04499). All steps were performed according to the kit's instructions.

Western blots were performed at room temperature with rocking. Membranes were blocked in 5% skim milk powder in tris buffered saline with tween-20 (TBST, 145 mM sodium chloride, 5 mM Tris-HCl pH 7.5, 0.1% Tween-20) for one hour, or, if it was convenient, overnight at 4°C. Primary antibodies were applied to the membranes and incubated for an additional hour. Antibody purchasing information and dilution factors can be found in Table 5. Diluent for all antibodies was 5% skim milk powder in TBST. Membranes were then washed four times for five minutes each time in TBST and incubated in secondary antibodies conjugated to horseradish peroxidase for one hour. Membranes were again washed four times for five minutes in TBST, then developed using ECL+ development reagent purchased from GE Healthcare (catalogue number

RPN2132) which interacts with horseradish peroxidases to produce a fluorescent substance that was imaged using a VersaDoc imaging system from BioRad.

Table 5 Antibody concentrations and purchasing information

Antibody	Dilution	Source
Flag	1:1000	Sigma cat. no. F1804
Ubiquitin	1:5000	Millipore cat. no. 662099
Tal	1:2000	Sigma T1200
Rab34	1:500	Abcam cat. no. 73383
KCNAB1	1:1000	Santa Cruz cat. no. sc-51106
Nemo	1:500	New England Bioloabs cat. no. 2685
Phos-ERK	1:500	Cell Signaling cat. no. 4377
Penta-His	1:2000	Qiagen cat. no. 34660
IpaH	1:1000	A gift from Régis Tournebize (Mavris *et al*, 2002)
Actin	1:2000	Cell Signaling cat. no. 4967
IκBα	1:400	Santa Cruz cat. no SC-371
Cortactin	1:1000	Millipore cat. no. 05-180
P62	1:1000	BD Bioscience cat. no. 610497
LC3	1:5000	Sigma cat. no. 7543
Mouse IgG	1:2000	New England Biolabs cat. no. 7076
Rabbit IgG	1:2000	New England Biolabs cat. no. 7074
Goat IgG	1:10,000	Sigma cat. no. A8919-2mL

2.18: Congo Red Assay

Ninety six strains from the *S. flexneri* M90T deletion collection (Onodera *et al*, submitted to Journal of Bacteriology) were pinned onto 14 cm diameter, round Congo red TSB plates in triplicate. Strains were pinned in different locations on each plate to avoid edge effects. As controls, the same ninety six strains were pinned onto Luria broth plates without Congo red, and ninety four strains from the Keio *E. coli* deletion collection were pinned onto a Congo red TSB plate. All strains were grown for sixteen hours at 37°C.

These plates were imaged using a VersaDoc imaging system from BioRad with an excitation wavelength of 430 nm and an emission wavelength of 503 nm. Densitometry was performed using Image Lab software from BioRad.

2.19: Statistical Methods

The IL-8 ELISA results shown in Figure 15 were analyzed using a variety of statistical methods. In all cases, the level of IL-8 produced by uninfected control U937 cells, which was approximately ten-fold less than that produced by M90T-infected cells, was subtracted from the levels produced by infected strains. Results from infections with *ΔmxiH* and *Δorf186* strains (Figure 15C) failed a test for normality, and so these data were analyzed using a nonparametric Friedman test followed by a Dunn's test. Results from infections with *Δorf186,* M90T and *Δorf186 porf186* were assumed to be normally distributed, although the number of replicates was not high enough to confirm this assumption. These data were analyzed using a one-way ANOVA followed by a Dunnett's test. Results shown in Figures 15A and B were not analyzed statistically due to their small sample sizes.

Chapter 3: Results

3.1: Using Protein Arrays to Identify Substrates of IpaHs.

3.1.1: Potential Targets of IpaH7.8 Include Cortactin, KCNAB1, Rab34, p62 and Tal.

Conventional methods for identifying protein-protein interactions, such as yeast-two-hybrid screens, are difficult to use for the purpose of identifying substrates of E3 ubiquitin ligases because a salient role of ubiquitination is to target proteins for destruction by the proteasome, rendering them undetectable. To avoid this difficulty, we used protoarrays to identify putative targets of IpaH7.8. Protoarrays are nitrocellulose-coated glass chips to which many proteins, in this case approximately 9,000 human proteins, most of which are involved in signaling cascades, have been applied. The protocol used is outlined in Figure 5A, and described in detail in the Materials and Methods. Briefly, IpaH7.8 was applied to protoarrays as a component of two assays: a binding assay, used to identify proteins to which IpaH7.8 can bind, and a ubiquitination assay, used to identify proteins that IpaH7.8 can ubiquitinate.

The results of binding and ubiquitination screens, as well as a high-confidence data set showing results obtained from both screens, are listed in Tables 6, 7 and 8. Tables 6 and 7 also show Z-scores as an indication of the fluorescent intensity of the proteins that are listed. A Z-score is defined as the number of standard deviation above the mean of a particular data point. Selected results that were chosen for follow-up are also described in Figure 5B. I chose to focus my efforts on validating five of these

putative substrates: Cortactin, KCNAB1, p62, Tsg101-Associated Ligase, or Tal, and Rab34. Tal is also referred to as "LRSAM1" by some groups, and p62 as "sequestosome-1, or SQSTM-1." P62 should not be confused with the nucleoporin that goes by the same name. Cortactin and KCNAB1 were present in the high-confidence data set. Tal and p62 were identified through the ubiquitination screen, and Rab34 was identified through the binding screen. Screens for substrates of an IpaH-homologue from *Salmonella enterica,* known as SspH1, were also performed. The ubiquitination screen identified PKN1, a known substrate of SspH1 (Haraga and Miller, 2006), thereby indicating that protoarrays can be used to identify substrates of IpaH-family E3 ubiquitin ligases.

Cortactin plays a role in actin polymerization and re-arrangement, is enriched in membrane ruffles, and may play a role in *S. flexneri's* invasion of epithelial cells (Dehio *et al*, 1995). Cortactin is also involved in building the actin scaffolding that links phagosomes with lysosomes (Lee *et al*, 2010): an activity *S. flexneri* might benefit from preventing, as some bacteria are destroyed by phagolysosomes. These previously-known links between Cortactin and bacterial pathogenesis, along with the commercially-available reagents for studying this protein, made it an attractive candidate for validation.

KCNAB1 is an accessory protein for a voltage-gated potassium channel (Shi *et al*, 1996). KCNAB1 was one of the top results in the protoarray screen for substrates of SspH1 as well as IpaH7.8. In addition, Persaud and coworkers (2009) identified KCNAB1 as a possible substrate of human Nedd4-2. This may mean that KCNAB1 is a "sticky protein" in this type of assay, meaning it is able to bind non-specifically to many proteins and will turn up in most protoarray screens, or it may mean that many IpaH-family E3 ubiquitin ligases target KCNAB1. Although we suspected the former of being true, I decided to follow up on KCNAB1, as well.

p62, also sometimes known as Sequestosome-1, is an adaptor that links ubiquitinated proteins, organelles and pathogens with autophagosomes: a useful tool for a eukaryotic cell trying to clear an infection (Zheng et al, 2009). p62 also promotes K63-linked ubiquitination of TRAF6, which activates the NF-κB cascade: a signaling pathway that is central to many innate immune responses (Wooten et al, 2005). Considering p62's strong link to innate immunity, we found it easy to imagine *S. flexneri* targeting p62 for destruction by the proteasome, thereby promoting its own survival. Therefore, I chose to follow up on p62.

Roles in vesicle transport and autophagy were common factors among many of the results from the screens for substrates of IpaH7.8. Because Fernandez-Prada and coworkers (2000) found a relationship between IpaH7.8 and escape from the phagocytic vacuole, we were intrigued by this relationship among the hits from the protoarrays. As stated above, p62 and Cortactin follow this trend. The last two results selected for follow-up, Tal and Rab34, were chosen because they also fit this theme. KCNAB1 does not have a known relationship to autophagy or vesicle transport, and in fact may be an artifact related to the type of screen performed, but ignoring the top hit from several different screens for substrates of IpaH-family proteins seemed inadvisable, and so we chose to follow up on KCNAB1, as well.

Tal is an E3 ubiquitin ligase that monoubiquitinates a protein named Tsg101. Unlike polyubiquitination, monoubiquitination does not target proteins for degradation by the proteasome. In this case, monoubiquitination deactivates Tsg101, thereby preventing it from fulfilling its normal responsibility for sorting ubiquitinated proteins originating from the golgi or the plasma membrane to the lysosome (Amit *et al*, 2004). Recently, Ng and coworkers (2011) showed that reducing levels of Tal in HeLa cells infected with *S.*

typhimurium resulted in lower rates of autophagy of *S. typhimurium*. This indicates that Tal plays a role in the innate immune response to bacterial infection. Tsg101 has also been implicated in the budding of some viruses, such as Human Immunodeficiency Virus (Martin-Serrano, 2007), and therefore its potential to play a role in pathology has already been established.

Rab34, like other Rabs, binds to vesicles and acts like an address, targeting the vesicles to their proper destinations within cells. Specifically, Rab34 colocalizes with membrane ruffles and transports large materials into the cell from the extracellular space in a process known as "macropinocytosis." (Sun *et al*, 2003). Four Rabs are present in our list of hits from the binding assay. I chose to focus on Rab34 over the others because a high-quality antibody for Rab34 was readily available, whereas functional antibodies against the other three proved harder to find.

A

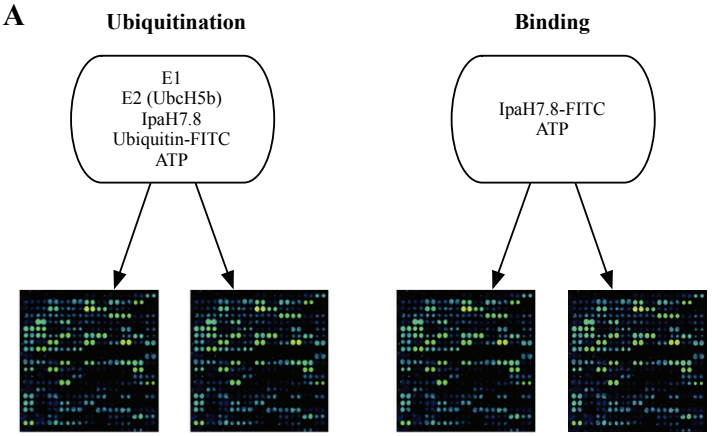

B

Hit Selected for Follow-Up	Identified Through Ubiquitination Screen?	Identified Through Binding Screen?	Gene Ontogeny Function
KCNAB1	Yes	Yes	Synaptic Transmission[1]
p62	Yes	No	Endosome Transport, Macroautophagy and Ubiquitin-Dependent Protein Catabolism.[1]
Rab34	No	Yes	Protein Transport and Small GTPase Mediated Signal Transduction[1]
Cortactin	Yes	Yes	Actin Polymerization and Rearrangement[2]
Tal	Yes	No	Negative Regulation of Endocytosis, Protein Polyubiquitination and Protein Transport.[1]

Figure 5: Procedure for **(A)** and selected results from **(B)** protoarray screens for substrates of IpaH7.8.

1: UniProt. "Protein Knowledgebase" http://www.uniprot.org/uniprot/ (Accessed Jan. 19, 2012)
2: Dehio *et al*, 1995

Table 6 Results from a screen for binding partners of IpaH7.8

Binding Hits	Z score	Genbank Accession number
cortactin (CTTN), transcript variant 2	18.4	NM_138565.1
potassium voltage-gated channel, shaker-related subfamily, beta member 1 (KCNAB1), transcript variant 1	14.1	NM_172160.1
spleen tyrosine kinase (SYK)	6.5	NM_003177.3
RAB7, member RAS oncogene family-like 1 (RAB7L1)	5.9	NM_005825.2
RAS guanyl releasing protein 2 (calcium and DAG-regulated) (RASGRP2), transcript variant 1	5.7	NM_005825.2
Uncharacterized protein LOC120376	5.3	XM_071712.11
piccolo (presynaptic cytomatrix protein) (PCLO)	5.2	BC001304.1
ATP synthase mitochondrial F1 complex assembly factor 2 (ATPAF2), nuclear gene encoding mitochondrial protein	5	NM_145691.3
RAB32, member RAS oncogene family (RAB32)	5	NM_006834.2
zinc finger protein 239 (ZNF239)	4.9	BC026030.1
RAS-like, family 11, member B (RASL11B)	4.9	NM_023940.1
Proline-rich protein 16	4.9	BC038838.1
sciellin (SCEL)	4.8	BC020726.1
zinc finger protein 650 (ZNF650)	4.8	NM_172070.2
CCR4-NOT transcription complex, subunit 8 (CNOT8)	4.7	NM_004779.4
Bone morphogenetic protein receptor type-1A	4.7	NM_004329.1
trafficking protein particle complex 2 (TRAPPC2), transcript variant 1	4.7	NM_001011658.1
Ras-related GTP binding C (RRAGC)	4.6	NM_022157.2
Band 4.1-like protein 4A	4.5	NM_022140.2
Cell division cycle 7-related protein kinase	4.4	NM_003503.2
TBC1 domain family member 22B	4.4	NM_017772.2
Serine/threonine-protein kinase 12	4.3	BC000442.1
Ras-related protein Rab-34	4.2	BC066904.1
RAB28, member RAS oncogene family (RAB28)	4.2	BC035054.2
cysteine and glycine-rich protein 2 (CSRP2)	4.2	NM_001321.1
Serine/threonine-protein kinase Sgk2	4.2	BC014037.1
Putative E3 ubiquitin-protein ligase SH3RF2	4.1	BC0031650.1
UNC-112 related protein 2 (URP2)	4.1	BC013366.2
RAB20, member RAS oncogene family (RAB20)	4.1	NM_017817.1
SHC-transforming protein 3	4.1	NM_016848.2
serine/threonine kinase 40 (STK40)	4.1	BC008344.1
peroxisome proliferator-activated receptor gamma (PPARG)	4.1	BC006811.1
protein kinase, AMP-activated, gamma 2 non-catalytic subunit (PRKAG2), transcript variant c, mRNA	4.1	NM_001040633.1
BMX non-receptor tyrosine kinase (BMX), transcript variant 2	4	NM_001721.2
zeta-chain (TCR) associated protein kinase 70kDa (ZAP70), transcript variant 2	3.8	NM_207519.1
pentatricopeptide repeat domain 2 (PTCD2)	3.8	NM_024754.2
Ribonuclease P protein subunit p14	3.8	NM_007042.1
CDK5 regulatory subunit associated protein 1-like 1 (CDKAL1)	3.7	BC064145.1
Mitogen-activated protein kinase kinase kinase 4	3.7	NM_005922.1

Table 7 Results from a screen for proteins ubiquitinated by IpaH7.8

Ubiquitination Screen Hit	Z-score	Genbank Accession Number
ankyrin repeat domain 13 family, member D (ANKRD13D)	22.4	BC044239.1
potassium voltage-gated channel, shaker-related subfamily, beta member 1 (KCNAB1), transcript variant 1	20.1	NM_172160.1
Cas-Br-M (murine) ecotropic retroviral transforming sequence b (CBLB)	14.4	BC032851.2
ring finger protein 4 (RNF4)	14.3	NM_002938.2
RIO kinase 3 (yeast) (RIOK3)	13.9	BC039729.1
ubiquitin fusion degradation 1 like (yeast) (UFD1L), transcript variant 1, mRNA.	13.6	NM_005689.1
sciellin (SCEL)	12.5	BC020726.1
RAS guanyl releasing protein 2 (calcium and DAG-regulated) (RASGRP2), transcript variant 1	11.2	NM_005825.2
DnaJ homolog subfamily B member 2	10.8	NM_006736.4
AF4/FMR2 family, member 4 (AFF4)	10.2	BC025700.1
ring finger protein 34 (RNF34), transcript variant 1	10.2	NM_194271.1
signal transducing adaptor molecule (SH3 domain and ITAM motif) 1 (STAM)	10.2	BC03586.2
TBC1 domain family member 22B	9.8	NM_017772.2
thymidylate synthetase (TYMS)	9.7	NM_001071.1
Isovaleryl-CoA dehydrogenase, mitochondrial	9.6	BC017202.2
p62 (sequestosome 1 (SQSTM1))	9.5	BC001874.1
polymerase (DNA directed) iota (POLI)	9.2	BC032662.1
RAD51 associated protein 1 (RAD51AP1)	9.2	NM_006479.2
RAD51 associated protein 1 (RAD51AP1)	9.2	NM_006479.2
coiled-coil domain containing 55 (CCDC55), transcript variant 1	9.1	NM_032141.1
crystallin, zeta (quinone reductase) (CRYZ)	8.9	NM_001889.2
DnaJ (Hsp40) homolog, subfamily B, member 2 (DNAJB2)	8.5	NM_006736.4
ataxin 3 (ATXN3)	8.4	BC033711.1
chromosome 1 open reading frame 63 (C1orf63)	8.3	NM_020317.2
ring finger protein 126 (RNF126)	8.3	NM_194460.1
Protein DDI1 homolog 1	8.2	NM_001001711.1
Nuclear protein localization protein 4 homolog	7.9	BC025930.1
Cytoplasmic polyadenylation element-binding protein 4	7.8	BC036899.1
2,4-dienoyl CoA reductase 2, peroxisomal (DECR2)	7.4	NM_020664.3
Tal (E3 ubiquitin-protein ligase LRSAM)1	7.3	BC009239.2
peptidylprolyl isomerase (cyclophilin)-like 2 (PPIL2), transcript variant 3	7.3	NM_148176.1
adenylosuccinate synthase like 1 (ADSSL1), transcript variant 2	7.2	NM_152328.3
RING finger protein 135	7.1	NM_197939.1
MAGUK p55 subfamily member 5	7	BC095485.1
membrane protein, palmitoylated 5 (MAGUK p55 subfamily member 5) (MPP5)	6.9	NM_022474.2
cortactin (CTTN), transcript variant 2	6.8	NM_138565.1
glutaredoxin 2 (GLRX2)	6.7	BC028113.1
SLAIN motif family, member 2 (SLAIN2)	6.7	BC031691.2

Ubiquitination Screen Hit	Z-Score	Genbank Accession Number
E3 ubiquitin-protein ligase LRSAM1	6.6	NM_001005373.1
Serine/threonine-protein kinase 12	6.6	BC000442.1
Glutaredoxin 2 (GLRX2) transcript variant 2	6.5	BC028113.1
Tripartite motif-containing protein 10	6.4	BC093926.1
protein kinase, AMP-activated, gamma 2 non-catalytic subunit (PRKAG2), transcript variant c, mRNA.	6.3	NM_001040633.1
potassium voltage-gated channel, shaker-related subfamily, beta member 2 (KCNAB2), transcript variant 1	6.2	NM_172160.1

Table 8 High-confidence data set from screens for substrates of IpaH7.8

High-Confidence Data Set	Genbank Accession Number
potassium voltage-gated channel, shaker-related subfamily, beta member 1 (KCNAB1), transcript variant 1	NM_172160.1
sciellin (SCEL)	BC020726.1
RAS guanyl releasing protein 2 (calcium and DAG-regulated) (RASGRP2), transcript variant 1	NM_005825.2
TBC1 domain family member 22B	NM_017772.2
Serine/threonine-protein kinase 12	BC000442.1
cortactin (CTTN), transcript variant 2	NM_138565.1
protein kinase, AMP-activated, gamma 2 non-catalytic subunit (PRKAG2), transcript variant c, mRNA.	NM_001040633.1

3.1.2: The IpaHs Do Not Target Other *S. flexneri* Effectors

Kubori et al (2010) recently demonstrated the ability of one *Legionella pneumophila* effector to modify others, thereby acting as a "metaeffector." This may be an emerging theme in bacterial pathogenesis, as CPAF, a protease from *Chlamydia*, was recently shown to cleave other *Chlamydia* proteins in addition to its mammalian substrates (Jorgensen *et al*, 2011). This lead me to wonder if the IpaHs ubiquitinate other *S. flexneri* effectors. I would not have observed such interactions using protoarrays because only human proteins are present on the protoarrays. To address this question, I isolated effectors from wild-type *S. flexneri*, then performed an *in vitro* ubiquitination reaction using these effectors in place of an E3 ubiquitin ligase and a substrate. Various control reactions were also performed, each lacking one component of the reaction, to ensure that any observed effects are attributable to the ubiquitination pathway. All reactions were treated with a buffer containing DTT, which disengages thioester bonds linking ubiquitin and cysteine residues while leaving the amide linkages between ubiquitin and lysine residues intact. I then separated the components of this reaction using SDS-PAGE and used silver staining to visualize the result (Figure 6). A complex containing the known substrate of IpaH9.8, Ste7, was included in one reaction as a positive control. In addition, a reaction containing Ste7 but lacking effectors was run to ensure Ste7 was being ubiquitinated in the positive control lane. Ubiquitination of a protein causes the band representing this protein to shift up in an SDS-PAGE gel because of the mass added by ubiquitin. I did not see a shift in any protein in the experimental reaction that I did not observe in at least one control reaction. The IpaHs do not appear to target other *S. flexneri* effectors in this system.

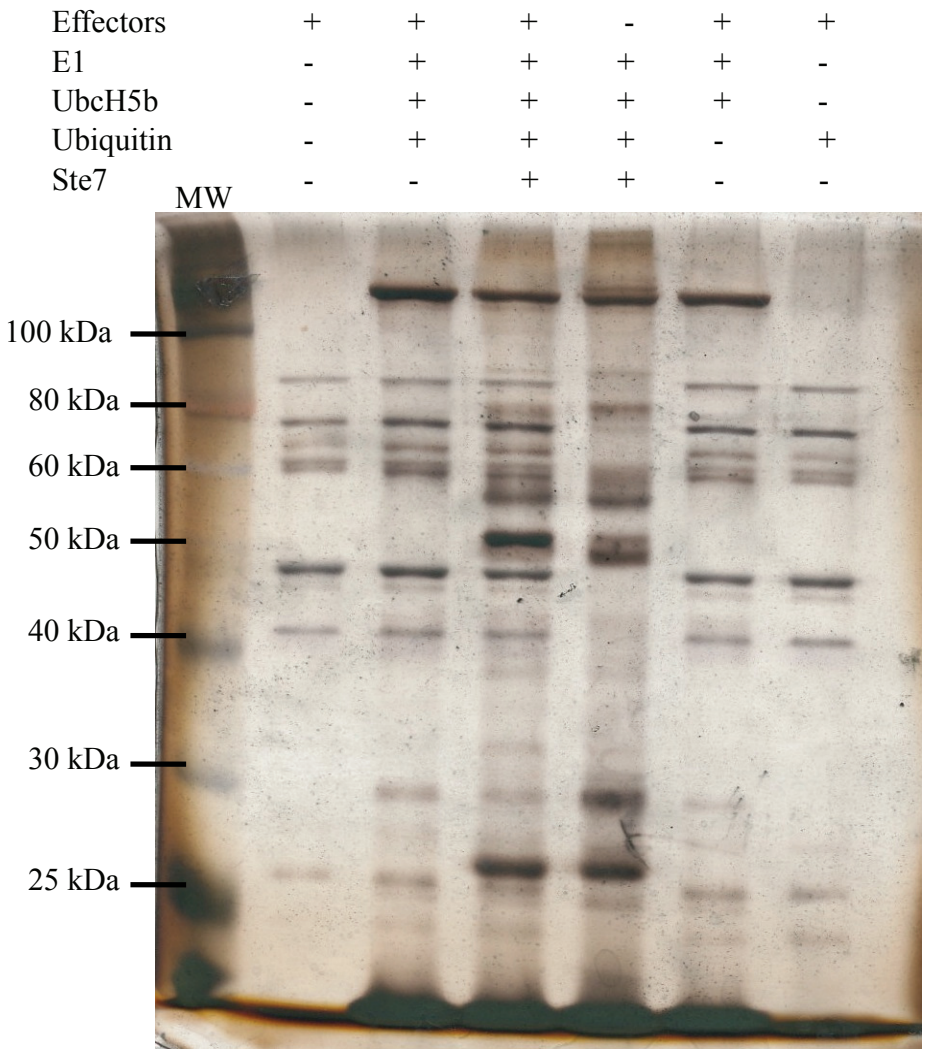

Figure 6: Effectors isolated from *S. flexneri* were used for in-vitro ubiquitination reactions in place of an E3 ubiquitin ligase and a substrate. Reaction components were then separated by SDS-PAGE and silver stained. The first lane shows a molecular weight marker.

3.1.3: Potential Substrates of IpaH7.8 Identified Through Protoarrays Are Not Ubiquitinated *In Vitro*.

I evaluated the ability of IpaH7.8 to ubiquitinate putative substrates identified through the protoarray screen in a simple reconstituted system that will hereafter be referred to as an "*in vitro* ubiquitination assay." Putative substrates were purified from *E. coli* and mixed with E1, UbcH5b (an E2 known to have the ability to charge IpaHs, Rohde *et al*, 2007), IpaH7.8 and ubiquitin. These reactions were incubated at room temperature for one hour and stopped with the addition of a DTT-containing buffer that disengages thioester linkages between ubiquitin and cysteine residues, while leaving the amide linkages between ubiquitin and lysine residues intact. This results in ubiquitin being removed from E1, UbcH5b or IpaH7.8, but not from substrates or other ubiquitin molecules. The reaction components were then separated by SDS-PAGE, transferred to PVDF membranes, and blotted using antibodies against the potential substrates. I was looking for high molecular weight bands that could represent polyubiquitinated species of the putative substrates. Various controls reactions were performed, each lacking a particular component of the reaction, to confirm that any high-molecular weight bands that I observed were dependent on the activity of the ubiquitination pathway, and were not attributable to cross-reactivity between the antibody against the putative substrate and another component of the reaction. Figure 7A shows results of *in vitro* reactions for p62, KCNAB1, Rab34, Tal and Cortactin, as well as two putative targets that were selected because of their high scores in the ubiquitination protoarray screen, RIOK3 and UFD1L. Control reactions lacking the E1 enzyme are shown for each putative substrate. For reactions in which bands were observed in the full reaction that were not present in the no

E1 control, an additional control reaction lacking IpaH7.8 is shown to address the possibility that high molecular weight bands were the result of cross-reactivity between the antibody against the putative substrate and the E1 enzyme (Figure 7B). Despite numerous attempts, reactions containing p62, KCNAB1, Rab34, Tal, RIOK3, UFD1L and Cortactin did not reveal any bands in the full reactions that were not present in either of the controls. As shown in Figure 7C, I also attempted to use IpaH9.8 to ubiquitinate Nemo: a substrate reported by Ashida *et al* (2009). I have been unable to replicate the results obtained by this group.

Figure 7D shows an *in-vitro* ubiquitination assay performed using p62 as a substrate along with five subsequent controls, each lacking one component of the reaction. These reactions were blotted with an antibody against ubiquitin instead of an antibody against p62. Multiple bands representing free ubiquitin chains can be seen in each lane representing a reaction containing E1, UbcH5b, IpaH7.8 and ubiquitin. I interpreted this as evidence that the ubiquitination machinery in my reactions was functional. However, my inability to observe conjugation of ubiquitin to the putative substrates led me to conclude that the putative substrates under consideration are not ubiquitinated by IpaH7.8 in this reconstituted system.

Figure 7: In-vitro ubiquitination reactions failed to reveal the ability of IpaH7.8 to ubiquitinate putative substrates identified through protoarray screens. **(A)** In vitro ubiquitination reactions using putative substrates were performed in the presence and absence of the E1 enzyme. Reaction components were separated by SDS-PAGE, transferred to PVDF, and western blotted using an antibody against the putative substrate. In the cases of RIOK3 and UFD1L, an antibody against the His-tag on these proteins was used. Because IpaH7.8 and the E1 and E2 enzymes are also His-tagged, annotations are provided to aid in the identification of bands. Bands that are not annotated were isolated with RIOK3 and UFD1L. **(B)** Putative substrates that appeared to be ubiquitinated in (A) were used in reactions with or without IpaH7.8 and analyzed as in part (A). **(C)** An in vitro ubiquitination reaction containing Nemo and IpaH9.8 was performed and analyzed as in part (A). **(D)** A reaction containing p62 was also performed along with five subsequent controls, each lacking one component of the reaction. The reaction components were separated by SDS-PAGE, transferred to PVDF and blotted using an antibody against Ubiquitin. Lane 1 = full reaction, lane 2 = no E1 control, lane 3 = no IpaH7.8 control, lane 4 = no Ubiquitin control, lane 5 = no p62 control

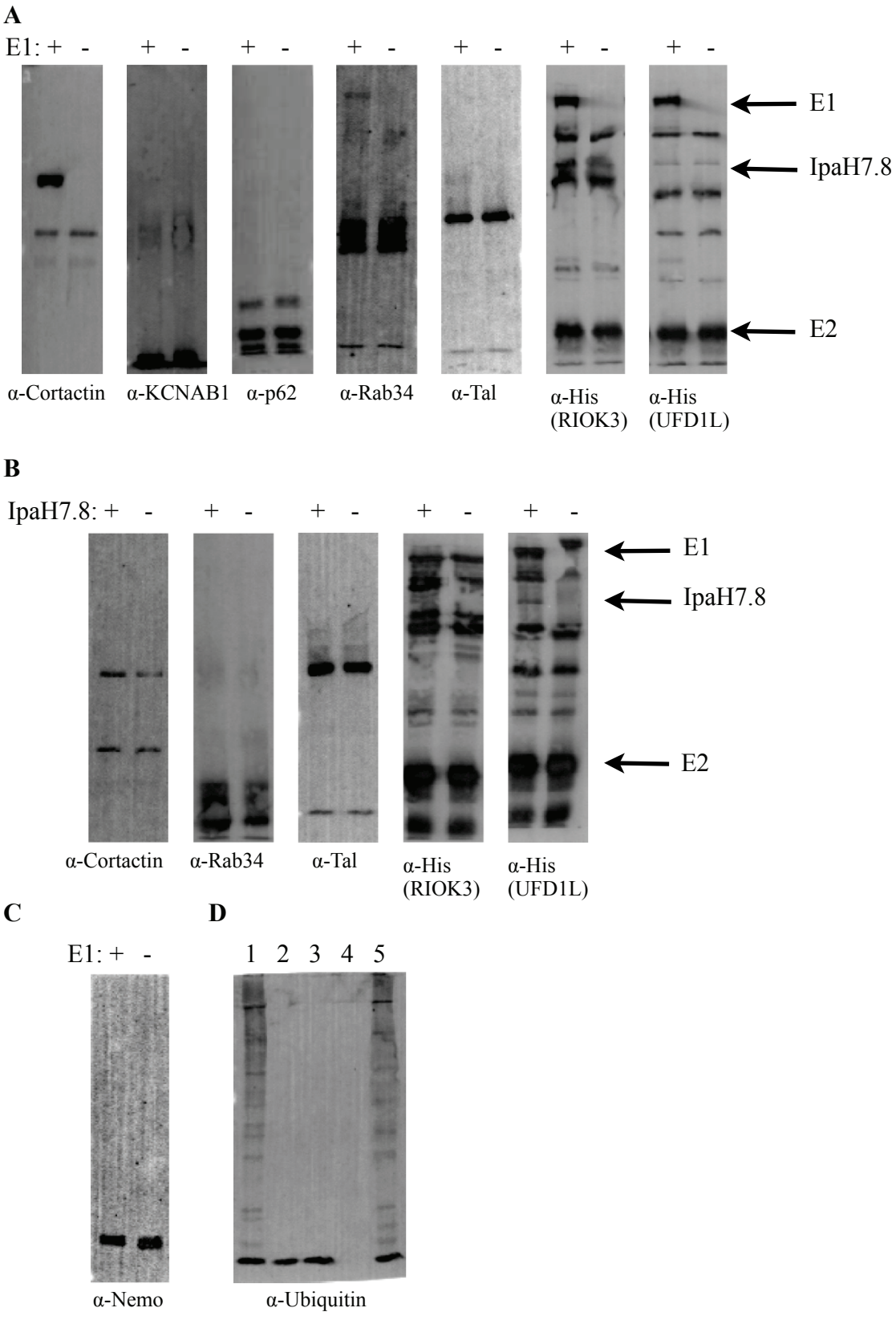
A
E1: + - + - + - + - + - + - + -
E1
IpaH7.8
E2
α-Cortactin
α-KCNAB1
α-p62
α-Rab34
α-Tal
α-His (RIOK3)
α-His (UFD1L)
B
IpaH7.8: + - + - + - + - + -
E1
IpaH7.8
E2
α-Cortactin
α-Rab34
α-Tal
α-His (RIOK3)
α-His (UFD1L)
C
E1: + -
α-Nemo
D
1 2 3 4 5
α-Ubiquitin

3.1.4: Immunoprecipitations of Putative Substrates of IpaH7.8 Do Not Reveal Ubiquitination.

Ubiquitination of proteins isolated from tissue culture can sometimes be observed by the presence of bands above the band corresponding to the isolated protein on a western blot using an antibody either against the immunoprecipitated protein or ubiquitin. I performed immunoprecipitations of Rab34, Tal and p62 from the colonic epithelial cell line Caco-2 cells and Cortactin, Tal and Rab34 from the macrophage-like cell line U937 infected with M90T and *ΔmxiE S. flexneri*. These cell types and others used throughout this study were chosen based on their relevance to the cell types infected by *S. flexneri in vivo*. I did not attempt to isolate KCNAB1 due to the lack of a high-quality antibody against this protein. I then separated the precipitated proteins by SDS-PAGE and blotted for the isolated protein and for ubiquitin (Figure 8). Although I observed laddering effects similar to those indicating ubiquitination when blotting against Rab34 and Tal, these effects were present in cells infected with M90T and *ΔmxiE S. flexneri*, indicating that they were not caused by an MxiE dependent factor such as IpaH7.8. Blots for ubiquitin also revealed the same patterns of bands when M90T infected cells were compared to *ΔmxiE* infected cells. Therefore, I did not observe any evidence of Cortactin, Rab34, Tal or p62 being ubiquitinated by IpaH7.8 using this method.

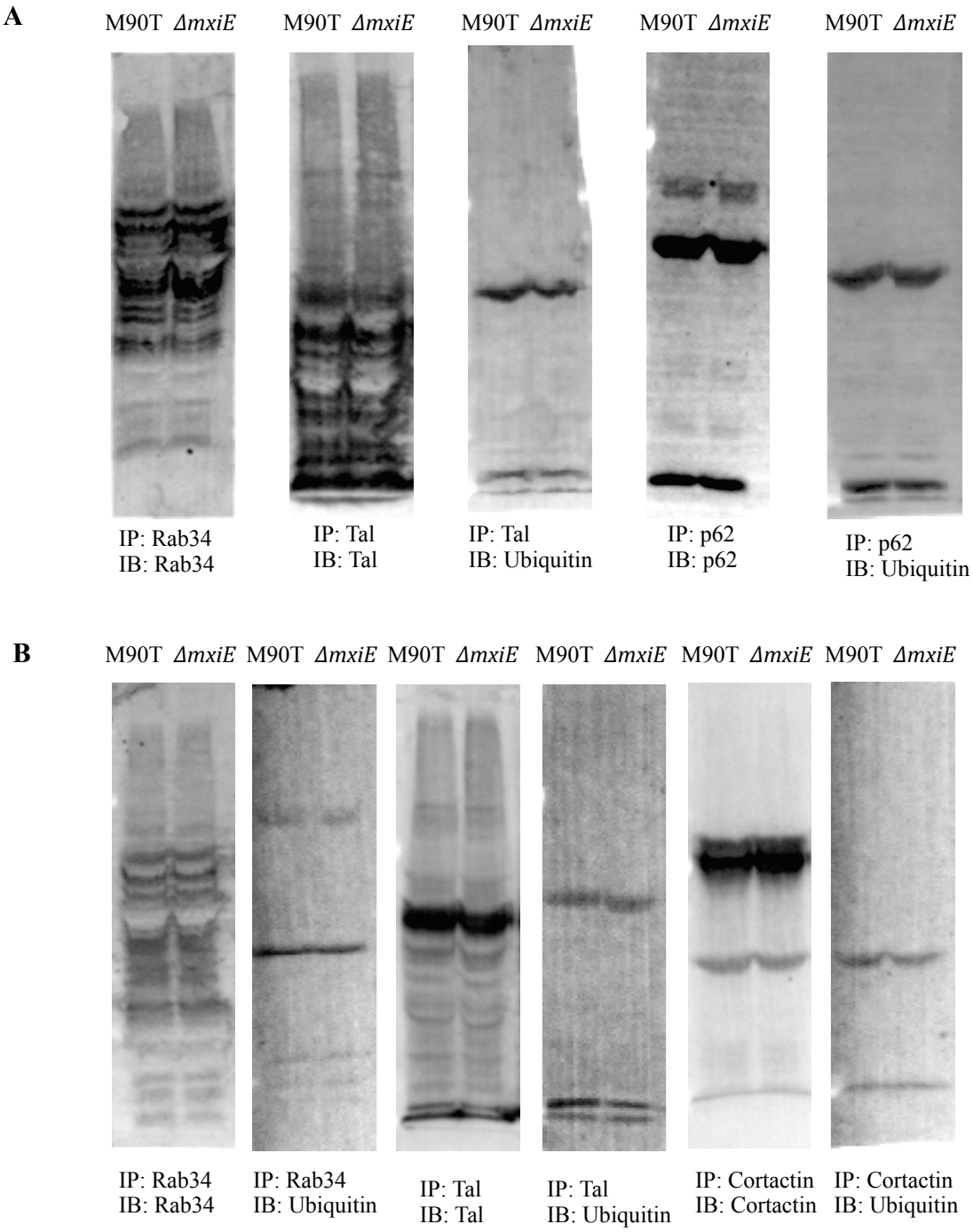

Figure 8: U937 cells **(A)** and Caco-2 cells **(B)** were infected with wild-type (M90T) *S. flexneri* or a mutant for the gene *mxiE*. Cells were lysed after two hours of infection, and the indicated putative substrates of IpaH7.8 were immunoprecipitated. Western blots were performed using antibodies against the precipitated proteins or ubiquitin. When no bands were observed on an anti-ubiquitin blot, the blot is not shown.

3.1.5: Levels of Cortactin, p62 and Tal Drop in M90T-Infected HeLa Cells, But This Effect is Not Observed Reliably.

Observing ubiquitination of immunoprecipitated substrates of IpaH7.8 may have been hindered by the fact that ubiquitination typically targets proteins for destruction by the proteasome. To avoid this difficulty, I infected HeLa, U937 and HT-29 cells with M90T and *ΔmxiE S. flexneri* and lysed the cells at time points ranging from 15 minutes to 3 hours. I then separated total cell lysates by SDS-PAGE and blotted against p62, Cortactin, Tal and Rab34. If these proteins are substrates of IpaH7.8, one would expect these proteins to be destroyed by the proteasome in cells infected by M90T, and therefore their levels would drop. This effect should be eliminated in cells infected with *ΔmxiE S. flexneri*. When using HeLa cells, results from these experiments varied widely between replicates. I observed decreased levels of Cortactin, p62 and Tal in some experiments, but I could not reproduce this effect reliably. Levels of Rab34 remained constant in M90T-infected cells. Figure 9 shows representative western blots against Cortactin, p62 and Tal, which illustrate the variability in this system, as well as a single western blot of Rab34 showing a typical result obtained when blotting against this protein. Anti-Actin western blots performed on the same membranes as blots against potential substrates are shown below each blot of a potential substrate as loading controls. None of these four potential targets appeared to be degraded in HT-29 or U937 cells**.** Figure 9 also shows a western blot illustrating that levels of IκBα, a protein that binds to NF-κB to prevent it from entering the nucleus, drop over the course of a three-hour infection of HeLa cells with M90T or *ΔmxiE S. flexneri*, indicating that the innate immune system of the HeLa

cells has been activated. A non-specific band below the band corresponding to IκBα is shown in place of a loading control.

An obvious source of error in these infections is the possibility that too few cells were infected for an effect to be observed. I used a technique known as a gentamicin protection assay to address this issue. This is a technique in which tissue culture cells are infected with bacteria, then a low dose of gentamicin is added to the cells to kill bacteria outside the cells without penetrating to the insides. The gentamicin is then removed, the cells are lysed, and serial dilutions of the released bacteria are plated. Assuming each fully-confluent well of a six-well dish contains 10^6 HeLa cells, which I have found to be a reliable estimate, I found that the average ratio of bacteria to HeLa cells was 2.2 during these infections, and that each infection had at least a ratio of 0.5.

Figure 9: HeLa cells were infected with wild-type (M90T) or *ΔmxiE S. flexneri* (UI = uninfected). Infections were stopped by the addition of Lamelli buffer at the indicated time points. Whole-cell lysates were separated by SDS-PAGE and blotted for putative substrates of IpaH7.8. Western blots against Actin were performed on the same membranes to serve as loading controls. A western blot using an antibody against IκBα was performed to show activation of the NF-κB pathway in response to infection. A non-specific background band is shown as a loading control for the IκBα western blot.

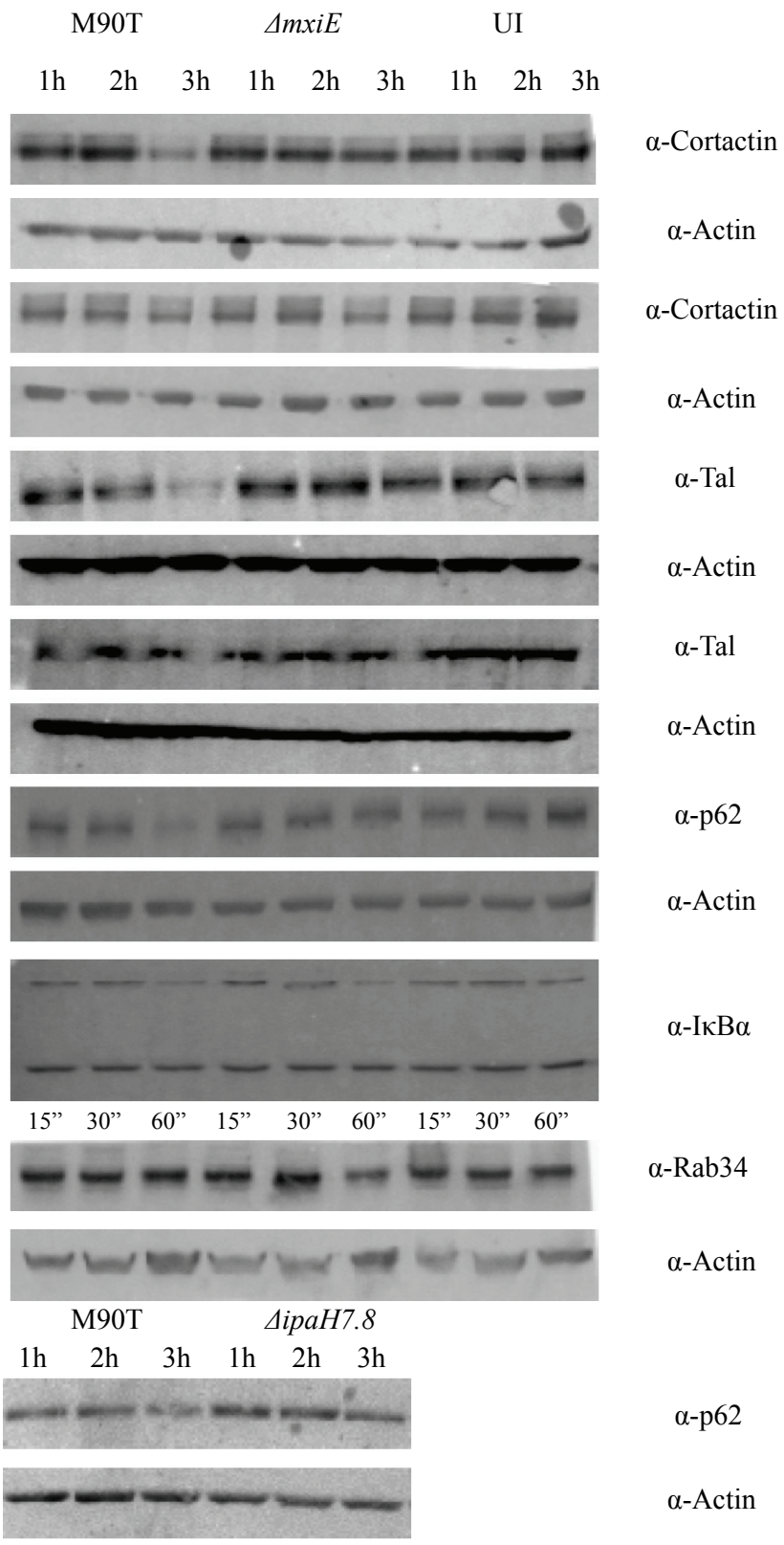
M90T
ΔmxiE
UI
1h 2h 3h 1h 2h 3h 1h 2h 3h
α-Cortactin
α-Actin
α-Cortactin
α-Actin
α-Tal
α-Actin
α-Tal
α-Actin
α-p62
α-Actin
α-IκBα
15” 30” 60” 15” 30” 60” 15” 30” 60”
α-Rab34
α-Actin
M90T
ΔipaH7.8
1h 2h 3h 1h 2h 3h
α-p62
α-Actin

3.1.6: An *ipaH7.8*-Expressing HeLa Cell Line Proves Difficult to Build

The difficulty I experienced in validating hits from the protoarray screens for substrates of IpaH7.8 prompted me to begin building a line of HeLa cells stably expressing *ipaH7.8* under an inducible promoter. Such a cell line would provide a simplified system for studying the effect of IpaH7.8 in which levels of this protein could be modulated and the potentially-conflicting actions of other *S. flexneri* effectors would be eliminated. In addition, issues regarding when *ipaH7.8* is expressed during an infection would be eliminated in a stable cell line. I used the pRetro-X system available from Clontech (Moutain View, CA) in my attempt to build this cell line. A detailed account of the method with which this system was employed can be found in the Materials and Methods under Chapter 2.12. Briefly, I incorporated the gene encoding a transactivator protein called "tTA-Advanced" into the genome of HeLa cells. tTA-advanced can be sequestered and rendered inactive by doxycycline. I then integrated *ipaH7.8* under the control of a promoter induced by tTA-advanced into the genomes of these cells. I also built a similar line of cells encoding *luciferase* under the tTA-advanced promoter. Although the *luciferase*-encoding cells produced approximately 173 times as much Luciferase in the absence of doxycycline as when doxycycline was present, a western blot of whole-cell lysates from *ipaH7.8*-encoding cells with and without doxycycline did not reveal IpaH7.8 under either condition. Thinking that levels of IpaH7.8 may have been too low to detect, I then transiently transduced HeLa cells with a plasmid encoding *ipaH7.8* under the control of the cytomegalovirus immediate early (CMV) promoter, which is typically highly active in mammalian cells. These transfected HeLa cells also did not appear to produce IpaH7.8 when assessed by western blot.

These results indicate that expression of *ipaH7.8* in HeLa cells is difficult to achieve. It is possible that codon bias has rendered HeLa cells ill equipped to produce IpaH7.8. Codon bias is a phenomenon in which the ratios of tRNAs produced by different organisms affect the frequencies with which they use particular codons to encode the same amino acids. This issue could be addressed through the synthesis of a codon-optimized version of *ipaH7.8*. It is also possible that IpaH7.8 is targeted for destruction post-translationally due to the inability of HeLa cells to recognize this foreign protein. Given that IpaH7.8 is normally injected directly into the cytosol of mammalian cells, it may not have the appropriate information to be properly processed when produced in mammalian cells. This issue would be more difficult to address than codon bias, but perhaps I would have better luck using a different cell line.

3.2: IpaH7.8 and Autophagy

3.2.1: LC3 Does Not Co-Localize With Wild-Type or *ΔmxiE S. flexneri* in HeLa Cells.

Because many of the top hits from the protoarray screens were proteins involved in autophagy, I chose to look for an association between *ΔmxiE S. flexneri* and the mammalian protein LC3. LC3 is a component of autophagosomes, and co-localization between LC3 and subcellular structures, such as protein complex, organelles or pathogens, is commonly used as an indication that these structures are being entrapped by autophagosomes (Tanida *et al*, 2004). I infected GFP-LC3-expressing HeLa cells (A gift from Dr. Craig McCormick) with the *S. flexneri* strains M90T (wild-type), *ΔmxiE* and *ΔipaH7.8,* all containing plasmids encoding the RFP variant mCherry. I did not see an

appreciable degree of colocalization between LC3 and any strain of *S. flexneri*, indicating that the IpaHs do not have an affect on autophagy under the conditions used to perform this experiment (Figure 10A).

Others have shown that LC3 has a dispersed pattern throughout the cytosol when levels of autophagy are low, and that it forms punctae when autophagy levels increase. I treated GFP-LC3 HeLa cells with the drug rapamycin, which is an inducer of autophagy, to obtain an example of a high number of LC3 punctae. I observed many punctae in rapamycin treated cells, however I observed similar numbers of punctae in uninfected, untreated cells (Figure 10A). This means that either the rapamycin did not effectively upregulate autophagy, or there was a high basal level of autophagy. Given the large number of LC3 punctae, I suspect that basal levels of autophagy were high in these HeLa cells. This may have prevented the cells from responding to an *S. flexneri* infection as they would when basal autophagy levels were lower.

3.2.2: Infections With Wild-Type and *ΔmxiE S. flexneri* Do Not Induce Increases in LC3-II Levels.

Upon induction of autophagy, LC3 is converted from the cytosolic form, LC3-I, to the form that is conjugated to autophagosomes, LC3-II, by the addition of a phosphatidylethanolamine (PE) group (Suzuki et al, 2001). This conversion can be observed by western blot, and because the level of LC3-II in a cell corresponds to the number of autophagosomes, an increase in LC3-II can be interpreted as an increase in autophagy within these cells. I infected HT-29, U937 and HeLa cells with M90T and *ΔmxiE S. flexneri* and compared levels of LC3-II in the two treatment groups by western blot. I did not observe a difference in LC3-II levels, which further supports the

hypothesis that the IpaHs do not have an effect on autophagy. Figure 10B shows representative results obtained using HeLa cells.

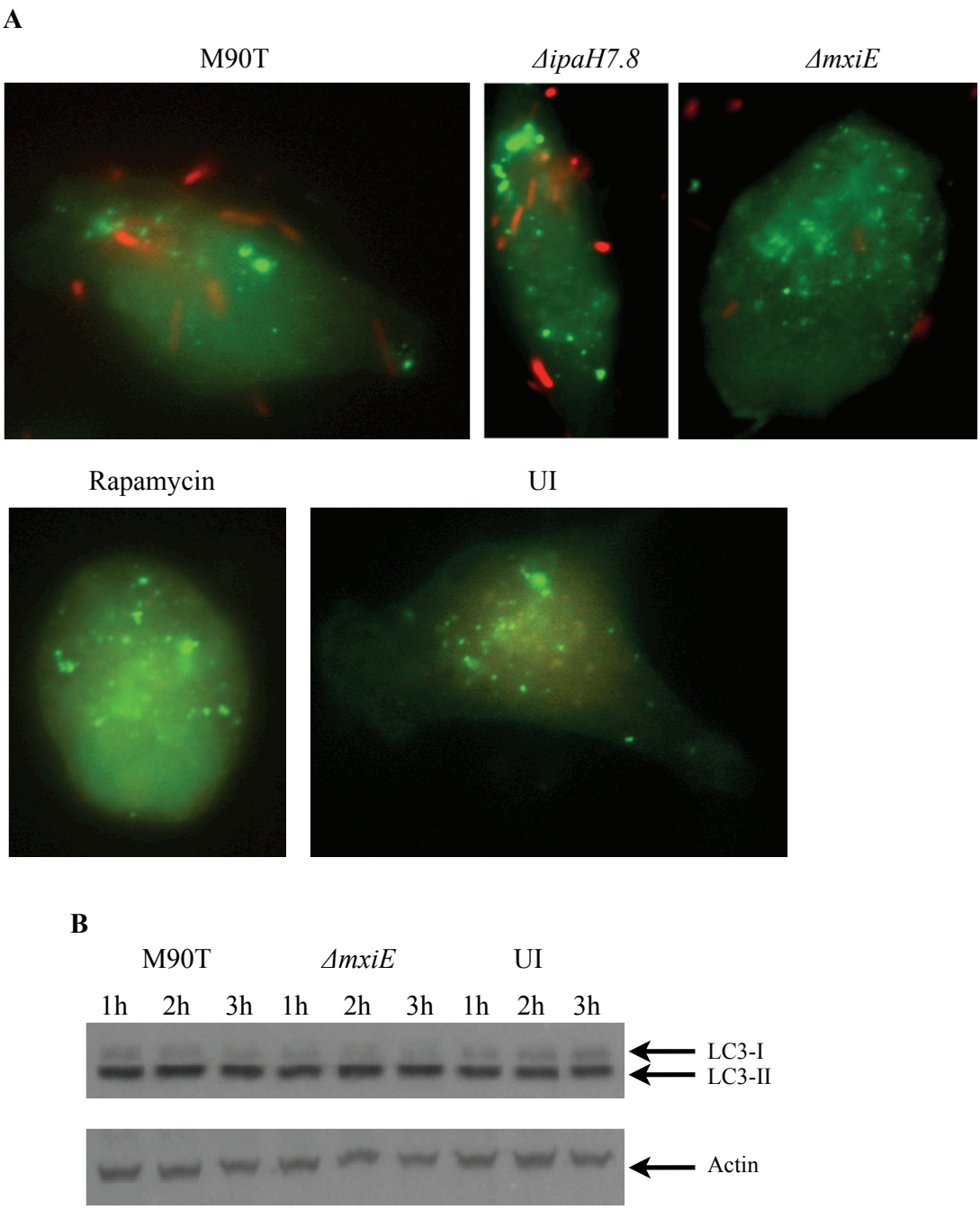

Figure 10: IpaH7.8 does not affect LC3 in HeLa cells. **(A)** HeLa cells expressing GFP-tagged LC3 were infected with mCherry-expressing *S. flexneri* and the indicated mutants for one hour (UI = uninfected). Rapamycin treatment was used as a positive control for LC3 punctae formation. **(B)** HeLa cells infected with M90T or *ΔmxiE S. flexneri* were lysed after 1, 2 and 3 hours of infection. Western blotting was used to compare levels of LC3-I and LC3-II between the two treatment groups and uninfected (UI) HeLa cells. An actin loading control is also shown.

3.3: Analysis of Cytokines Elicited in Response to *S. flexneri* Infection.

3.3.1: Development of a Protocol for Analyzing Cytokine Production by U937 Macrophages in Response to *S. flexneri* Infection.

Because *Shigella* researchers lack a robust animal model for shigellosis, many questions remain regarding the immunological response to *S. flexneri* infection. We decided to investigate some of these questions while simultaneously addressing our lab's interest in the functions of *S. flexneri's* effectors. To this end, I developed a protocol for collecting cytokines produced by U937 cells in response to infection with wild-type *S. flexneri* and various mutant strains. U937 cells are a monocyte cell line that differentiates to form macrophage-like cells upon contact with phorbol 12-myristate 13-acetate (PMA). As described in Chapter 1.2, macrophages residing beneath the epithelial lining of the gut are instrumental in the immunological response to *S. flexneri*, and therefore knowledge regarding the effects of virulence factors secreted into these cells could be useful in understanding the broader immunological landscape.

I infected U937 cells with wild-type (M90T) or plasmid-cured (BS176, a gift from Dr. Claude Parsot, Pasteur Institute) *S. flexneri* at an approximate multiplicity of infection (MOI) of 0.01. I incubated the cells at 37°C with 5% CO_2 for twelve to eighteen hours, then collected the medium overlaying the cells. At least 50% of the infected cells were alive at all time points between twelve and eighteen hours, as assessed by Trypan blue exclusion (Figure 11A).

I used the presence of IL-8 as an indication that medium collected from infected U937 cells contained cytokines. My preliminary experiments revealed that infected U937

cells produced high levels of IL-8 after infection with *S. flexneri*, making this cytokine easy to measure. In addition, IL-8 is produced in response to NF-κB activation (Philpott *et al*, 2000), as are other cytokines associated with bacterial infections such as TNFα and IL-1β (Baeuerle and Henkel, 1994). It is, therefore, a useful indicator that a bacterial infection has been established. IL-8 was produced at all time points from twelve to eighteen hours (Figure 11B) and levels produced in response to a plasmid-cured strain of *S. flexneri*, BS176, were significantly lower than those produced by M90T, or wild-type, *S. flexneri*. I chose to use a sixteen hour time point for further cytokine analysis because it allowed for the convenience of running experiments overnight, and was in line with the time points used in previous characterizations of cytokines produced in response to *Shigella* infection (e.g., van de Verg *et al*, 1995).

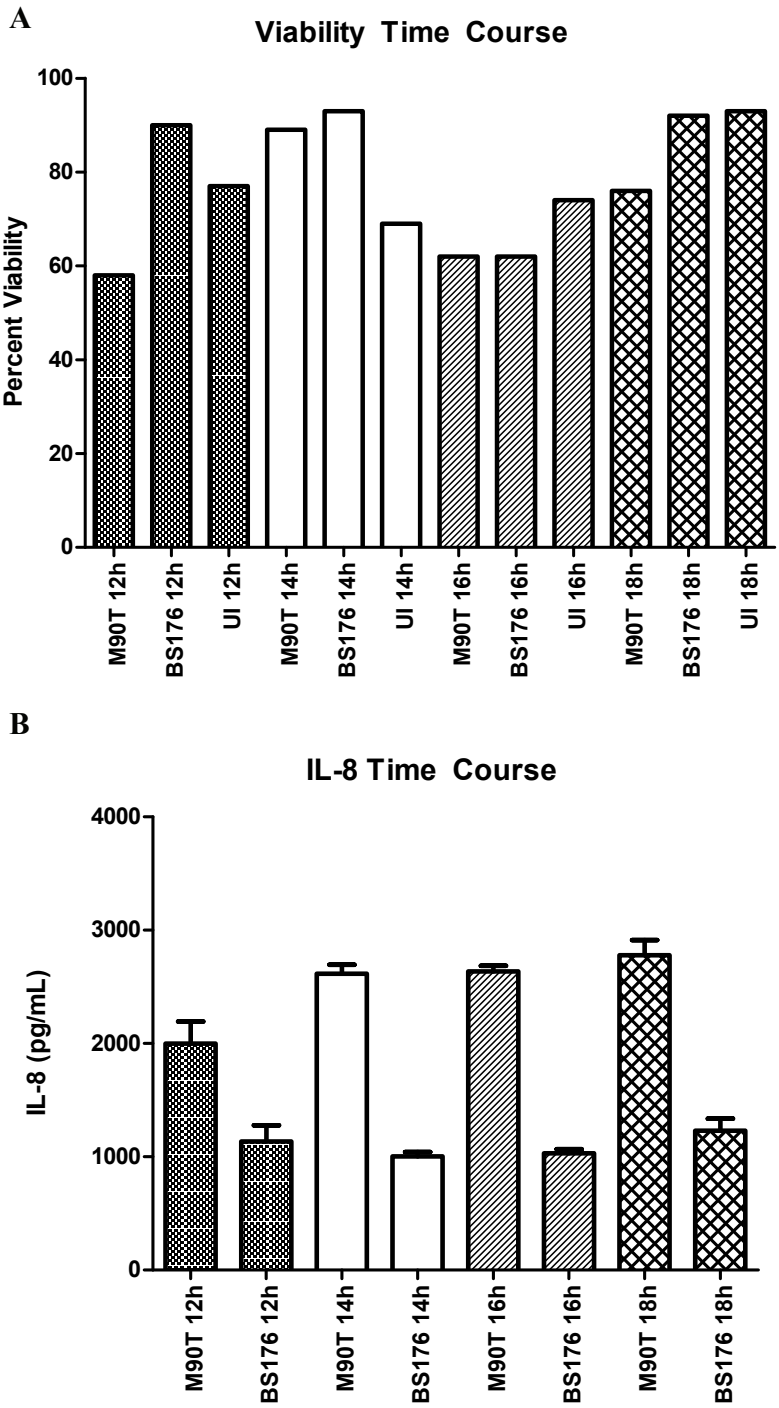

Figure 11: Appropriate conditions under which to collect cytokines produced by U937 cells were determined based on **(A)** Percent viability and **(B)** IL-8 production. Infections were performed using wild-type (M90T) or plasmid-cured (BS176) *S. flexneri* or an uninfected control (UI) at time points ranging from twelve to eighteen hours. Error bars represent standard deviation of four technical replicates.

3.3.2: RayBio Cytokine Antibody Arrays Identify Cytokines Potentially Affected by Virulence Factors

The cytokine milieu produced in response to *Shigella* infection has been characterized using *in vivo* models such as the mouse pulmonary model (Sellge *et al*, 2010) and rectal biopsies from shigellosis patients (Raqib *et al*, 1995) and *in vitro* using epithelial cell lines (Sperandio *et al*, 2008). I was interested in determining which, if any, of these cytokine responses were related to the presence of effectors encoded by the virulence plasmid. To address this question, I used commercially available arrays of anti-cytokine antibodies, purchased from RayBiotech Inc, to screen for cytokines present at different levels in the supernatants of U937 macrophages infected with M90T and the plasmid cured strain BS176. Densitometry analysis revealed that CCL3, CCL8 (MCP-2) and M-CSF were present in higher levels in the supernatants of BS176-infected macrophages than M90T-infected macrophages, whereas CXCL5 (ENA-78) and G-CSF levels were higher in M90T-infected cells than BS176-infected (Table 9). G-CSF levels were further analyzed using the Luminex system, however levels of this cytokine were too low to be quantified. One possible explanation for this discrepancy is that another cytokine cross-reacts with the G-CSF antibody found on RayBio cytokine arrays.

Levels of CCL3 produced by macrophages were previously shown to increase in response to Major Outer Membrane Protein (MOMP) from *S. flexneri* (Pore et al, 2010). MOMP is not encoded by the virulence plasmid and so these results indicate that there may be an additional regulatory mechanism for CCL3 that is dependent on a virulence plasmid-encoded factor, or such a factor may modify MOMP. Follow-up would be necessary to confirm this potentially useful result.

Table 9 Cytokines that may be regulated by effectors from *S. flexneri*

Cytokine	Ratio (M90T: BS176)
CCL3	0.63
G-CSF	1.64
CXCL5	1.85
CCL8	0.38
M-CSF	0.21

3.4: Proof-of-Principle Experiments Using the *S. flexneri* Deletion Collection

3.4.1: Quantification of Congo Red Sequestration by Mutants from the Deletion Collection

Congo red is a synthetic compound that induces expression of the T3SS apparatus in *Shigella*. Congo red is also bound by secreted effectors, and this binding is manifested as a red-coloured colony when *Shigella* is grown on an agar plate containing Congo red (Parsot et al, 1995). I developed a method for quantifying the degree to which the mutants in the Rohde lab's deletion collection were capable of binding Congo red. As an inability to bind Congo red correlates with a decreased ability to produce effectors, this tool could help identify effectors that control secretion of one or more factor(s). Briefly, ninety six strains from the deletion collection were grown on Congo-red containing TSB agar plates. I imaged these plates using a BioRad VersaDoc. Conveniently, I've found that *S. flexneri* produces light of 503 nm when excited with light of 430 nm: the same conditions used for imaging chemifluorescent western blot detection reagents. Congo red quenches this fluorescence. I was therefore able to use the VersaDoc on a setting under which it emits light of 503 nm to obtain grayscale images representing the degree to

which mutants from the deletion collection bound Congo red. Those that were highly Congo red positive (IE, had a dark red colour) appeared as dark gray colonies, and those that were Congo red negative (IE, had a lighter red colour) appeared white or nearly white (Figure 12). I was then able to quantify the saturation of colour in these images, thereby assigning a Congo red "score" to each mutant (Figure 13).

To assess the specificity of this technique to *S. flexneri* grown in the presence of Congo red, I also analyzed ninety six mutants of K-12 *E. coli* obtained from the Keio Deletion Collection (Baba *et al*, 2006) plated on Congo red containing medium, as well as the *S. flexneri* deletion collection plated on medium without Congo red. *E. coli* was not previously known to respond to Congo red. Although this expectation largely held, an *E. coli* mutant for a gene encoding LldP, a lactate permease, was Congo red positive. The ratio of the standard deviation to the average of the Congo red scores obtained from these two controls was less than that obtained from the *S. flexneri* deletion collection plated on Congo red-containing medium (about 0.12, as opposed to 0.2), indicating that, of the conditions examined, this effect is most pronounced using the combination of *S. flexneri* and Congo red. *ΔipaD*, a mutant for a component of *S. flexneri's* T3SS that produces effectors constitutively and is known to be highly Congo red positive, had the highest Congo red score of the *S. flexneri* mutants that I screened. Mutants for transcription factors such as *ΔvirF* had very low Congo red scores. These expected results are satisfying, and lend validity to the assay.

Several proteins of unknown function had Congo red scores that were higher than wild-type *S. flexneri*. However, the majority of the mutants analyzed had Congo red scores lower than those of M90T, which may indicate that most mutations in *S. flexneri's* virulence plasmid reduce effector secretion. A logical hypothesis regarding the mutants

that were more Congo red positive than wild-type *S. flexneri* was that these strains hypersecreted effectors. A summer student in the Rohde lab, Amit Mishra, tested this hypothesis by analyzing the secretion profiles of two such mutants: *Δorf157* and *Δorf131b*. Secretion of effectors was induced using Congo red, and the profile of the resulting effectors was analyzed using SDS-PAGE followed by silver staining. These profiles were not noticeably different from that of wild-type *S. flexneri*. Although enhanced effector secretion is correlated with the Congo red positive phenotype (Parsot *et al*, 1995), the exact combination of effectors necessary to produce this effect is unknown. Perhaps *Δorf157* and *Δorf131b* mutants hypersecrete one or a few effectors that are especially important for the Congo red positive phenotype, but this change in secretion profile is not obvious on a silver stained gel.

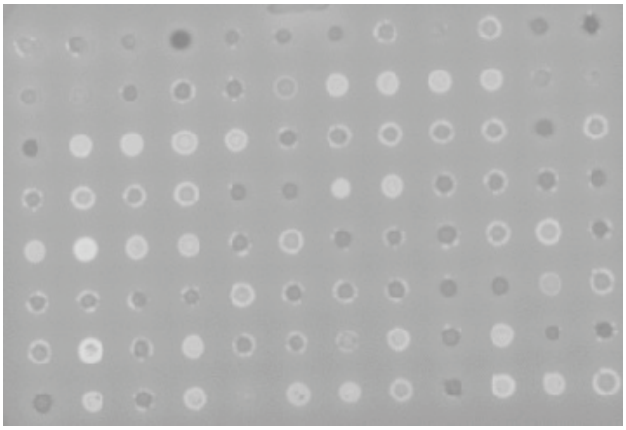

S. flexneri Deletion Collection

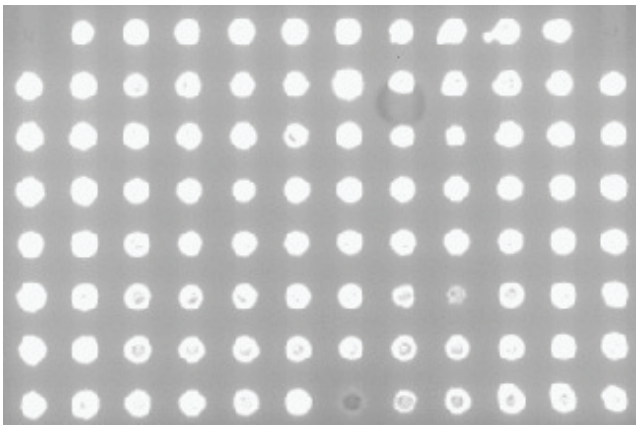

Keio *E. coli* Deletion Collection

Figure 12: Images of the *S. flexneri* deletion collection and a plate from the Keio *E. coli* deletion collection pinned onto Congo red TSB plates.

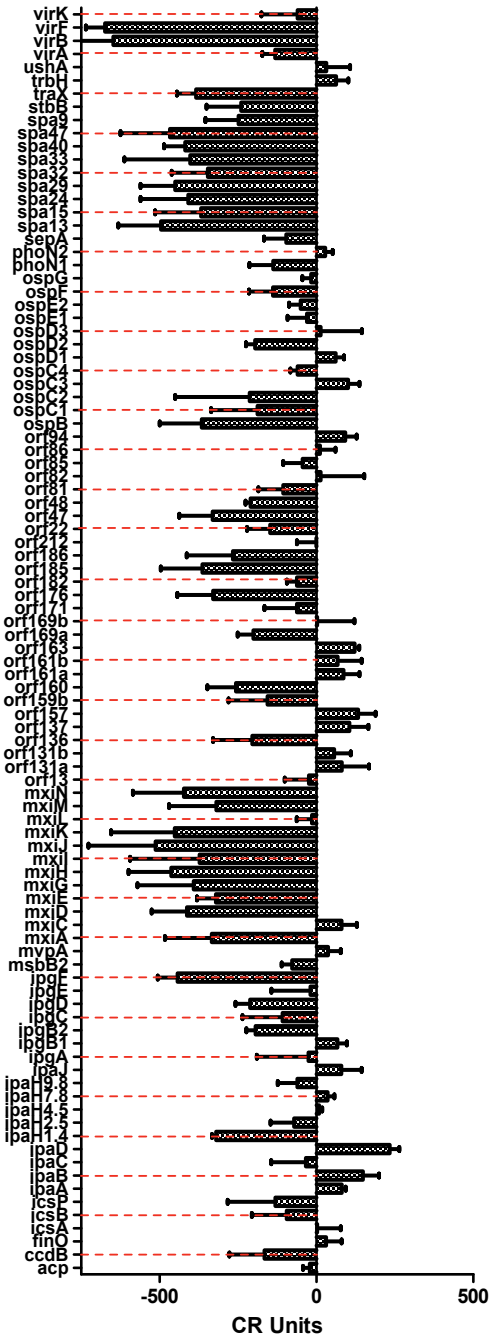

Figure 13: Densitometry analysis performed using Image Lab software from BioRad reveals the degree to which *S. flexneri* mutants for genes indicated on the Y-axis bind the dye Congo red. CR units are defined as the density of the indicated strain minus the density of wild-type *S. flexneri*. The average density of the wild-type strain was 902. Error bars indicate standard deviation over three replicates.

3.4.2: Luminex Cytokine Analysis Reveals Varied IL-8 Secretion by Macrophages Infected with the *S. flexneri* Deletion Collection

As a second proof-of-principle experiment related to the deletion collection, I looked for *S. flexneri* mutants that elicited altered levels of IL-8, TNFα, IL-6, EGF, CCL24 (Eotaxin-2) and G-CSF from U937 macrophages when compared to M90T. Using the Luminex cytokine analysis platform, I quantified the amounts of these cytokines produced by U937 cells after sixteen hours of infection with seventy nine strains of *S. flexneri*. Results from the IL-8 screen are shown in Figure 14. Levels of TNFα, IL-6, EGF, CCL24 and G-CSF were too low to warrant follow-up, however four mutants that produced high levels of IL-8, *ΔmxiH, ΔmxiK, ΔospB* and *Δorf186,* were analyzed further. In addition, the difference in levels of IL-8 elicited by U937 cells infected with wild-type (M90T) and plasmid-cured (BS176) *S. flexneri* was analyzed. In all cases, the level of IL-8 produced by uninfected U937 cells, which was approximately 10-fold lower than that produced by wild-type *S. flexneri* infected cells, was subtracted from the levels produced by infected cells. As shown in Figure 15A, BS176 elicited lower levels of IL-8 than wild-type *S. flexneri* in two independent experiment. A flowchart shown in Figure 16 outlines the process used to analyze the remaining four mutants.. Mutants for the genes *mxiK* and *ospB* produced higher levels of IL-8 than wild-type *S. flexneri* in two independent experiments (Figure 15B). A mutant for the gene *mxiH* elicited higher levels of IL-8 than wild-type *S. flexneri* in seven experiments. Values from these experiments were averaged, and the difference between *mxiH* and wild-type was found to be significant (Figure 15C). Although mutants for the gene *orf186* did not produce a statistically significant difference from wild-type in this set of

experiments, a separate set in which a complemented *orf186* mutant was also included showed that an *orf186* mutant did elicit significantly higher levels of IL-8 than wild-type *S. flexneri*, and this effect was reversed in the complemented strain, which elicited significantly lower levels of IL-8 than wild-type *S. flexneri* (Figure 15D). In all cases, although these trends were consistent over multiple independent biological replicates, the absolute levels of IL-8 varied widely between replicates, sometimes going as high as 10,000 pg/mL. One possible explanation for this variation is that more U937 cells were removed from the tissue culture dishes during wash steps in one experiment than the other, leaving fewer cells to produce IL-8. Despite the apparent reproducibility of M90T eliciting more IL-8 than BS176, others in the Rohde lab have since observed the opposite trend: M90T eliciting less IL-8 than BS176. The cause for these conflicting results is not known.

OspB is a largely uncharacterized effector, however this mutant was previously shown to elicit higher levels of IL-8 than wild-type *S. flexneri* upon infection of epithelial cells (Zurawski et al, 2009). My results show that this effect can be observed in macrophages, as well. MxiH and MxiK are both components of the T3SS needle apparatus. It is interesting that deleting these specific components of the needle causes more IL-8 to be produced than M90T, whereas BS176, a plasmid-cured strain of *S. flexneri* that lacks a T3SS entirely, elicits less. Orf186 has not been characterized in *Shigella*, however its homologue in *E. coli* modifies lipopolysaccharide (LPS) through the addition of an N-acetylglucosamine (GlcNAc) group to the inner core oligosaccharide (Kaniuk et al, 2004).

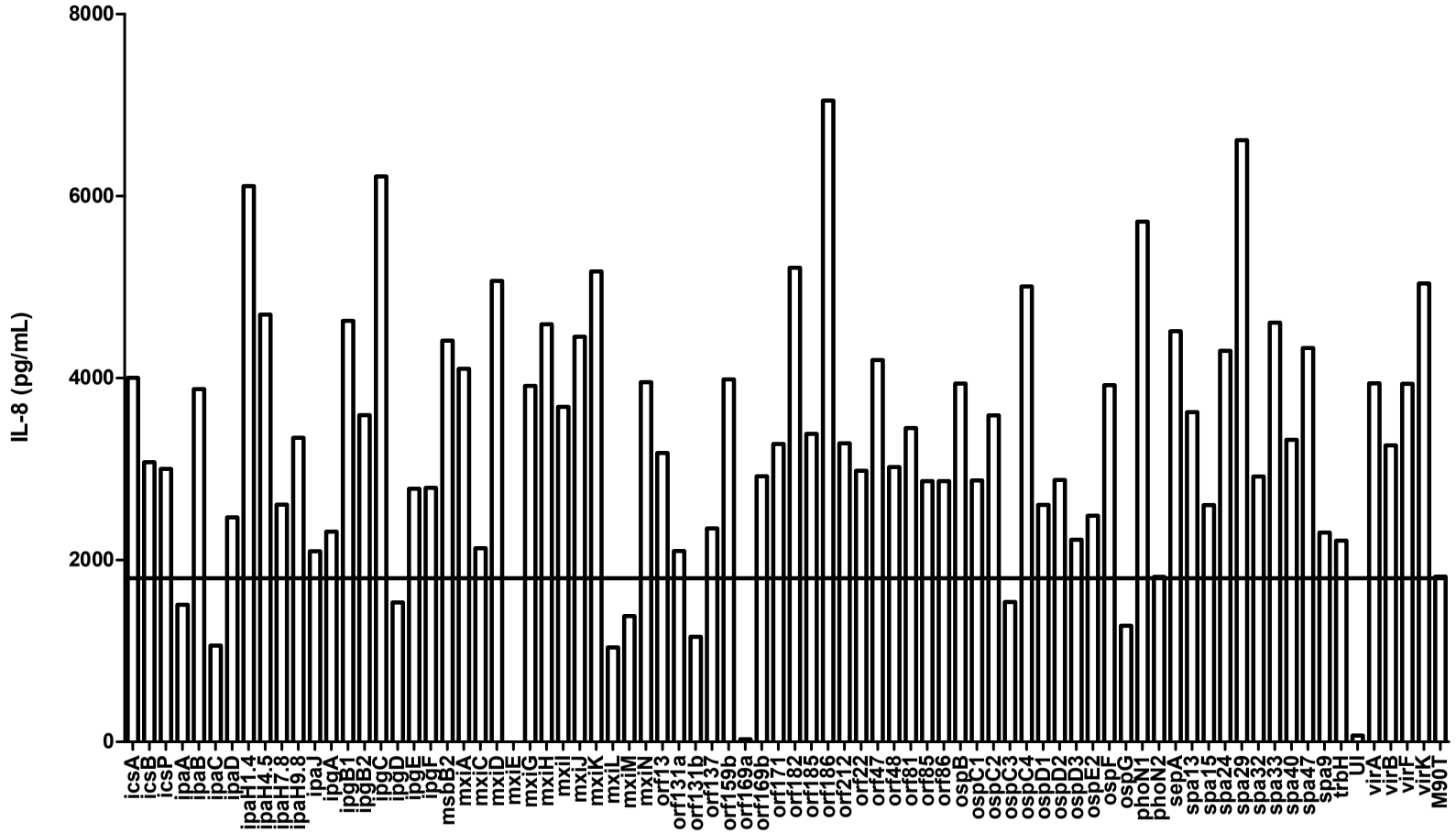

Figure 14: Levels of IL-8 produced by U937 cells in response to infection with wild-type (M90T) and seventy eight mutant strains of *S. flexneri*, as assessed by Luminex (UI = uninfected). The mutated gene is indicated on the X-axis, and the level of IL-8 produced in response to infection with wild-type *S. flexneri* is indicated by a horizontal black line.

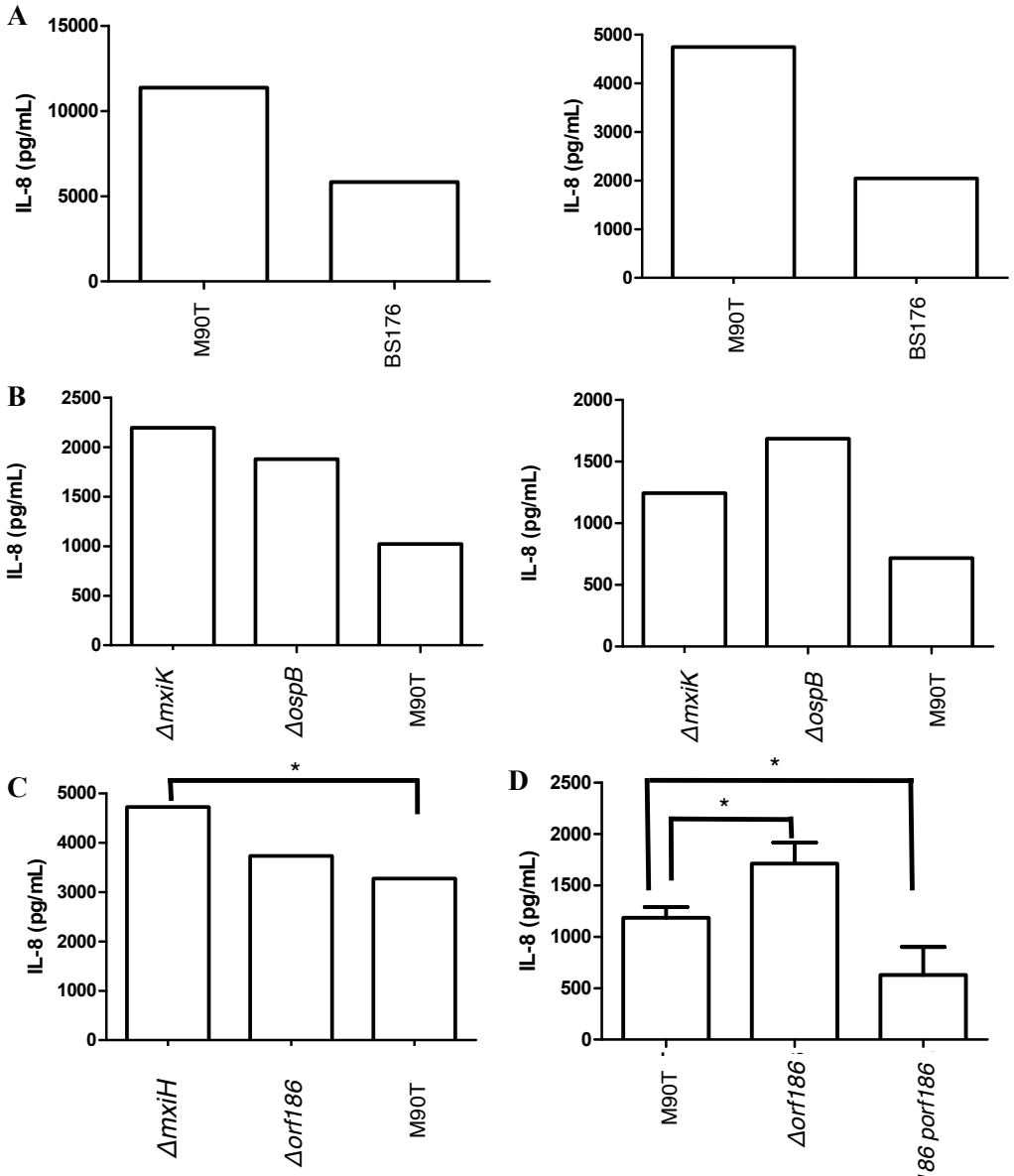

Figure 15: (A) A strain of *S. flexneri* lacking the virulence plasmid (BS176) elicited less IL-8 from U937 cells than wild-type *S. flexneri* (M90T) in two independent experiments. **(B)** Deletion mutants for the genes *mxiK* and *ospB* elicited more IL-8 from U937 cells than M90T in two independent experiments. **(C)** A deletion mutant for the gene *mxiH* elicited more IL-8 than M90T, and this difference was significant. **(D)** A deletion mutant for the gene *orf186* elicited more IL-8 from U937 cells than M90T, and the complemented mutant elicited less. These differences were significant. Complementation of the *orf186* mutant was performed by Julie Ryu. * = $0.01 < P < 0.05$. Statistical methods are outlined in Chapter 2.19.

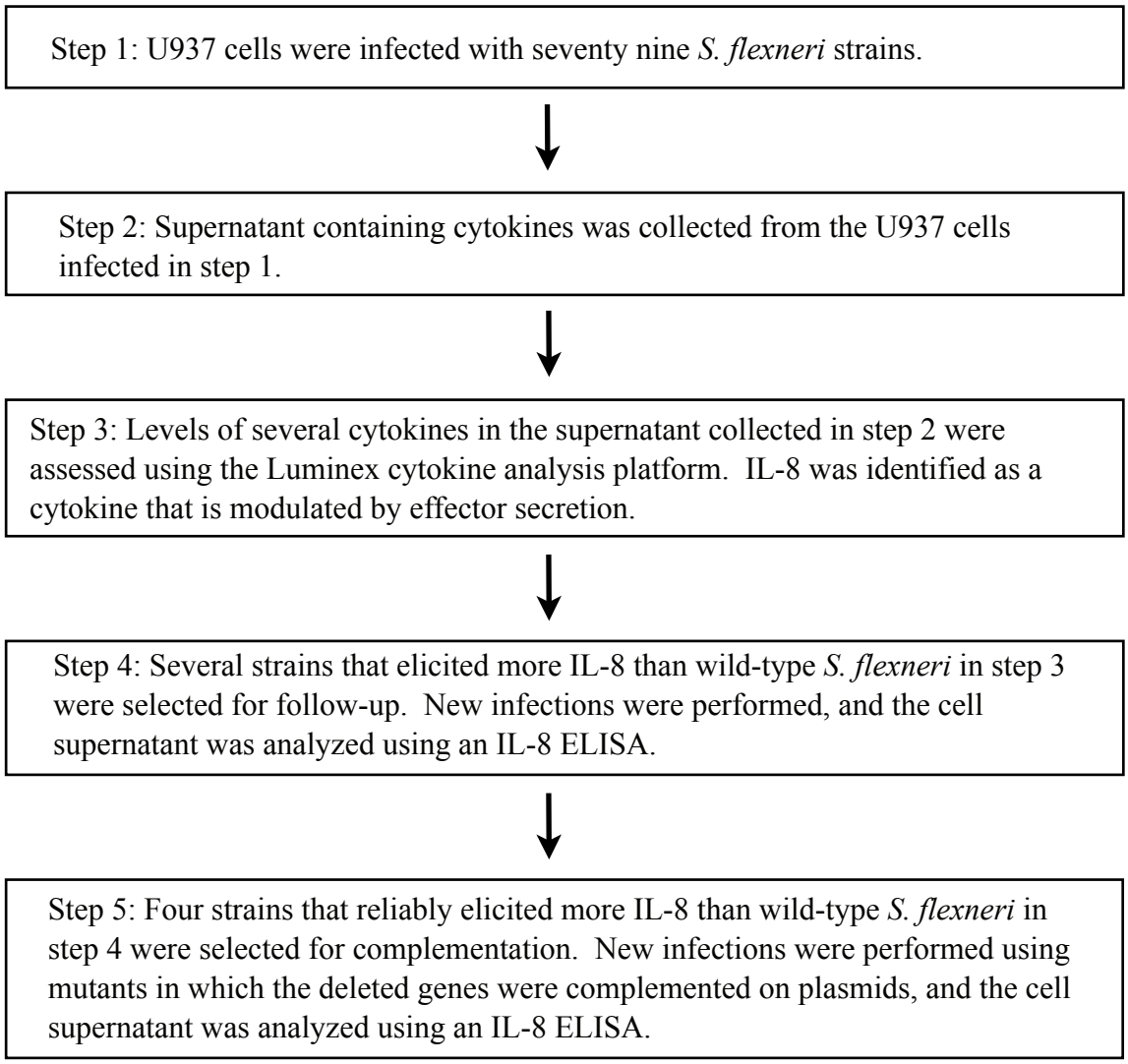

Figure 16 An outline of the strategy used to identify *S. flexneri* deletion mutants that elicited more IL-8 from U937 cells than wild-type.

Chapter 4: Discussion

4.1: Protoarrays as Tools for Identifying Functions of Effectors

Attempts to definitively validate several putative targets of IpaH7.8 identified through protoarrays were unsuccessful. Seven putative substrates did not appear to be ubiquitinated in a reconstituted system, and immunoprecipitations performed against four of these proteins also failed to reveal evidence of ubiquitination. The former is a curious finding, given that ubiquitinating a protein on a chip should be very similar to ubiquitinating a protein in a test tube. One difference in these two systems arises from the fact that the proteins on the protoarray chips were isolated from insect cells, whereas I isolated the proteins used in my *in vitro*-ubiquitination reactions from *E. coli*. Specifically, there may be eukaryotic-specific modifications on the proteins on the protoarray that govern IpaH recognition. However, it seems unlikely that this could explain the inability of IpaH7.8 to ubiquitinate all seven of the hits that I tested. Similarly, it is possible that the cell lines I chose to use when performing immunoprecipitations of the putative targets are not cell lines in which IpaH7.8 is active. Again, this seems unlikely, as epithelial cells and macrophages were chosen because they are among the main cell types infected by *S. flexneri* (Sansonetti, 2001).

Some of the proteins that I attempted to ubiquitinate *in vitro* are known to interact with ubiquitin in the absence of an E3 ubiquitin ligase. For example, p62 binds to ubiquitin chains and links the structures to which they are attached with autophagosomes (Zheng *et al*, 2009). Perhaps proteins such as p62 appeared in the list of hits because of the presence of ubiquitin in the reaction mixture, not because of the presence of IpaH7.8.

A control in which a chip is exposed to a reaction mixture containing only FITC-labeled ubiquitin could have been used to address this question. However, protoarray chips cost several thousand dollars each, and performing controls that were not strictly necessary was not an option. Another potential source of error associated with the protoarray screens stemmed from the fact that I lacked information regarding how much of each protein was present on each spot. Invitrogen adjusts the amount of protein per spot to account for differences in the intrinsic fluorescent intensities of different proteins, and so it is possible that some of the proteins that appeared among the top hits were identified only because larger amounts of protein were present on those spots than on others.

Gupta *et al* (2007) and Persaud *et al* (2009), who successfully used protoarrays to identify targets of HECT-domain E3 ubiquitin ligases, had an advantage in that the enzymes they were studying were known to recognize proteins containing (L/P)PXY motifs. Another example of an E3 ubiquitin ligase recognizing a particular sequence, or "degron," is the SCF complex, which targets proteins containing a (I/L)(I/L/P)pTP[K/R]$_4$ sequence, where pT indicates phosphorylated threonine and square brackets indicate disfavoured residues (Tang *et al*, 2005). Whether or not the IpaHs recognize a degron is an open question. The SCF E3 ligase illustrates another critical factor involved in identifying substrates of some E3 ubiquitin ligases. This complex binds phosphorylated substrates with a much higher affinity than their non-phosphorylated counterparts (Carrano *et al*, 1999). A similar situation is found with the E3 ubiquitin ligase RNF4, which recognizes proteins modified by conjugation to the ubiquitin-like protein Sumo (Tatham *et al*, 2008). Similarly, if the IpaHs do recognize a degron, it may also contain post-translational modifications. If, in the future, such structural information regarding

the IpaHs is discovered, results obtained through protoarray screens will be easier to assess, and hits worthy of follow-up will be easier to identify.

Despite difficulty ubiquitinating putative substrates of IpaH7.8 *in vitro*, levels of several of these proteins dropped over the course of a three-hour infection in HeLa cells using wild-type *S. flexneri*. This drop was not observed in similar infections using a *ΔmxiE* strain of *S. flexneri*, in which transcription of the *ipaHs* is greatly decreased. However, this effect was not reproduced reliably. Perhaps the IpaHs require some yet-unknown stimulus to become active that was fortuitously present during several infections. This stimulus could be related to the density of the cells being infected or to the multiplicity of infection.

Phenotypes associated with *ΔipaH7.8* mutants, such as the defect in vacuole escape observed by Fernandez-Prada *et al* (2000) or the reduced toxicity to macrophages observed by Paetzold *et al* (2007), could be useful in identifying the function of this effector. Future studies could capitalize on these phenotypes by using a forward-genetics approach to identify cellular factors associated with these phenotypes. For example, siRNA could be used to reduce translation of mammalian proteins known to be involved in vacuole formation and maintenance, and one could look to see if the difference in vacuole escape between wild-type *S. flexneri* and a *ΔipaH7.8* mutant is eliminated. Classical methods of identifying protein-protein interactions, such as a Yeast-Two-Hybrid screen, could also be employed to identify IpaH7.8's interacting partners. The issue associated with this technique is that substrates of IpaH7.8 will, presumably, be quickly destroyed by the proteasome, and so their interaction may be too transient to be identified. However, the known substrates of IpaH9.8 and SspH1, Nemo and PKN1, were both identified using Yeast-Two-Hybrid screens using either portions of the E3 ligase or

catalytically dead E3s, so there is reason to believe that this method could be used with a modified version of IpaH7.8. SILAC, a technique involving stable isotope labeling linked to mass spectrometry (Ong *et al*, 2002), could also be applied to the identification of substrates of IpaH7.8. SILAC involves comparing proteins from two treatment groups, one of which comes from cells that have incorporated an isotopically-labeled amino acid into their proteins. The change in mass resulting from the labeled amino acid can be detected by mass spectrometry, and this can be used to differentiate between proteins from the two groups. Levels of corresponding proteins from the two groups can then be compared. We could use this to look for proteins that are ubiquitinated in cells infected with wild-type *S. flexneri*, but not ubiquitinated upon infection with a strain lacking *ipaH7.8*. This method has been used successfully for the identification of substrates of E3 ubiquitin ligases in the past. For example, Tatham and coworkers (2008) used SILAC to identify substrates of the mammalian E3 ubiquitin ligase RNF4. By combining results from the protoarray screens with results from a Yeast-2-Hybrid screen or SILAC, we may be able to find putative substrates identified using more than one screening technique, which would provide strong rationale for following up on those hits.

4.2: IpaH7.8 and Autophagy

The protoarray screens for substrates of IpaH7.8 identified proteins such as p62, Tal and Cortactin that play roles in autophagy. This combined with the observations made by Fernandez-Prada and coworkers (2000) regarding a relationship between IpaH7.8 and a vesicle-related process prompted me to examine the relationship between IpaH7.8 and autophagy. However, I did not observe an association between *ΔipaH7.8* or *ΔmxiE S. flexneri* and the autophagosome marker LC3. However, high levels of LC3

punctae observed in an uninfected control lead me to question the validity of this experiment. LC3 is usually dispersed throughout the cytosol when cells are not under conditions of stress, and so these LC3 punctae may indicate that I inadvertently placed the cells under non-optimal conditions, such as those associated with low nutrient levels. This could be the result of a step in our infection protocol, such as washes in serum-free media that we perform to remove dead cells prior to infection, or a shift from 37°C to room temperature that occurs for approximately half an hour at the time of infection to synchronize the bacterial invasion of the cells. This issue should be addressed if this experiment is repeated.

It was also difficult to tell if the bacteria used to infect were inside the HeLa cells, or simply sticking to the outsides. Dr. Armelle Phalipon's group has solved this problem by infecting with GFP-expressing *S. flexneri,* then staining *S. flexneri* with an antibody against Lipopolysaccharide and a secondary antibody conjugated to Alexa Fluor 350 before permeabilizing tissue culture cells. Alexa Fluor 350 appears blue, and so *S. flexneri* outside cells will appear in both the blue and green channels, whereas *S. flexneri* inside cells will only appear in the green channel (Konradt *et al*, 2011). Using this system would be propitious if subsequent experiments of this type are performed.

The conversion of LC3-I to LC3-II also did not differ between HeLa cells infected with wild-type *S. flexneri* or *ΔmxiE S. flexneri*. These experiments may have been subject to the same caveats discussed above for the fluorescent colocalization experiment, and, if they are repeated, a control in which cells are treated with rapamycin to induce autophagy would help elucidate such potential problems.

Finally, indicators of autophagic flux other than those associated with LC3 in epithelial cells should be examined before ruling out the possibility that the IpaHs affect

autophagy. For example, autophagy is involved in antigen processing and display on Major Histocompatibility Complexes (Münz, 2006). Some pathogens, such as *S. enterica*, interfere with antigen processing, thereby reducing the ability of antigen-presenting cells to activate T-cells (Cheminay *et al*, 2005). It is possible that an interaction between the IpaHs and the autophagy machinery could result in reduced antigen presentation without affecting the total number of autophagosomes that are associated with the more heavily studied autophagy-associated process of xenophagy. In this case, antigen-presenting cells, such as dendritic cells, would be a more appropriate model than epithelial cells, and the ability of these cells to activate T cells could be a more appropriate read-out than LC3 localization or conversion of LC3-I to LC3-II.

4.3: Cytokines Regulated by Virulence Factors

I have identified CCL3, CCL8 and M-CSF as cytokines that may be produced in lower quantities by U937 cells infected with wild-type *S. flexneri* than those infected with a strain lacking the virulence plasmid (BS176). Conversely, CXCL5 may be produced in a higher quantity in wild-type *S. flexneri* infected cells than BS176-infected. While these results were acquired through a qualitative approach (RayBiotech cytokine antibody array screening), they provide starting points for future projects.

M-CSF, or Macrophage Colony Stimulating Factor, is a cytokine involved in stimulating the differentiation of hematopoietic stem cells into macrophages (Stanley *et al*, 1998). CCL8 is a chemokine capable of attracting a wide range of immune cells including T cell subsets, NK cells, eosinophils and basophils to the site of infection (Proost *et al*, 1996). In addition, an N-terminally truncated form of CCL8 is able to inhibit the activities of other cytokines such as CCL2 (MCP-1), CCL7 (MCP-3) and

CCL5, as well as non-truncated CCL8 (Proost *et al*, 1998). M-CSF and CCL8 could make contributions to the host's ability to eliminate *S. flexneri*, and so this pathogen may have evolved the ability to block production of these cytokines to avoid premature clearance. These results may inform hypothesis-based research in the area of immune evasion by *S. flexneri*.

The involvement of CCL3 and CXCL5 in *S. flexneri* infection is also not surprising. Both of these cytokines are chemotactic for neutrophils: a type of immune cell that plays a major role in the clearance of *S. flexneri* (Haelens *et al*, 1996, Walz, 1991). Pore *et al* (2010) have shown that macrophages release CCL3 upon treatment with a protein called MOMP that is found on the outer membrane of *S. flexneri*. My results indicate that a factor encoded by the virulence plasmid may partially counteract the effect of MOMP, thereby reducing levels of CCL3 produced by infected macrophages (Table 9).

CXCL5 is a major cytokine produced by intestinal epithelial cells (Z'Graggen *et al*, 1997) that shares many similarities with IL-8. Besides sharing a high degree of sequence similarity, both cytokines are encoded by a region of chromosome four, the promoters for both are bound, and activated, by NF-κB, and both are chemotactic for neutrophils (Chang *et al*, 1994, Walz *et al*, 1991). Given my results showing that wild-type *S. flexneri* elicits higher levels of IL-8 than a strain lacking the virulence plasmid, observing the same trend with the highly similar cytokine CXCL5 is logical.

4.4: The *S. flexneri* Deletion Collection as a Tool for Studying Pathogenesis

Deletion collections have become an important tool for studying genetics in organisms such as *S. cerevisiae* and *E. coli* (e.g., Glaever *et al*, 2002, Steinmetz *et al*,

2002, Tong *et al*, 2001, Baba *et al*, 2006, Typas *et al*, 2008). Results presented here show the utility of the newly-created *S. flexneri* deletion collection in studying bacterial pathogenesis.

I assessed the ability of ninety six *S. flexneri* mutants to bind the dye Congo red. Congo red activates Type III Secretion, and the ability of a strain to sequester Congo red has been correlated with virulence and with an ability to secrete effectors (Parsot *et al*, 1995). There are examples of effectors that, once secreted, can regulate release of other virulence factors. For example, YopK is an effector from *Yersinia pseudotuberculosis* that docks at the interface of the bacterium and the host cell and regulates the passage of other effectors through the T3SS (Holmström *et al*, 1997). Therefore, there was a precedent that led us to believe we might find an effector that would have a similarly global effect on secretion. The most Congo red-positive strain identified in this screen was a mutant for *ipaD*, which has previously been show to hypersecrete effectors in the presence of Congo red (Ménard *et al*, 1993). Mutants for *virF* and *virB*, two transcription factors that are necessary for expression of components of the T3SS (Adler *et al*, 1989), were among the most Congo red-negative strains. These results were satisfying, and gave me confidence in this technique.

Several genes of unknown function, such as *orf157, orf137* and *orf163* were more Congo red-positive than wild-type *S. flexneri*, indicating that the proteins encoded by these genes may regulate secretion of one or several other effectors. However, most of the mutants that I screened were more Congo red-negative than wild-type *S. flexneri*. This is logical, as most genes encoded by the virulence plasmid are thought to be involved in virulence. Two families of effectors, the IpaHs and the OspDs, had members that behaved differently than the rest. A *ΔipaH1.4* mutant was as Congo red-negative as

mutants for components of the T3SS such as *Δspa40* and *Δspa33*. Other *ipaH* mutants, including a mutant for *ipaH2.5*, a gene that has a nucleotide sequence nearly identical to that of *ipaH1.4,* behaved similarly to wild-type *S. flexneri*. In addition, *ΔospD2*, a mutant for a gene of unknown function (Buchreiser *et al*, 2000) was more Congo red-negative than either *ΔospD1* or *ΔospD3*. In both cases, these results indicate that there are factors that set *ipaH1.4* and *ospD2* apart from other closely-related genes. One such factor could be differences in the levels of the proteins produced by these genes.

As a second proof-of-principle experiment, I used the Luminex cytokine analysis platform to measure levels of IL-8, IL-6, TNFα, G-CSF, EGF and CCL24 elicited from U937 cells infected with strains from the *S. flexneri* deletion collection. IL-8 levels were found to be high (between 500 and 1,500 pg/mL) for most strains. However, levels of all other cytokines were low (under 20 pg/mL) or too low to be quantified. I selected four mutants that elicited high levels of IL-8, and confirmed these results by ELISA. Among these was a *ΔospB* mutant, which was previously shown to elicit higher levels of IL-8 than wild-type *S. flexneri* upon infection of epithelial cells (Zurawski *et al*, 2009). My results are consistent with the published literature, and show that high levels of IL-8 can be observed in association with a *ΔospB* mutant upon infection of macrophages as well as epithelial cells. The significance of other results associated with this screen will be discussed in Chapter 4.5.

The low levels of TNFα, IL-6, CCL24, G-CSF and EGF observed in the Luminex screen were disappointing, as we were unable to look for effectors that change levels of these cytokines. However, we can use these negative results to gain information regarding the signaling pathways activated by *S. flexneri* in U937 cells.

IL-8, IL-6 and TNF are regulated by complex combinations of transcription factors. The promoter regions for the genes encoding all three of these cytokines have been shown to include binding sites for the transcription factors NF-κB and C/EBP (Smith *et al*, 2001, Trede *et al*, 1995, Sitaraman *et al*, 2001). This region of the promoter is necessary and sufficient to induce transcription of the gene encoding IL-8 (Mukaida *et al*, (1990). In the cases of IL-6 and TNFα, the transcription factor Sp1 is also necessary to induce transcription (Borgatti *et al*, 2007, Tsai *et al*, 2000). This implies that NF-κB and C/EBP are able to promote transcription in response to *S. flexneri* infection in U937 cells, but perhaps Sp1 is inactive. It is plausible that *S. flexneri* interferes with Sp1 production so as to reduce levels of certain proinflammatory cytokines.

Regulation of the gene encoding CCL24 appears relatively straight-forward compared to IL-8, IL-6 and TNFα. CCL24 expression is dependent on the transcription factor STAT6 (Zimmermann *et al*, 2000). My results suggest that *S. flexneri* interferes with factors involved in the JAK/STAT signaling program.

S. flexneri may also prevent secretion of IL-6, TNFα, G-CSF, CCL24 and EGF post-translationally. Cytokines exit cells through a number of pathways. For example, Murray and coworkers (2005) have shown that TNFα is delivered to the plasma membrane in vesicles associated with Vesicle-Associated Membrane Protein 3, or VAMP3. Perhaps this pathway has been altered in cells infected with *S. flexneri*. In addition, Murray and coworkers (2005b) identified Syntaxin 6 and Vti1b, two SNARE proteins, as regulators of TNFα secretion from macrophages, raising the possibility that *S. flexneri* prevents one of these two proteins from functioning. Further research on cytokines that are modulated by *S. flexneri's* effectors should address both pre- and post-translational factors that regulate secretion.

Part of the value of deletion collections originates in the user's ability to investigate proteins that would otherwise go un-studied. For example, I would never have thought to look at Orf186, one of the virulence encoded factors that I connected with altered levels of IL-8 produced by U937 cells, had it not been identified through a screen involving the deletion collection. In addition, my screen for the Congo red phenotype shows that some techniques that are normally applied to only a few strains can be scaled to a high-throughput format in order to take advantage of the deletion collection. The Congo red phenotype is normally used mainly to confirm that the strain being worked with is still virulent, and has not acquired a mutation that changes effector secretion. Here, I show that by scaling this technique to the 96-well format I was able to take advantage of the deletion collection and gain information that could elucidate the functions of several effectors. The Luminex screen for factors that alter IL-8 production by U937 cells shows that multiplexing, or using the same sample to perform more than one assay at a time, can be used to further enhance the versatility of the deletion collection.

4.5: Virulence Factors that Affect IL-8 Production

I identified *ΔmxiH, ΔmxiK, Δorf186* and *ΔospB* as *S. flexneri* mutants that elicit higher levels of IL-8 from infected U937 cells than wild-type *S. flexneri*. Similar results were previously obtained when using a *ΔospB* mutant to infect epithelial cells (Zurawski *et al*, 2009), and my results show that OspB is involved in reducing levels of IL-8 produced by macrophages, as well. Zurawski *et al* (2009) attributed this decrease in IL-8 to the ability of OspB to interact with a modulator of transcription called Retinoblastoma Protein, or Rb. They hypothesize that these two proteins, along with the *S. flexneri*

effector OspF, remodel chromatin, thereby reducing transcription of *interleukin-8*. Further research could involve testing the theory that OspB and Rb also interact in macrophages, so as to determine whether or not the mechanism by which OspB reduces IL-8 levels in macrophages is the same as in epithelial cells. A BLAST search using the amino acid sequence of OspB reveals homologues in other gastrointestinal pathogens such as *Vibrio cholerae,* Enterohemmorhagic *Escherichia coli* and *Salmonella enterica*, indicating that knowledge regarding this protein could expand our understanding of other diseases as well as shigellosis.

MxiH is a component of the Type III Secretion System needle apparatus (Blocker *et al,* 2001) and MxiK is required for assembly of the needle (Jouihri *et al*, 2003). While mutants for *mxiH* and *mxiK*, which lack needle complexes, elicit more IL-8 than wild-type *S. flexneri*, BS176, a strain lacking the needle complex entirely, elicited less IL-8 in experiments I performed. However, others in the Rohde lab have observed the opposite trend in BS176 infections. The reasons behind this discrepancy are not known. If BS176 does elicit less IL-8 than M90T, this implies that one or more factor(s) encoded on the virulence plasmid elicit IL-8 production in a T3SS-independent manner. In addition, it appears as though assembly of the needle structure can reduce this effect, most likely due to the efficient delivery of one or more effectors secreted through this system. A model in which BS176 elicits more IL-8 than M90T is simpler, as this would mean that that eliminating the T3SS causes *S. flexneri* to elicit more IL-8, with or without eliminating the effectors that pass through it.

MxiH and MxiK are encoded by a part of the virulence plasmid known as the "entry region," which contains a large number of densely-packed genes (Buchrieser *et al*, 2000). Due to the close spatial proximity of these genes, it seems likely that *mxiH* and

mxiK may be part of an operon, meaning a cluster of genes under the control of a single promoter. In situations such as this, it can be difficult to ensure that deleting one gene does not affect transcription of the surrounding genes. Therefore, complementation of these deletions is essential if we are to attribute increased levels of IL-8 to mutations in *mxiH* and *mxiK* specifically. Mutants for two genes encoded between *mxiH* and *mxiK*, *mxiI* and *mxiJ,* also elicited high levels of IL-8 when assessed by Luminex, although I did not confirm these results by ELISA. This may indicate that the increased levels of IL-8 that I observed are attributable to loss of the needle structure generally, rather than deletions in *mxiH* and *mxiK* specifically. Miao and coworkers (2010) recently found that, in macrophages, MxiI, a component of the T3SS, is recognized by the intracellular pattern recognition receptor NLRC4, or Ipaf. This leads to activation of Caspase 1: a necessary step in the signaling pathway leading to pyroptosis. Perhaps the induction of pyroptosis precludes secretion of maximal levels of IL-8.

Orf186 has not been characterized in *S. flexneri*, but its close homologue in *Enteropathic E. coli* is known to modify Lipopolysaccharide, or LPS, which suggests that Orf186 may serve a similar function. *Orf186* is part of an operon that includes the gene *msbB2*, which encodes a protein that is known to modify LPS (Goldman *et al*, 2008, d'Hauteville *et al*, 2002). Genes in operons often have similar functions (Lodish *et al*, 2004), and so the function of MsbB2 supports this hypothesis regarding the role of Orf186. The homologue of Orf186 from *E. coli*, WabB, is responsible for addition of an N-acetylglucosamine (GlcNAc) group to the inner core oligosaccharide of LPS (Kaniuk *et al*, 2004). Toll-like Receptor Four (TLR4) is the main receptor for LPS found on mammalian immune cells (Hoshino *et al*, 1999). This interaction takes place in association with several cofactors: LPS Binding Protein (LBP), CD14 and MD-2 (Lu *et*

al, 2008). Perhaps the addition of a GlcNAc group to LPS reduces the ability of either TLR4 or one of these cofactors to bind LPS, thereby reducing the ability of U937 cells to respond to *S. flexneri.*

Effectors that modify external saccharides and lipids have been found in other pathogens, as well. For example, *Yersinia pestis* alters the lipid A portion of LPS from being hexa-aceylated to being penta- or tetra-aceylated in response to a shift from 21°C to 37°C. Penta- and tetra-aceylated lipid A elicit less TNF than hexa-aceylated lipid A in mammalian hosts, whereas hexa-aceylated lipid A is thought to protect against killing by antimicrobial peptides while *Y. pestis* inhabits insect hosts (Rebeil *et al*, 2004). Another example of effectors causing immune evasion by modification of external molecules is the effector PgdA from *Listeria monocytogenes*, which causes N-deacetylation of peptidoglycan: the thick layer of sugars and amino acids that forms the external layer of gram-positive bacteria (Boneca *et al*, 2007, White, 2007). This interferes with the recognition of peptidoglycan by the intracellular pattern recognition receptors Nod1 and Nod2. The virulence of a *ΔpgdA* mutant of *L. monocytogenes* is highly attenuated (Boneca *et al*, 2007).

The different serotypes of *S. flexneri* and other *Shigella* species are determined based on the structure of the O-antigen component of LPS (Lindbert *et al*, 1991). Protection against reinfection is serotype-specific, indicating that the immune response to *S. flexneri* depends heavily on the structure of LPS. This has been a major impediment in the development of a vaccine offering broad protection against shigellosis (Germani and Sansonetti, 2011). Variations in the O-antigen can have dramatic effects on the virulence of *S. flexneri*. For example, replacing the O-antigen of *S. flexneri* with that of *E. coli* strain O8 eliminated the ability of the bacterium to invade epithelial cells and cause

inflammation when applied to a rabbit's eye (Lindbert *et al*, 1991). However, attempts to create vaccines by expressing the O-antigens of *S. flexneri* in commensal *E. coli* failed to protect vaccinated volunteers (Germani and Sansonetti, 2011), indicating that the O-antigen is necessary but not sufficient to elicit immunological memory. Therefore, knowledge regarding modifications to the O-antigen and other external molecules found on *S. flexneri*, such as those that may result from the actions of Orf186, could be valuable in the context of vaccine development.

4.6: Conclusions

This thesis covers four areas of research related to *S. flexneri*: the use of protoarrays to identify substrates of IpaH7.8, the identification of cytokines that may have their production altered by effectors, validation of an *S. flexneri* deletion collection as a tool for studying bacterial pathogenesis, and identification of effectors that alter production of IL-8.

Protoarrays were an ineffective tool for the identification of substrates of IpaH7.8. I was not able to replicate results obtained through protoarrays either *in vitro* or reproducibly using tissue culture. In addition, despite the presence of many proteins involved in autophagy in the results of the protoarray screens, I did not find an association between IpaH7.8 and autophagy. However, information regarding the mechanisms by which the IpaHs function may be embedded in these negative results. The contrast between the success of using protoarrays to identify substrates of HECT domain E3s (Gupta *et al*, 2007) and our experience implies that we are missing a piece of information regarding how the IpaHs function. This could be used as motivation to look for other bacterial effectors that function in combination with the IpaHs, or to look for post-

translational modifications on known substrates of the IpaHs and their homologues that may influence their interactions with the IpaHs.

Work regarding the identification of cytokines that may be affected by factors encoded by the virulence plasmid was more successful. I identified CCL8, CCL3, CXCL5 and M-CSF as cytokines that may have their production altered in U937 cells by secreted effectors. Confirmation of these findings, and investigation into which effectors are responsible for altering their levels upon infection of U937 cells, could be useful directions for future research.

In contrast to the protoarray screens, the deletion collection proved to be an effective tool for studying *S. flexneri* pathogenesis. I used the deletion collection to obtain new information about the ability of ninety six *S. flexneri* mutants to bind the dye Congo red, and performed a screen for effectors that change production of the cytokine IL-8. Results obtained from the Congo red screen included the fact that mutants for *ipaH1.4* and *ospD2* behaved differently than mutants for other genes included in their respective families. This implies that sequence similarity between these genes and others like them may not indicate that the proteins they encode have similar functions.

I identified four mutants that elicit higher levels of IL-8 from U937 cells than wild-type *S. flexneri.* These four mutants have deletions in the genes *mxiH, mxiK, orf186* and *ospB*. A complemented *Δorf186* mutant elicits significantly lower levels of IL-8 than the non-complemented strain, indicating that this effect can indeed be attributed to Orf186. Complementation of the remainder of these mutants and identification of the mechanisms by which the effectors these genes encode alter IL-8 production could prove to be valuable contributions to the field.

Shigellosis is a global health problem (Kotloff *et al*, 1999, Sansonetti, 2001), and therefore research related to the pathogenicity of *S. flexneri* could help raise standards of living, particularly in the developing world. My results elucidate several ways in which *S. flexneri's* effectors interact with immune cells and with *S. flexneri* itself. For example, I have demonstrated that Orf186, which is hypothesized to modify *S. flexneri's* LPS, can modulate elicitation of cytokines from U937 cells. This is one small step along the road to completing our understanding of shigellosis and how this disease can be prevented. In addition, *S. flexneri* is an easy pathogen to grow and manipulate genetically, which makes it a useful model for studying bacteriology in general. Therefore, extending research performed using *S. flexneri* to other pathogens could produce useful results. OspB, for example, is an effector that has homologues in many pathogens, and so research regarding the function of OspB in *S. flexneri* can be extended to many other fields of bacteriology. As the Rohde lab grows, the methods I have developed and the results I have obtained will provide starting points for future students who will undoubtedly reveal new and fascinating aspects of bacteriology.

References:

Adam, T., Arpin, M., Prevost, M.C., Gounon, P., and Sansonetti, P.J. (1995). Cytoskeletal rearrangements and the functional role of T-plastin during entry of *Shigella flexneri* into HeLa cells. J Cell Biol 129, 367-381.

Adler, B., Sasakawa, C., Tobe, T., Makino, S., Komatsu, K., and Yoshikawa, M. (1989). A dual transcriptional activation system for the 230 kb plasmid genes coding for virulence-associated antigens of *Shigella flexneri*. Mol Microbiol 3, 627-635.

Allaoui, A., Mounier, J., Prevost, M.C., Sansonetti, P.J., and Parsot, C. (1992). *IcsB:* a *Shigella flexneri* virulence gene necessary for the lysis of protrusions during intercellular spread. Mol Microbiol 6, 1605-1616.

Amit, I., Yakir, L., Katz, M., Zwang, Y., Marmor, M.D., Citri, A., Shtiegman, K., Alroy, I., Tuvia, S., Reiss, Y., Roubini, E., Cohen, M., Wides, R., Bacharach, E., Schubert, U. and Yarden, Y. (2004). Tal, a Tsg101-specific E3 ubiquitin ligase, regulates receptor endocytosis and retrovirus budding. Genes & Development 18, 1737-1752.

Arbibe, L., Kim, D.W., Batsche, E., Pedron, T., Mateescu, B., Muchardt, C., Parsot, C., and Sansonetti, P.J. (2007). An injected bacterial effector targets chromatin access for transcription factor NF-kappaB to alter transcription of host genes involved in immune responses. Nat Immunol 8, 47-56.

Ashida, H., Kim, M., Schmidt-Supprian, M., Ma, A., Ogawa, M., Sasakawa, C. (2009). A bacterial E3 ubiquitin ligase IpaH9.8 targets NEMO/IKKgamma to dampen the host NF-kB-mediated inflammatory response. Nature Cell Biology 12, 66-75.

Baba, T., Ara, T., Hasegawa, M., Takai, Y., Okumura, Y., Baba, M., Datsenko, K.A., Tomita, M., Wanner, B.L., and Mori, H. (2006). Construction of *Escherichia coli* K-12 in-frame, single-gene knockout mutants: the Keio collection. Mol Syst Biol 2, 2006 0008.

Baeuerle, P.A., and Henkel, T. (1994). Function and activation of NF-kappa B in the immune system. Annu Rev Immunol 12, 141-179.

Beatty, W.L., and Sansonetti, P.J. (1997). Role of lipopolysaccharide in signaling to subepithelial polymorphonuclear leukocytes. Infect Immun 65, 4395-4404.

Behrends, C., and Harper, J.W. (2011). Constructing and decoding unconventional ubiquitin chains. Nat Struct Mol Biol 18, 520-528.

Bernal-Bayard, J., and Ramos-Morales, F. (2009). *Salmonella* type III secretion effector SlrP is an E3 ubiquitin ligase for mammalian thioredoxin. J Biol Chem 284, 27587-27595.

Bernassola, F., Karin, M., Ciechanover, A., and Melino, G. (2008). The HECT family of E3 ubiquitin ligases: multiple players in cancer development. Cancer Cell 14, 10-21.

Blocker, A., Jouihri, N., Larquet, E., Gounon, P., Ebel, F., Parsot, C., Sansonetti, P., and Allaoui, A. (2001). Structure and composition of the *Shigella flexneri* "needle complex", a part of its type III secreton. Mol Microbiol 39, 652-663.

Boneca, I.G., Dussurget, O., Cabanes, D., Nahori, M.A., Sousa, S., Lecuit, M., Psylinakis, E., Bouriotis, V., Hugot, J.P., Giovannini, M., et al. (2007). A critical role for peptidoglycan N-deacetylation in *Listeria* evasion from the host innate immune system. Proc Natl Acad Sci U S A 104, 997-1002.

Borgatti, M., Bezzerri, V., Mancini, I., Nicolis, E., Dechecchi, M.C., Lampronti, I., Rizzotti, P., Cabrini, G., and Gambari, R. (2007). Induction of IL-6 gene expression in a CF bronchial epithelial cell line by *Pseudomonas aeruginosa* is dependent on transcription factors belonging to the Sp1 superfamily. Biochem Biophys Res Commun 357, 977-983.

Buchrieser, C., Glaser, P., Rusniok, C., Nedjari, H., D'Hauteville, H., Kunst, F., Sansonetti, P., and Parsot, C. (2000). The virulence plasmid pWR100 and the repertoire of proteins secreted by the type III secretion apparatus of *Shigella flexneri*. Mol Microbiol 38, 760-771.

Canton, R., and Lumb, J. (2011). Emerging resistance in Gram-negative pathogens and implications for clinical practice. Future Microbiol 6, 19-22.

Carrano, A.C., Eytan, E., Hershko, A., and Pagano, M. (1999). SKP2 is required for ubiquitin-mediated degradation of the CDK inhibitor p27. Nat Cell Biol 1, 193-199.

Casselli, T., Lynch, T., Southward, C.M., Jones, B.W., and DeVinney, R. (2008). *Vibrio parahaemolyticus* inhibition of Rho family GTPase activation requires a functional chromosome I type III secretion system. Infect Immun 76, 2202-2211.

Center for Disease Control (2009) Shigellosis www.cdc.gov/nczved/divisions/dfbmd/diseases/shigellosis/ (Accessed March 3, 2012)

Chang, M.S., McNinch, J., Basu, R., and Simonet, S. (1994). Cloning and characterization of the human neutrophil-activating peptide (ENA-78) gene. J Biol Chem 269, 25277-25282.

Cheminay, C., Mohlenbrink, A., and Hensel, M. (2005). Intracellular *Salmonella* inhibit antigen presentation by dendritic cells. J Immunol 174, 2892-2899.

Cherepanov, P.P., and Wackernagel, W. (1995). Gene disruption in *Escherichia coli*: TcR and KmR cassettes with the option of Flp-catalyzed excision of the antibiotic-resistance determinant. Gene 158, 9-14.

Clark, J.M. (1988). Novel non-templated nucleotide addition reactions catalyzed by procaryotic and eucaryotic DNA polymerases. Nucleic Acids Res 16, 9677-9686.

Datsenko, K.A., and Wanner, B.L. (2000). One-step inactivation of chromosomal genes in Escherichia coli K-12 using PCR products. Proc Natl Acad Sci U S A *97*, 6640-6645.

D'Hauteville, H., Khan, S., Maskell, D.J., Kussak, A., Weintraub, A., Mathison, J., Ulevitch, R.J., Wuscher, N., Parsot, C., and Sansonetti, P.J. (2002). Two *msbB* genes encoding maximal acylation of lipid A are required for invasive *Shigella flexneri* to mediate inflammatory rupture and destruction of the intestinal epithelium. J Immunol 168, 5240-5251.

Dehio, C., Prévost, M.C. and Sansonetti, P.J. (1995). Invasion of epithelial cells by *Shigella flexneri* induces tyrosine phosophorylation of cortactin by a pp60c-src-mediated signalling pathway. The EMBO Journal 14, 2471-2482.

Deshaies, R.J., and Joazeiro, C.A. (2009). RING domain E3 ubiquitin ligases. Annu Rev Biochem 78, 399-434.

Diao, J., Zhang, Y., Huibregtse, J.M., Zhou, D., and Chen, J. (2008). Crystal structure of SopA, a *Salmonella* effector protein mimicking a eukaryotic ubiquitin ligase. Nat Struct Mol Biol 15, 65-70.

El-Gendy, A.M., Mansour, A., Weiner, M.A., Pimentel, G., Armstrong, A.W., Young, S.Y., Elsayed, N., and Klena, J.D. (2012). Genetic diversity and antibiotic resistance in *Shigella dysenteriae* and *Shigella boydii* strains isolated from children aged <5 years in Egypt. Epidemiol Infect 140, 299-310.

Fernandez-Prada, C.M., Hoover, D.L., Tall, B.D., Hartman, A.B., Kopelowitz, J., Venkatesan, M.M. (2000). *Shigella flexneri* IpaH7.8 Facilitates Escape of Virulent Bacteria from the Endocytic Vacuoles of Mouse and Human Macrophages. Infection and Immunity 2000, 3608 -- 3619.

Fink, S.L., and Cookson, B.T. (2005). Apoptosis, pyroptosis, and necrosis: mechanistic description of dead and dying eukaryotic cells. Infect Immun 73, 1907-1916.

Galan, J.E. (2009). Common themes in the design and function of bacterial effectors. Cell Host Microbe 5, 571-579.

Garrus, J.E., von Schwedler, U.K., Pornillos, O.W., Morham, S.G., Zavitz, K.H., Wang, H.E., Wettstein, D.A., Stray, K.M., Cote, M., Rich, R.L., et al. (2001). Tsg101 and the vacuolar protein sorting pathway are essential for HIV-1 budding. Cell 107, 55-65.

Germain, Y., Sansonetti, P.J. (2011). Live-Attenuated *Shigella* Vaccines. Is Encouraging Good Enough? In Replicating Vaccines, P.R. Dormitzer, ed. (Springer Basel), pp. 99 -- 117.

Gimenez-Ibanez, S., Hann, D.R., Ntoukakis, V., Petutschnig, E., Lipka, V., and Rathjen, J.P. (2009). AvrPtoB targets the LysM receptor kinase CERK1 to promote bacterial virulence on plants. Curr Biol 19, 423-429.

Girardin, S.E., Tournebize, R., Mavris, M., Page, A.L., Li, X., Stark, G.R., Bertin, J., DiStefano, P.S., Yaniv, M., Sansonetti, P.J., et al. (2001). CARD4/Nod1 mediates NF-kappaB and JNK activation by invasive *Shigella flexneri*. EMBO Rep 2, 736-742.

Girardin, S.E., and Philpott, D.J. (2004). Mini-review: the role of peptidoglycan recognition in innate immunity. Eur J Immunol 34, 1777-1782.

Glaever, G., Chu, A.M., Ni, L., Connelly, C., Riles, L., Veronneau, S., et al (2002). Functional profiling of the *Saccharomyces cerevisiae* genome. Nature 418, 387-391.

Gohre, V., Spallek, T., Haweker, H., Mersmann, S., Mentzel, T., Boller, T., de Torres, M., Mansfield, J.W., and Robatzek, S. (2008). Plant pattern-recognition receptor FLS2 is directed for degradation by the bacterial ubiquitin ligase AvrPtoB. Curr Biol 18, 1824-1832.

Goldman, S. R., Y. Tu, and Goldberg, M.B. (2008). Differential regulation by magnesium of the two MsbB paralogs of *Shigella flexneri*. J Bacteriol 190, 3526-3537.

Gupta, R., B Kus, C Fladd, J Wasmuth, R Tonikian, S Sidhu, NJ Krogan, J Parkinson, D Rotin (2007). Ubiquitination screen using protein microarrays for comprehensive identification of Rsp5 substrates in yeast. Molecular Systems Biology 3, 10.1038.

Hachani, A., Biskri, L., Rossi, G., Marty, A., Menard, R., Sansonetti, P., Parsot, C., Van Nhieu, G.T., Bernardini, M.L., and Allaoui, A. (2008). IpgB1 and IpgB2, two homologous effectors secreted via the Mxi-Spa type III secretion apparatus, cooperate to mediate polarized cell invasion and inflammatory potential of *Shigella flexenri*. Microbes Infect 10, 260-268.

Haelens, A., Wuyts, A., Proost, P., Struyf, S., Opdenakker, G., and van Damme, J. (1996). Leukocyte migration and activation by murine chemokines. Immunobiology 195, 499-521.

Haglund, K., Di Fiore, P.P., and Dikic, I. (2003). Distinct monoubiquitin signals in receptor endocytosis. Trends Biochem Sci 28, 598-603.

Haraga, A., and Miller, S.I. (2006). A *Salmonella* type III secretion effector interacts with the mammalian serine/threonine protein kinase PKN1. Cell Microbiol 8, 837-846.

Hemrajani, C., Marches, O., Wiles, S., Girard, F., Dennis, A., Dziva, F., Best, A., Phillips, A.D., Berger, C.N., Mousnier, A., et al. (2008). Role of NleH, a type III secreted effector from attaching and effacing pathogens, in colonization of the bovine, ovine, and murine gut. Infect Immun 76, 4804-4813.

Hernandez, L.D., Hueffer, K., Wenk, M.R., and Galan, J.E. (2004). *Salmonella* modulates vesicular traffic by altering phosphoinositide metabolism. Science 304, 1805-1807.

Hershko, A., and Ciechanover, A. (1998). The ubiquitin system. Annu Rev Biochem 67, 425-479.

Hicks, S.W., and Galan, J.E. (2010). Hijacking the host ubiquitin pathway: structural strategies of bacterial E3 ubiquitin ligases. Curr Opin Microbiol 13, 41-46.

High, N., Mounier, J., Prevost, M.C., and Sansonetti, P.J. (1992). IpaB of *Shigella flexneri* causes entry into epithelial cells and escape from the phagocytic vacuole. EMBO J 11, 1991-1999.

Hilbi, H., Moss, J.E., Hersh, D., Chen, Y., Arondel, J., Banerjee, S., Flavell, R.A., Yuan, J., Sansonetti, P.J., and Zychlinsky, A. (1998). *Shigella*-induced apoptosis is dependent on caspase-1 which binds to IpaB. J Biol Chem 273, 32895-32900.

Hochstrasser, M. (2006). Lingering mysteries of ubiquitin-chain assembly. Cell 124, 27-34.

Holmgren, A., and Lu, J. (2010). Thioredoxin and thioredoxin reductase: current research with special reference to human disease. Biochem Biophys Res Commun 396, 120-124.

Holmstrom, A., Petterson, J., Rosqvist, R., Hakansson, S., Tafazoli, F., Fallman, M., Magnusson, K.E., Wolf-Watz, H., and Forsberg, A. (1997). YopK of *Yersinia pseudotuberculosis* controls translocation of Yop effectors across the eukaryotic cell membrane. Mol Microbiol 24, 73-91.

Hoshino, K., Takeuchi, O., Kawai, T., Sanjo, H., Ogawa, T., Takeda, Y., Takeda, K., and Akira, S. (1999). Cutting edge: Toll-like receptor 4 (TLR4)-deficient mice are hyporesponsive to lipopolysaccharide: evidence for TLR4 as the Lps gene product. J Immunol 162, 3749-3752.

Huang, L., Kinnucan, E., Wang, G., Beaudenon, S., Howley, P.M., Huibregtse, J.M., and Pavletich, N.P. (1999). Structure of an E6AP-UbcH7 complex: insights into ubiquitination by the E2-E3 enzyme cascade. Science 286, 1321-1326.

Huibregtse, J.M., Scheffner, M., Beaudenon, S., and Howley, P.M. (1995). A family of proteins structurally and functionally related to the E6-AP ubiquitin-protein ligase. Proc Natl Acad Sci U S A 92, 2563-2567.

Huitema, Carly “Plasmid Preps” http://www.carlyhuitema.com/cloning.html Accessed April 20, 2012.

Janjusevic, R., Abramovitch, R.B., Martin, G.B., and Stebbins, C.E. (2006). A bacterial inhibitor of host programmed cell death defenses is an E3 ubiquitin ligase. Science 311, 222-226.

Johnson, S., and Blocker, A. (2008). Characterization of soluble complexes of the *Shigella flexneri* type III secretion system ATPase. FEMS Microbiol Lett 286, 274-278.

Jorgensen, I., Bednar, M.M., Amin, V., Davis, B.K., Ting, J.P., McCafferty, D.G., and Valdivia, R.H. (2011). The *Chlamydia* protease CPAF regulates host and bacterial proteins to maintain pathogen vacuole integrity and promote virulence. Cell Host Microbe 10, 21-32.

Jouihri, N., Sory, M.P., Page, A.L., Gounon, P., Parsot, C. and Allaoui, A. (2003). MxiK and MxiN interact with the Spa47 ATPase and are required for transit of the needle components MxiH and MxiI, but not of Ipa proteins, through the type III secretion apparatus of *Shigella flexneri*. Molecular Microbiology 49, 755-767.

Kaniuk, N.A., Vinogradov, E., Li, J., Monteiro, M.A., and Whitfield, C. (2004). Chromosomal and Plasmid-encoded Enzymes Are Required for Assembly of the R3-type Core Oligosaccharide in the Lipopolysaccharide of *Escherichia coli* O157:H7. The Journal of Biological Chemistry 279, 31237-31250.

Karlinsey, J.E. (2007). lambda-Red genetic engineering in *Salmonella enterica* serovar *Typhimurium*. Methods Enzymol 421, 199-209.

Kerneis, S., Guerin, P.J., von Seidlein, L., Legros, D., and Grais, R.F. (2009). A look back at an ongoing problem: *Shigella dysenteriae* type 1 epidemics in refugee settings in Central Africa (1993-1995). PLoS One 4, e4494.

Kim, D.W., Lenzen, G., Page, A.L., Legrain, P, Sansonetti, P.J., and Parsot, C. (2005). The *Shigella flexneri* effector OspG interferes with inate immune responses by targeting ubiquitin-conjugating enzymes. Proceedings of the National Academy of Science 102, 14046 -- 14051.

Kim, M., Ogawa, M., Fujita, Y., Yoshikawa, Y., Nagai, T., Koyama, T., Nagai, S., Lange, A., Fassler, R., and Sasakawa, C. (2009). Bacteria hijack integrin-linked kinase to stabilize focal adhesions and block cell detachment. Nature 459, 578-582.

Kinsella, T.M., and Nolan, G.P. (1996). Episomal vectors rapidly and stably produce high-titer recombinant retrovirus. Hum Gene Ther 7, 1405-1413.

Konradt, C., Frigimelica, E., Nothelfer, K., Puhar, A., Salgado-Pabon, W., di Bartolo, V., Scott-Algara, D., Rodrigues, C.D., Sansonetti, P.J., and Phalipon, A. (2011). The *Shigella flexneri* type three secretion system effector IpgD inhibits T cell migration by manipulating host phosphoinositide metabolism. Cell Host Microbe 9, 263-272.

Kotloff, K.L., Winickoff, J.P., Ivanoff, B., Clemens, J.D., Swerdlow, D.L., Sansonetti, P.J., Adak, G.K., and Levine, M.M. (1999). Global burden of *Shigella* infections: implications for vaccine development and implementation of control strategies. Bull World Health Organ 77, 651-666.

Kubori, T., N Shinzawa, H Kanuka, H Nagai (2010). *Legionella* Metaeffector Exploits Host Proteasome to Temporally Regulate Cognate Effector. PLoS Pathogens 6.

Kubori, T., Hyakutake, A., and Nagai, H. (2008). *Legionella* translocates an E3 ubiquitin ligase that has multiple U-boxes with distinct functions. Mol Microbiol 67, 1307-1319.

Kunsch, C., and Rosen, C.A. (1993). NF-kappa B subunit-specific regulation of the interleukin-8 promoter. Mol Cell Biol 13, 6137-6146.

Kunsch, C., and Rosen, C.A. (1993). NF-kappa B subunit-specific regulation of the interleukin-8 promoter. Mol Cell Biol 13, 6137-6146.

Lara-Tejero, M., Kato, J., Wagner, S., Liu, X., and Galan, J.E. (2011). A sorting platform determines the order of protein secretion in bacterial type III systems. Science 331, 1188-1191.

Lee, J.Y., Koga, H., Kawaguchi, Y., Tang, W., Wong, E., Gao, Y.S., Pandey, U.B., Kaushik, S., Tresse, E., Lu, J., Taylor, J.P., Cuervo, A.M. and Yao, T.P. (2010). HDAC6 controls autophagosome maturation essential for ubiquitin-selective quality-control autophagy. The EMBO Journal 29, 969-980.

Le Gall, T., Mavris, M., Martino, M.C., Bernardini, M.L., Denamur, E., and Parsot, C. (2005). Analysis of virulence plasmid gene expression defines three classes of effectors in the type III secretion system of *Shigella flexneri*. Microbiology *151*, 951-962.

Levin, I., Eakin, C., Blanc, M.P., Klevit, R.E., Miller, S.I., and Brzovic, P.S. (2010). Identification of an unconventional E3 binding surface on the UbcH5 ~ Ub conjugate recognized by a pathogenic bacterial E3 ligase. Proc Natl Acad Sci U S A 107, 2848-2853.

Li, H., Xu, H., Zhou, Y., Zhang, J., Long, C., Li, S., Chen, S., Zhou, J.M., and Shao, F. (2007). The phosphothreonine lyase activity of a bacterial type III effector family. Science 315, 1000-1003.

Lindberg, A.A., Karnell, A., and Weintraub, A. (1991). The lipopolysaccharide of *Shigella* bacteria as a virulence factor. Rev Infect Dis 13 Suppl 4, S279-284.

Lodish, H., Berk, A., Matsudaira, P., Kaiser, C., Krieger, M., Scott, M., Zipursky, S.L., Darnell, J. (2004). Molecular Cell Biology (New York, W. H. Freeman and Company).

Lu, Y.C., Yeh, W.C., and Ohashi, P.S. (2008). LPS/TLR4 signal transduction pathway. Cytokine 42, 145-151.

Mallo, G.V., Espina, M., Smith, A.C., Terebiznik, M.R., Aleman, A., Finlay, B.B., Rameh, L.E., Grinstein, S., and Brumell, J.H. (2008). SopB promotes phosphatidylinositol 3-phosphate formation on *Salmonella* vacuoles by recruiting Rab5 and Vps34. J Cell Biol 182, 741-752.

Martin-Serrano, J. (2007). The Role of Ubiquitin in Retroviral Egress. Traffic 8, 1297 -- 1303.

Matsusaka, T., Fujikawa, K., Nishio, Y., Mukaida, N., Matsushima, K., Kishimoto, T., and Akira, S. (1993). Transcription factors NF-IL6 and NF-kappa B synergistically activate transcription of the inflammatory cytokines, interleukin 6 and interleukin 8. Proc Natl Acad Sci U S A 90, 10193-10197.

Mattoo, S., Lee, Y.M., and Dixon, J.E. (2007). Interactions of bacterial effector proteins with host proteins. Curr Opin Immunol 19, 392-401.

Mavris, M., Page, A.L., Tournebize, R., Demers, B., Sansonetti, P., and Parsot, C. (2002). Regulation of transcription by the activity of the *Shigella flexneri* type III secretion apparatus. Mol Microbiol 43, 1543-1553.

Menard, R., Sansonetti, P., Parsot, C., and Vasselon, T. (1994). Extracellular association and cytoplasmic partitioning of the IpaB and IpaC invasins of *S. flexneri*. Cell 79, 515-525.

Menard, R., Sansonetti, P.J., and Parsot, C. (1993). Nonpolar mutagenesis of the *ipa* genes defines IpaB, IpaC, and IpaD as effectors of *Shigella flexneri* entry into epithelial cells. J Bacteriol 175, 5899-5906.

Menard, R., Sansonetti, P.J., and Parsot, C. (1993). Nonpolar mutagenesis of the ipa genes defines IpaB, IpaC, and IpaD as effectors of *Shigella flexneri* entry into epithelial cells. J Bacteriol 175, 5899-5906.

Miao, E.A., Mao, D.P., Yudkovsky, N., Bonneau, R., Lorang, C.G., Warren, S.E., Leaf, I.A., and Aderem, A. (2010). Innate immune detection of the type III secretion apparatus through the NLRC4 inflammasome. Proc Natl Acad Sci U S A 107, 3076-3080.

Morita-Ishihara, T., Ogawa, M., Sagara, H., Yoshida, M., Katayama, E., and Sasakawa, C. (2006). *Shigella* Spa33 is an essential C-ring component of type III secretion machinery. J Biol Chem 281, 599-607.

Mounier, J., Vasselon, T., Hellio, R., Lesourd, M., and Sansonetti, P.J. (1992). *Shigella flexneri* enters human colonic Caco-2 epithelial cells through the basolateral pole. Infect Immun 60, 237-248.

Mukaida, N., Mahe, Y., and Matsushima, K. (1990). Cooperative interaction of nuclear factor-kappa B- and cis-regulatory enhancer binding protein-like factor binding elements in activating the interleukin-8 gene by pro-inflammatory cytokines. J Biol Chem 265, 21128-21133.

Munz, C. (2006). Autophagy and antigen presentation. Cell Microbiol 8, 891-898.

Murray, R.Z., Kay, J.G., Sangermani, D.G., and Stow, J.L. (2005). A role for the phagosome in cytokine secretion. Science *310*, 1492-1495.

Murray, R.Z., Wylie, F.G., Khromykh, T., Hume, D.A., and Stow, J.L. (2005b). Syntaxin 6 and Vti1b form a novel SNARE complex, which is up-regulated in activated macrophages to facilitate exocytosis of tumor necrosis Factor-alpha. J Biol Chem 280, 10478-10483.

Nataro, J.P., Seriwatana, J., Fasano, A., Maneval, D.R., Guers, L.D., Noriega, F., Dubovsky, F., Levine, M.M., and Morris, J.G., Jr. (1995). Identification and cloning of a novel plasmid-encoded enterotoxin of enteroinvasive *Escherichia coli* and *Shigella* strains. Infect Immun 63, 4721-4728.

Navarro, S., Debili, N., Bernaudin, J.F., Vainchenker, W., and Doly, J. (1989). Regulation of the expression of IL-6 in human monocytes. J Immunol 142, 4339-4345.

Ng, A.C., Eisenberg, J.M., Heath, R.J., Huett, A., Robinson, C.M., Nau, G.J., and Xavier, R.J. (2011). Human leucine-rich repeat proteins: a genome-wide bioinformatic categorization and functional analysis in innate immunity. Proc Natl Acad Sci U S A 108 Suppl 1, 4631-4638.

Niebuhr, K., Jouihri, N., Allaoui, A., Gounon, P., Sansonetti, P.J., and Parsot, C. (2000). IpgD, a protein secreted by the type III secretion machinery of *Shigella flexneri*, is chaperoned by IpgE and implicated in entry focus formation. Mol Microbiol 38, 8-19.

Nobe, R., Nougayrede, J.P., Taieb, F., Bardiau, M., Cassart, D., Navarro-Garcia, F., Mainil, J., Hayashi, T., and Oswald, E. (2009). Enterohaemorrhagic *Escherichia coli* serogroup O111 inhibits NF-(kappa)B-dependent innate responses in a manner independent of a type III secreted OspG orthologue. Microbiology 155, 3214-3225.

Ogawa, M., Suzuki, T., Tatsuno, I., Abe, H., and Sasakawa, C. (2003). IcsB, secreted via the type III secretion system, is chaperoned by IpgA and required at the post-invasion stage of *Shigella* pathogenicity. Mol Microbiol 48, 913-931.

Ogawa, M., Yoshimori, T., Suzuki, T., Sagara, H., Mizushima, N., and Sasakawa, C. (2005). Escape of intracellular *Shigella* from autophagy. Science 307, 727-731.

Ong, S.E., Blagoev, B., Kratchmarova, I., Kristensen, D.B., Steen, H., Pandey, A., and Mann, M. (2002). Stable isotope labeling by amino acids in cell culture, SILAC, as a simple and accurate approach to expression proteomics. Mol Cell Proteomics 1, 376-386.

Onodera, N.T., Ryu, J., Durbic, T., Nislow, C., Archibald, J.M., Rohde, J.R. The genome sequence of *Shigella flexneri* serotype 5a strain M90T Sm. Journal of Bacteriology (submitted).

Paetzold, S., Lourido, S., Raupach, B., and Zychlinsky, A. (2007). *Shigella flexneri* phagosomal escape is independent of invasion. Infect Immun 75, 4826-4830.

Page, A.L., Sansonetti, P., and Parsot, C. (2002). Spa15 of *Shigella flexneri*, a third type of chaperone in the type III secretion pathway. Mol Microbiol 43, 1533-1542.

Parsot, C., R Menard, P Gounon, P Sansonetti (1995). Enhanced secretion through the *Shigella flexneri* Mxi-Spa translocon leads to assembly of extracellular proteins into macromolecular structures. Molecular Microbiology 16, 291--300.

Parsot, C. (2009). *Shigella* type III secretion effectors: how, where, when, for what purposes? Curr Opin Microbiol 12, 110-116.

Parsot, C., Ageron, E., Penno, C., Mavris, M., Jamoussi, K., d'Hauteville, H., Sansonetti, P., and Demers, B. (2005). A secreted anti-activator, OspD1, and its chaperone, Spa15, are involved in the control of transcription by the type III secretion apparatus activity in *Shigella flexneri*. Mol Microbiol 56, 1627-1635.

Patel, J.C., and Galan, J.E. (2006). Differential activation and function of Rho GTPases during *Salmonella*-host cell interactions. J Cell Biol 175, 453-463.

Patel, J.C., Hueffer, K., Lam, T.T., and Galan, J.E. (2009). Diversification of a *Salmonella* virulence protein function by ubiquitin-dependent differential localization. Cell 137, 283-294.

Persaud, A., Alberts, P., Amsen, E.M., Xiong, X., Wasmuth, J., Saadon, Z., Fladd, C., Parkinson, J., and Rotin, D. (2009). Comparison of substrate specificity of the ubiquitin ligases Nedd4 and Nedd4-2 using proteome arrays. Molecular Systems Biology 5, 333.

Petroski, M.D., and Deshaies, R.J. (2005). Mechanism of lysine 48-linked ubiquitin-chain synthesis by the cullin-RING ubiquitin-ligase complex SCF-Cdc34. Cell 123, 1107-1120.

Phalipon, A., Sansonetti, P.J. (2007). *Shigella's* way of manipulating the host intestinal innate and adaptive immune system: a tool box for survival? Immunology and Cell Biology 85, 119 -- 129.

Philpott, D.J., Yamaoka, S., Israel, A., and Sansonetti, P.J. (2000). Invasive *Shigella flexneri* activates NF-kappa B through a lipopolysaccharide-dependent innate intracellular response and leads to IL-8 expression in epithelial cells. J Immunol 165, 903-914.

Pore, D., Mahata, N., Pal, A., and Chakrabarti, M.K. (2010). 34 kDa MOMP of *Shigella flexneri* promotes TLR2 mediated macrophage activation with the engagement of NF-kB and p38 MAP kinase signaling. Molecular Immunology 47, 1739 -- 1746.

Price, C.T., Al-Quadan, T., Santic, M., Rosenshine, I., and Abu Kwaik, Y. (2011). Host proteasomal degradation generates amino acids essential for intracellular bacterial growth. Science 334, 1553-1557.

Proost, P., Struyf, S., Couvreur, M., Lenaerts, J.P., Conings, R., Menten, P., Verhaert, P., Wuyts, A., and Van Damme, J. (1998). Posttranslational modifications affect the activity of the human monocyte chemotactic proteins MCP-1 and MCP-2: identification of MCP-2(6-76) as a natural chemokine inhibitor. J Immunol 160, 4034-4041.

Proost, P., Wuyts, A., and Van Damme, J. (1996). Human monocyte chemotactic proteins-2 and -3: structural and functional comparison with MCP-1. J Leukoc Biol 59, 67-74.

Rebeil, R., Ernst, R.K., Gowen, B.B., Miller, S.I., and Hinnebusch, B.J. (2004). Variation in lipid A structure in the pathogenic *Yersiniae*. Mol Microbiol 52, 1363-1373.

Reed, W.P. (1975). Serum factors capable of opsonizing *Shigella* for phagocytosis by polymorphonuclear neutrophils. Immunology 28, 1051-1059.

Rohde, J., and Parsot, C. (2007). Type III Secretion Effectors of the IpaH Family are E3 Ubiquitin Ligases. Cell Host & Microbe 1, 77-83.

Rosebrock, T.R., Zeng, L., Brady, J.J., Abramovitch, R.B., Xiao, F., and Martin, G.B. (2007). A bacterial E3 ubiquitin ligase targets a host protein kinase to disrupt plant immunity. Nature 448, 370-374.

Sack, D.A., Lyke, C., McLaughlin, C., Suwanvanichkij, V. (2001). Antimicrobial resistance in shigellosis, cholera and campylobacteriosis. World Health Organization.

Sambrook, J., Russell, D. (2001). SDS-PAGE Electrophoresis. In Molecular Cloning: A Laboratory Manual (Cold Spring Harbor, NY, Cold Spring Harbor Laboratory Press), pp. A8.40 -- A48.51.

Sansonetti, P.J. (2001). Microbes and Microbial Toxins: Paradigms for Microbial-Mucosal Interactions III. Shigellosis: from symptoms to molecular pathogenesis. Am J Physiol Gastrointest Liver Physiol 280, G319-G323.

Sansonetti, P.J. (2006). Shigellosis: an old disease in new clothes? PLoS Med 3, e354.

Schuch, R., and Maurelli, A.T. (2001). MxiM and MxiJ, base elements of the Mxi-Spa type III secretion system of *Shigella*, interact with and stabilize the MxiD secretin in the cell envelope. J Bacteriol 183, 6991-6998.

Scudiero, O., Galdiero, S., Cantisani, M., Di Noto, R., Vitiello, M., Galdiero, M., Naclerio, G., Cassiman, J.J., Pedone, C., Castaldo, G., et al. (2010). Novel synthetic, salt-resistant analogs of human beta-defensins 1 and 3 endowed with enhanced antimicrobial activity. Antimicrob Agents Chemother 54, 2312-2322.

Sellge, G.e.a. (2010). Th17 Cells are the Dominant T Cell Subtype Primed by *Shigella flexneri* Mediating Protective Immunity. Journal of Immunology 184.

Shi, G., K Nakahira, S Hamond, KJ Rhodes, LE Schechter and JS Trimmer (1996). Beta Subunits Promote K+ Channel Surface Expression through Effects Early in Biosynthesis. Neuron 16, 843-852.

Singer, A.U., Rohde, J.R., Lam, R., Skarina, T., Kagan, O., Dileo, R., Chirgadze, N.Y., Cuff, M.E., Joachimiak, A., Tyers, M., et al. (2008). Structure of the *Shigella* T3SS effector IpaH defines a new class of E3 ubiquitin ligases. Nat Struct Mol Biol 15, 1293-1301.

Sitaraman, S.V., Merlin, D., Wang, L., Wong, M., Gewirtz, A.T., Si-Tahar, M., and Madara, J.L. (2001). Neutrophil-epithelial crosstalk at the intestinal lumenal surface mediated by reciprocal secretion of adenosine and IL-6. J Clin Invest 107, 861-869.

Smith, R.S., Fedyk, E.R., Springer, T.A., Mukaida, N., Iglewski, B.H., and Phipps, R.P. (2001). IL-8 production in human lung fibroblasts and epithelial cells activated by the *Pseudomonas* autoinducer N-3-oxododecanoyl homoserine lactone is transcriptionally regulated by NF-kappa B and activator protein-2. J Immunol 167, 366-374.

Sperandio, B., Regnault, B., Guo, J., Zhang, Z., Stanley, S.L., Sansonetti, P.J., and Pédron, T. (2008). Virulent *Shigella flexneri* subverts the host innate immune response through manipulation of antimicrobial peptide gene expression. Journal of Experimental Medicine 205, 1121 -- 1132.

Stanley, E.R., Berg, K.L., Einstein, D.B., Lee, P.S.W., Pixley, F.J., Wang, Y., Yeung, Y.G. (1998). Biology and action of colony-stimulating factor-1. Molecular Reproduction and Development 46, 4 -- 10.

Stavrinides, J., McCann, H.C., and Guttman, D.S. (2008). Host-pathogen interplay and the evolution of bacterial effectors. Cell Microbiol 10, 285-292.

Steinmetz, L.M., Scharfe, C., Deutschbauer, A.M., Mokranjac, D., Herman, Z.S., Jones, T., Chu, A.M., Giaever, G., Prokisch, H., Oefner, P.J., et al. (2002). Systematic screen for human disease genes in yeast. Nat Genet 31, 400-404.

Strockbine, N.A., Jackson, M.P., Sung, L.M., Holmes, R.K., and O'Brien, A.D. (1988). Cloning and sequencing of the genes for Shiga toxin from *Shigella dysenteriae* type 1. J Bacteriol 170, 1116-1122.

Sun, L., Deng, L., Ea, C.K., Xia, Z.P., and Chen, Z.J. (2004). The TRAF6 ubiquitin ligase and TAK1 kinase mediate IKK activation by BCL10 and MALT1 in T lymphocytes. Mol Cell 14, 289-301.

Sun, P., Yamamoto, H., Suetsugu, S., Miki, H., Takenawa, T. and Endo, T. (2003). Small GTPase Rah/Rab34 Is Associated with Membrane Ruffles and Macropinosomes and Promotes Macropinosome Formation. The Journal of Biological Chemistry 278, 4063-4071.

Suzuki, K., Kirisako, T., Kamada, Y., Mizushima, N., Noda, T., and Ohsumi, Y. (2001). The pre-autophagosomal structure organized by concerted functions of APG genes is essential for autophagosome formation. EMBO J 20, 5971-5981.

Suzuki, T., Franchi, Luigi, Toma, Claudia, Ashida, Hiroshi, Ogawa, Michinaga, Yoshikawa, Yuko, HItomi, MImuro, Inohara, Naohiro, Sasakawa, Chihiro and Nunez, Gabriel (2007). Differential Regulation of Caspase-1 Activation, Pyroptosis, and Autophagy via Ipaf and ASC in *Shigella*-Infected Macrophages. PLoS Pathogens 3, e111.

Tamae, C., Liu, A., Kim, K., Sitz, D., Hong, J., Becket, E., Bui, A., Solaimani, P., Tran, K.P., Yang, H.*, et al.* (2008). Determination of antibiotic hypersensitivity among 4,000 single-gene-knockout mutants of *Escherichia coli*. J Bacteriol 190, 5981-5988.

Tang, X., Orlicky, S., Liu, Q., Willems, A., Sicheri, F., and Tyers, M. (2005). Genome-wide surveys for phosphorylation-dependent substrates of SCF ubiquitin ligases. Methods Enzymol 399, 433-458.

Tanida, I., Ueno, T., and Kominami, E. (2004). LC3 conjugation system in mammalian autophagy. Int J Biochem Cell Biol 36, 2503-2518.

Tatham, M.H., Geoffroy, M.C., Shen, L., Plechanovova, A., Hattersley, N., Jaffray, E.G., Palvimo, J.J., and Hay, R.T. (2008). RNF4 is a poly-SUMO-specific E3 ubiquitin ligase required for arsenic-induced PML degradation. Nat Cell Biol 10, 538-546.

Tong, A.H., Evangelista, M., Parsons, A.B., Xu, H., Bader, G.D., Page, N., Robinson, M., Raghibizadeh, S., Hogue, C.W., Bussey, H., et al. (2001). Systematic genetic analysis with ordered arrays of yeast deletion mutants. Science 294, 2364-2368.

Trede, N.S., Tsytsykova, A.V., Chatila, T., Goldfeld, A.E., and Geha, R.S. (1995). Transcriptional activation of the human TNF-alpha promoter by superantigen in human monocytic cells: role of NF-kappa B. J Immunol 155, 902-908.

Tsai, E.Y., Falvo, J.V., Tsytsykova, A.V., Barczak, A.K., Reimold, A.M., Glimcher, L.H., Fenton, M.J., Gordon, D.C., Dunn, I.F., and Goldfeld, A.E. (2000). A lipopolysaccharide-specific enhancer complex involving Ets, Elk-1, Sp1, and CREB binding protein and p300 is recruited to the tumor necrosis factor alpha promoter in vivo. Mol Cell Biol 20, 6084-6094.

Typas, A., Nichols, R.J., Siegele, D.A., Shales, M., Collins, S.R., Lim, B., Braberg, H., Yamamoto, N., Takeuchi, R., Wanner, B.L., et al. (2008). High-throughput, quantitative analyses of genetic interactions in *E. coli*. Nat Methods 5, 781-787.

van de Verg, L.L., Mallett, C.P., Collins, H.H., Larsen, T., Hammack, C., and Hale, T.L. (1995). Antibody and cytokine responses in a mouse pulmonary model of *Shigella flexneri* serotype 2a infection. Infect Immun 63, 1947-1954.

VerPlank, L., Bouamr, F., LaGrassa, T.J., Agresta, B., Kikonyogo, A., Leis, J., and Carter, C.A. (2001). Tsg101, a homologue of ubiquitin-conjugating (E2) enzymes, binds the L domain in HIV type 1 Pr55(Gag). Proc Natl Acad Sci U S A 98, 7724-7729.

Walsh, T.R., Weeks, J., Livermore, D.M., and Toleman, M.A. (2011). Dissemination of NDM-1 positive bacteria in the New Delhi environment and its implications for human health: an environmental point prevalence study. Lancet Infect Dis 11, 355-362.

Walz, A., Burgener, R., Car, B., Baggiolini, M., Kunkel, S.L., and Strieter, R.M. (1991). Structure and neutrophil-activating properties of a novel inflammatory peptide (ENA-78) with homology to interleukin 8. J Exp Med 174, 1355-1362.

Wan, F., Weaver, A., Gao, X., Bern, M., Hardwidge, P.R., and Lenardo, M.J. (2011). IKKbeta phosphorylation regulates RPS3 nuclear translocation and NF-kappaB function during infection with *Escherichia coli* strain O157:H7. Nat Immunol 12, 335-343.

Wassef, J.S., Keren, D.F., Mailloux, J.L. (1989). Role of M cells in initial antigen uptake and in ulcer formation in the rabbit intestinal loop model of shigellosis. Infection and Immunity 57, 858 -- 863.

White, D. (2007). The Physiology and Biochemistry of Prokaryotes (New York, Oxford University Press), pp. 323-328.

Wooten, M.W.e.a. (2005). The p62 Scaffold Regulates Nerve Growth Factor-induced NF-kB Activation by Influencing TRAF6 Polyubiquitination. The Journal of Biological Chemistry 280, 35625 -- 35629.

Xu, P., Duong, D.M., Seyfried, N.T., Cheng, D., Xie, Y., Robert, J., Rush, J., Hochstrasser, M., Finley, D., and Peng, J. (2009). Quantitative proteomics reveals the function of unconventional ubiquitin chains in proteasomal degradation. Cell 137, 133-145.

Z'Graggen, K., Walz, A., Mazzucchelli, L., Strieter, R.M., and Mueller, C. (1997). The C-X-C chemokine ENA-78 is preferentially expressed in intestinal epithelium in inflammatory bowel disease. Gastroenterology 113, 808-816.

Zheng, Y. T., Shahnazari, S., Brech, A., Lamark, T., Johansen, T., Brumell, J. (2009). The Adaptor Protein p62/SQSTM1 Targets Invading Bacteria to the Autophagy Pathway. The Journal of Immunology 183, 5909-5916.

Zhou, D., Chen, L.M., Hernandez, L., Shears, S.B., and Galan, J.E. (2001). A *Salmonella* inositol polyphosphatase acts in conjunction with other bacterial effectors to promote host cell actin cytoskeleton rearrangements and bacterial internalization. Mol Microbiol 39, 248-259.

Zhu, Y., and Shao, F. (2008). Structure of a *Shigella* effector reveals a new class of ubiquitin ligases. Nature Structural & Molecular BIology 15, 1302 -- 1308.

Zimmermann, N., Hogan, S.P., Mishra, A., Brandt, E.B., Bodette, T.R., Pope, S.M., Finkelman, F.D., and Rothenberg, M.E. (2000). Murine Eotaxin-2: a constitutive eosinophil chemokine induced by allergen challenge and IL-4 overexpression. J Immunol 165, 5839-5846.

Zurawski, D.V., Mumy, K.L, Faherty, C.S., McCormick, B.A. and Maurelli, A.T. (2009). *Shigella flexneri* type III secretion system effectors OspB and OspF target the nucleus to downregulate the host inflammatory response via interactions with retinoblastoma protein. Molecular Microbiology 71, 350 -- 368.

Zurawski, D.V., Mitsuhata, C., Mumy, K.L., McCormick, B.A., and Maurelli, A.T. (2006). OspF and OspC1 are *Shigella flexneri* type III secretion system effectors that are required for postinvasion aspects of virulence. Infect Immun 74, 5964-5976.

Zychlinsky, A., Fitting, C., Cavaillon, J.M., and Sansonetti, P.J. (1994). Interleukin 1 is released by murine macrophages during apoptosis induced by *Shigella flexneri.* J Clin Invest 94, 1328-1332.

Zychlinsky, A., Prevost, M.C., and Sansonetti, P.J. (1992). *Shigella flexneri* induces apoptosis in infected macrophages. Nature 358, 167-169.

Zychlinsky, A., Thirumalai, K., Arondel, J., Cantey, J.R., Aliprantis, A.O., and Sansonetti, P.J. (1996). In vivo apoptosis in *Shigella flexneri* infections. Infect Immun 64, 5357-5365.